Fall 1983

Close-Coupling Calculations for NaAr, NaNe, and NaHe

Linda Lindroth Vahala
Old Dominion University

CLOSE-COUPLING CALCULATIONS FOR NaAr, NaNe, AND NaHe

by
Linda Lindroth Vahala
B.S. June, 1969, University of Illinois
M.S. December, 1971, University of Iowa

A Dissertation Submitted to the Faculty of
Old Dominion University in Partial Fulfillment of the
Requirements for the Degree of

DOCTOR OF PHILOSOPHY
APPLIED PHYSICS

OLD DOMINION UNIVERSITY
December, 1983

Approved by:

Mark D. Havey (Director)

ABSTRACT

CLOSE-COUPLING CALCULATIONS
FOR NaAr, NaNe, AND NaHe

Linda Lindroth Vahala
Old Dominion University, 1983
Director: Dr. Mark D. Havey

The non-adiabatic close-coupled theory, developed by Mies and by George, is employed in a time-independent molecular calculation for Na-rare gas collisions in a radiations field. The intensity of the Na D1/D2 lines is calculated for both blue- and red-wing excitation and is in good agreement with the experimental results of Havey, Copeland, and Wang for NaAr. The effects of different Born-Oppenheimer potentials on D1/D2 line intensity is considered by also treating NaNe and NaHe. The individual parity contributions to the line intensities are significantly different from each other.

ACKNOWLEDGEMENTS

I would like to thank Dr. Mark Havey for not only suggesting this dissertation problem and obtaining the experimental results for the NaAr system, but also for the many discussions and useful physical insights; Dr. Paul Julienne and Dr. Fred Mies of the National Bureau of Standards for supplying me with the basic close-coupling numerical code and for important guidance ; Dr. Pascale and Dr. Peach for supplying me with the NaHe and NaNe potentials ; Dr. Gary Copeland for helping me to transfer this code from the IBM to the DEC 10 system ; and Dr. Gilbert Hoy for useful discussions.

I am grateful to the Oral Exam Committee for their reading of this dissertation and their comments, as well as to my fellow graduate students for their encouragement and support.

TABLE OF CONTENTS

LIST OF TABLES

TABLES

LIST OF FIGURES

FIGURES

CHAPTER 1

INTRODUCTION

It has long been recognized [1] that in the low energy scattering of two atoms, one can conveniently express the scattering process by using the continuum wave functions of the diatomic molecule consisting of the two combined atoms. In particular, the adiabatic electronic states of the molecule (also called the molecular Born-Oppenheimer (BO) states) are a very useful truncated basis with which to describe the scattering and should lead to more rapidly convergent results than the choice of the asymptotic individual atomic states as a basis. As the BO states are implicit functions of the interatomic separation R between the two atoms, they incorporate within the molecular basis itself effects like electron exchange, valence forces, and interatomic polarization effects. Mies [2] has very carefully examined and systematically discussed the usual techniques [1,3,4] and approximations employed to handle the coupling between the different BO states. In particular, he presented a detailed [2] molecular theory of atomic collisions resulting in fine structure transitions. Attention has recently focused on how atomic collisions are

affected by the presence of a strong radiation field. These studies have considered the possibilities of laser modified energy transfer [5], as well as chemical reactions [6], and isotope separations [7]. The introduction of the laser field introduces considerable complexity and this has led George and his colleagues [8,9] to investigate whether the intrinsic angular momentum of the photon field must be fully incorporated quantum mechanically. This work is also reviewed by Mies [10] as well as the approximation they introduce so as to limit the internal coupling of the projection of the total molecular angular momentum (due to the lack of rotational invariance in the molecule-radiation field system).

In this dissertation we shall consider in some detail the inelastic processes that occur in the collisions between alkali and rare gas atoms in the presence of a radiation field. Considerable experimental [11-13] and theoretical efforts [14-16] are currently being expended on studying these systems (and related ones) since these results can lead to a basic understanding of a variety of collisional effects such as electronic quenching [17], fine-structure changing collisions [17-18], coherence transfer [19], and radiative collisions [20]. Such processes are important in understanding a wide range of phenomena such as molecular dissociation [21], non-radiative electronic transitions [17], the formation of spectral line wings [14-16], and the approach of systems towards thermodynamic equilibrium.

Since the interaction of ground state alkali and rare gas atoms in the presence of a non-resonant radiation field-- non-resonant with respect to the atomic alkali or the rare gas energy levels--allows one to treat the rare-gas atom as atomically unchanged, this system can be probed both experimentally and theoretically to some degree of thoroughness and can lead us to some insight as to the role of the BO (adiabatic) potentials, non-adiabatic mixing of states and the effects of detuning on the emitted radiation.

Theoretically, the work of Cooper [14] and his group has centered on the density matrix formulation while we follow the more intuitive approach of Mies [2,10] and Julienne [16] in developing the non-adiabatic theory of atomic collisions in the presence of a radiation field by a time-independent molecular formulation. In particular we will be concerned with "optical" collisions in a non-resonant laser field

$$Na(^2S_{1/2}) + B + nh\nu \longrightarrow Na(^2P_{1/2})$$

$$\text{or } Na(^2P_{3/2}) + B + (n-1)h\nu$$

This excited molecule then dissociates and the excited sodium atom eventually decays, emitting photons at the D1 ($^2P_{1/2} - {}^2S_{1/2}$) and D2 ($^2P_{3/2} - {}^2S_{1/2}$) resonance transitions.

In considering the molecular dynamics we will find (numerically) the regions of internuclear separation where the various angular momenta are good quantum numbers (i.e.

how the various Hund angular momentum coupling schemes are encountered during the molecular motion). Because of the complexity of the hierarchy of coupled equations in the 'exact' close-coupled theory, heavy numerics must be employed to obtain the solutions. These solutions can then be used to set up simple physical arguments as to the radial (internuclear) regions where important coupling of molecular states can occur, or to the degree of depolarization of the radiation emitted following molecular dissociation. In particular we will concentrate on the experiment of Havey, Copeland, Wang [13] on NaAr and show how the nonadiabatic close coupled theory can recover these results (preliminary results have just been published by Kulander and Rebentrost [22] on the intensities of the D1/D2 lines as a function of the detuning of the incident laser photon frequency from the atomic sodium resonance lines). We will then investigate the changes brought about by changing the rare gas from Ar to He and Ne.

CHAPTER 2

EXPERIMENTAL RESULTS AND HEURISTIC ARGUMENTS

Interesting effects can be introduced into the well studied field of scattering phenomena by the introduction of intense laser radiation fields. In particular one can study the effects of the laser field on the internal states and the final scattering wave functions for atom-atom collisions. By choosing the laser frequency to be well outside an inverse collision time ($\tau \sim 10^{-12}$ sec) of the atomic resonance, so that the photon absorption takes place in the far wings, we come across the situation in which the atom-atom dynamics are strongly correlated (Burnett [14]).

Fine structure changing collisions are readily examined in the atomic collision of an alkali atom (in our case Na) and a rare gas atom mediated by an intense laser field. Alkali atoms are chosen since they have essentially a one valence electron structure, while rare gas atoms behave as a polarizable charge distribution during the collision. This leads to interatomic interactions which are principally that of the weak van der Waal force. Since the excited states of a rare gas atom lie very much above the ionization energy of the alkali atom, the only important interactions for

initially ground state alkali atoms will be that of exciting the alkali atom to an excited state while leaving the rare gas atom in its ground state.

The following is a synopsis of details of an experiment on such collisions by Havey, Copeland, Wang [13]. The experimental technique consists of containing an optically thin alkali-rare atom gas mixture in a Pyrex cell with a production of alkali atoms to create a central density of $\sim 10^{10}$ / cm^3 . The perturber rare gas atom pressure is kept high -- typically in the range of 1-50 Torr. A vertically polarized laser beam from a ring dye laser is focussed into the central section of the Pyrex cell yielding a radiation field power density of $\sim 10^3$ W/cm^2 there. The laser is tuned to a frequency in the far wings of the collisionally perturbed alkali resonance transition. For example in the case of Na-Ar binary collisions excitation on the high frequency ("blue") side of the atomic resonance of $Na(^2P_{3/2})$-$Na(^2S_{1/2})$ corresponds to free-free transitions between the molecular $X\,^2\Sigma_{1/2}$ and $B\,^2\Sigma_{1/2}$ states, while excitation on the low frequency ("red") side of the allowed Na atomic resonance frequency could lead to free-free, free-bound transitions between the molecular $X\,^2\Sigma_{1/2}$ and the $A\,^2\Pi_{1/2,3/2}$ states. There is a change in the relative kinetic energy of the atom-atom system before and after the laser mediated strong collision so that total energy is conserved. After the photon absorption, the Na-Ar molecule dissociates and there is a relative probability that the Na atom will be

left in either the excited $^2P_{1/2}$ or excited $^2P_{3/2}$ state. Thus the non-resonant excitation will produce atomic fluorescence at the Na D1 and D2 lines. This fluorescence is detected perpendicular to the incident laser beam and its linear polarization vector. The fluorescence is spectrally dispersed by a one-third - meter scanning monochromator, and detected by a photomultiplier tube operating in the photon counting mode. The resulting signals are recorded on a multichannel analyzer whose time base is synchronized to the scan rate of the monochromator. The analyzer enables us to integrate the resulting emission line intensities I(D1) and I(D2) for the Na D1 and D2 atomic lines. Because of the background pressure of the rare gas, fine structure changing collisions can occur after the far wing photon absorption and the Na-Ar molecular dissociation. Hence the ratio of the emission line intensities I(D1)/I(D2) is dependent on the background pressure of the rare gas. The probability ratio of finding the excited Na atom in the $^2P_{1/2}$ state rather than in the $^2P_{3/2}$ state is obtained by extrapolating the emission line intensity ratio I(D1)/I(D2) to zero background rare gas pressure.

However, there are several systematic effects which can distort the experimentally measured values of the line intensities I(D1)/I(D2) and lead to errors in the extrapolation to the probability of excited Na-population of the $^2P_{1/2}$ over $^2P_{3/2}$ states.

One systematic effect that must be considered is radiation trapping, or reabsorption, of the emitted (asymptotic) atomic resonance radiation by the Na atoms in the cell before this radiation can escape the cell and be detected. It can be shown that this photon reabsorption is greater for the D2 resonance line rather than for the D1 line, thus decreasing the experimentally measured D2 radiation line intensity over the D1 line intensity. Since this subsequently absorbed radiation will be reradiated out of the cell but will not, in general, be detected in the light collection experimental optics, the emission line intensities I(D1)/I(D2) will be systematically increased by this effect. One can reduce this reabsorption effect by decreasing the alkali pressures below 10^{-6} Torr. At this Na pressure, one can safely radiation trapping effects.

Another systematic error is due to the spatial anisotropy of the emitted atomic resonance radiation. The spatial anisotropy arises from electric dipole radiation from the m_j magnetic sublevels of the j=1/2 and j=3/2 Na asymptotic states, which will generally be unequally populated by the laser photon absorption of the Na-Ar molecule, and its eventual disintegration into either the $^2P_{1/2}$ or $^2P_{3/2}$ atomic Na states. Walkup, Migdall, Pritchard [23] give the emitted radiation intensity

$$I(\theta) = I_o [1+\beta P_2 (\cos\theta)]$$

where θ is the angle between the linear polarization of the incident (vertically polarized) photon beam and the linear polarization of the scattered light, I_o is the total emitted intensity , β is a complicated non-zero parameter encompassing the effects of rare gas pressure, the frequency of the incident laser radiation, the hyperfine depolarization of the excited alkali state, and $P_2(\cos\theta) = (1/2)(3\cos^2\theta - 1)$ is a Legendre polynomial. To avoid this spatial anisotropy in the emitted radiation one can introduce a polaroid placed in the light detection arm at $\theta_* = 54.7^\circ$ so that $P_2(\cos\theta_*) = 0$.

A third systematic effect is the dependence of the cross section ratio of populating the excited alkali atom state on the rare gas pressure.

Using a simple model based on a rate equation analysis of the asymptotic alkali collision dynamics with rare gas atoms we find that the pressure dependence is given by

$$\frac{I(D1)}{I(D2)} = \frac{\nu_1}{\nu_2}\left[\frac{\gamma(P1/P2) + \Gamma_{21}(1+P1/P2)}{\gamma + \Gamma_{12}(1+P1/P2)}\right]$$

where ν_1 and ν_2 are the D1 and D2 emission frequencies, γ^{-1} is the spontaneous decay time for the alkali excited state (typically $\gamma \sim 10^6$ sec^{-1}). Γ_{12} is the fine structure mixing rate for population transfer from the $^2P_{1/2}$ to the $^2P_{3/2}$ alkali states (while Γ_{21} is the rate for population

transfer from $^2P_{3/2}$ to the $^2P_{1/2}$ levels) and is linearly dependent on the rare gas pressure. Thus

$$\frac{P1}{P2} = \frac{(\gamma + \Gamma_{12}) - \Gamma_{21}(\nu_1/\nu_2)(I_2/I_1)}{(\gamma + \Gamma_{21})(\nu_1/\nu_2)(I_2/I_1) - \Gamma_{12}}$$

since the right hand side is known or can be experimentally measured, we can determine the relative probability P1/P2. Experimentally one makes a nonlinear least squares fit to the data I_1/I_2 and then extrapolates to zero rare gas pressure.

Figure 1 schematically illustrates the Na-Ar interatomic potentials, while Figure 2 illustrates the Ar pressure dependence of the intensity ratio I(D1)/I(D2) of the Na D lines for red wing excitation at -11.5 cm^{-1} detunings. Figure 3 illustrates the zero-pressure extrapolations of the Na D1/D2 intensity ratios measured experimentally. For asymptotic blue wing excitation (detuning $\Delta \rightarrow +\infty$), D1/D2 intensity approaches 1.6 (2), while for asymptotic red wing excitation (detuning $\Delta \rightarrow -\infty$), D1/D2 intensity approaches 0.50 (4). If we were considering a single Na-Ar collision, the D1/D2 intensity ratio gives the ratio of the probability of making a transition from Na $^2P_{1/2} \rightarrow$ Na $^2S_{1/2}$ relative to the transition Na $^2P_{3/2} \rightarrow$ Na $^2S_{1/2}$. If one is allowing for many Na-Ar collisions then the D1/D2 intensity ratio gives the ratio of these transition probabilities from one of the excited

FIGURE 1

Schematic NaAr interatomic potentials as a function of internuclear separation

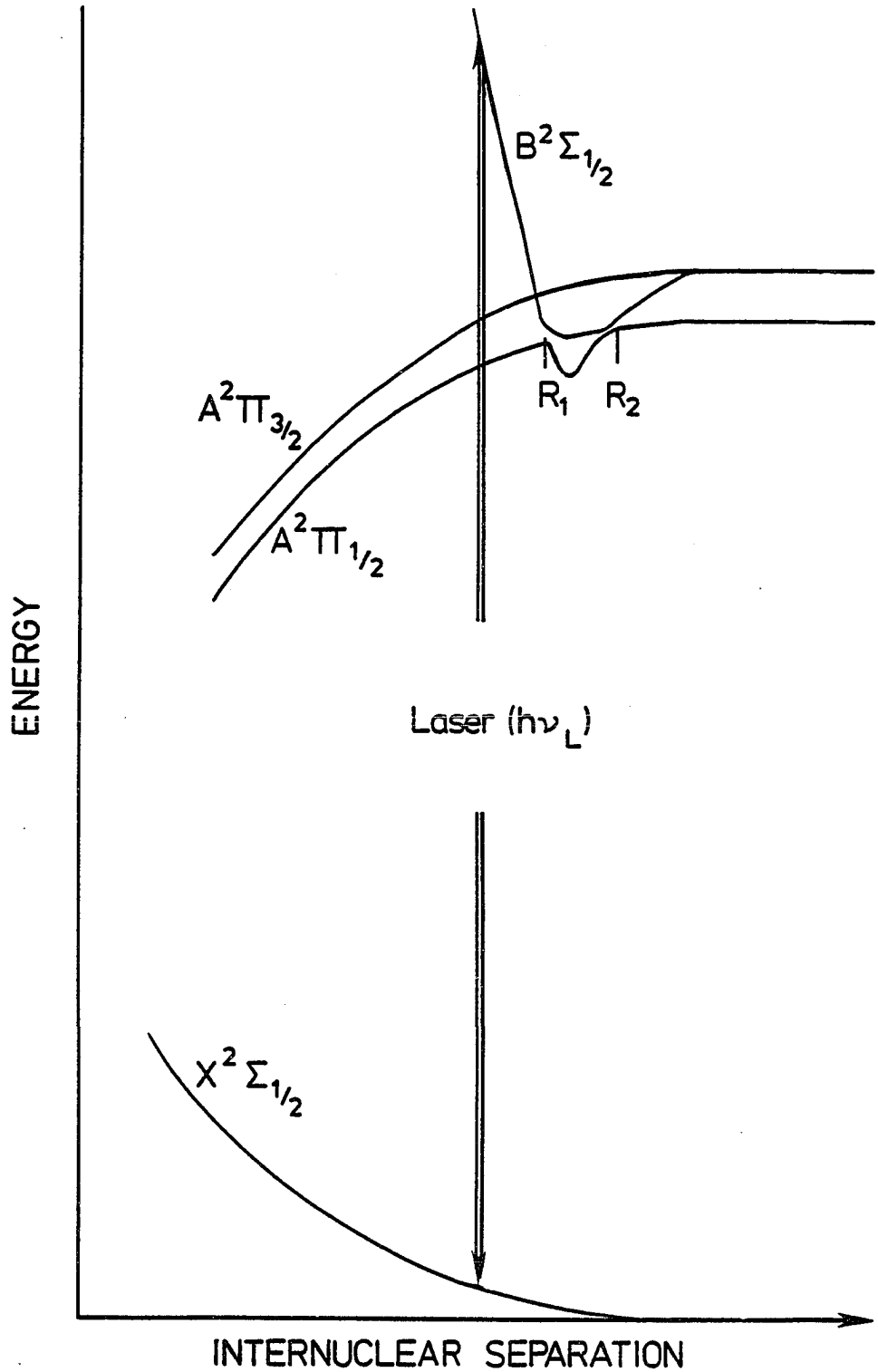

FIGURE 2

Experimental intensity ratio I(D1)/I(D2) for NaAr as a function of background Ar gas pressure. This data is for a detuning of - 11.5 cm^{-1} from the D1 line.

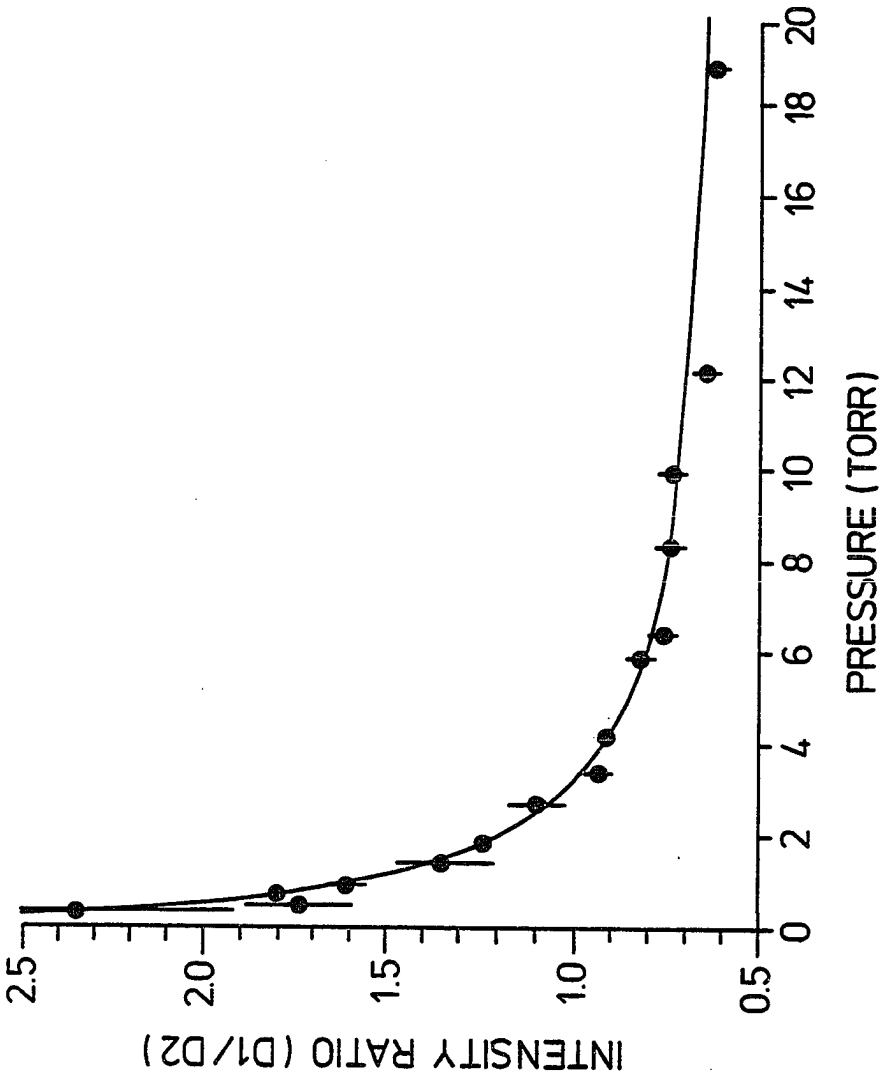

FIGURE 3

Experimental NaAr intensity ratio D1/D2 as a function of detuning. These results are for zero background gas pressure.

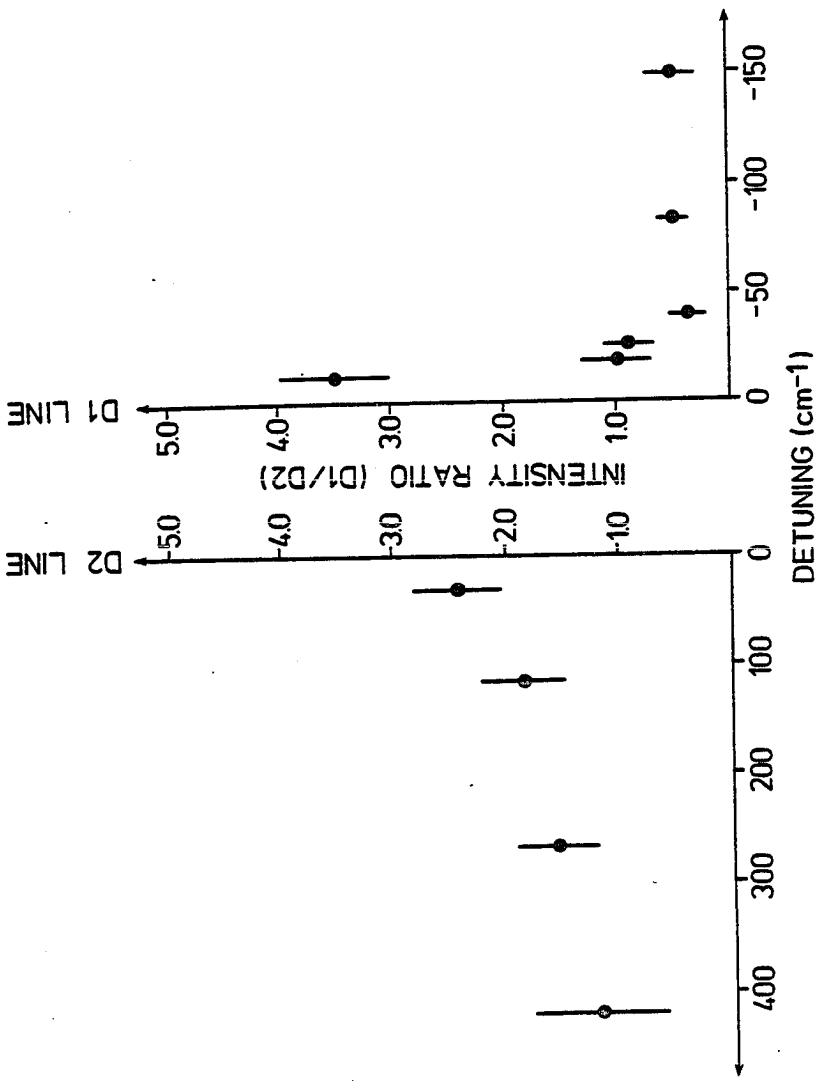

states to the final asymptotic atomic ground state ($^2S_{1/2}$), but all these probabilities are averaged over all the impact parameters (0-R) possible for wing excitation at R.

A. PRELIMINARY HEURISTIC ARGUMENTS

We now present in some detail the heuristic arguments of Havey [39] to explain the asymptotic blue and red wing excitation D1/D2 intensities.

blue wing: D1/D2 $\approx$ 1.6 (2)

red wing: D1/D2 $\approx$ .50 (4)

Consider the adiabatic interatomic potential curves of Figure 1. If the NaAr molecule in $X\,^2\Sigma_{1/2}$ state absorbed a non-resonant photon, and if the subsequent breakup of the Na-Ar molecule into its atomic constituents followed the adiabatic approximation, then, since the $B\,^2\Sigma_{1/2}$ state correlates to the atomic Na $^2P_{3/2}$ ($m_j = \pm 1/2$) state, we would have equal probability amplitutes for populating the $^2P_{3/2}$ ($m_j = \pm 1/2$ $^2P_{3/2}$) states, but zero probability of populating the $^2P_{1/2}$ state. Thus in the adiabatic approximation, I (D1/D2) = 0% for blue wing excitation, and the emission will be 60% for blue wing excitation polarized in the absence of hyperfine effects.

In the sudden approximation one assumes that for internuclear separations where we have avoided adiabatic potential curve crossings ($R_1 < R < R_2$ in Figure 1) the molecular system changes suddenly from Hund case (a) and cylindrical symmetry to atomic Hund case (c) and spherical symmetry (Pritchard [23]). That is, we go from the uncoupled angular momentum Hund case (a) with quantum numbers $J\ M\ p;\ S\ \Lambda\ \Sigma\ >$ to the coupled Hund case (c) representation $J\ M\ p\ ;\ S\ j\ \Omega\ >$ by

$$|J\ M\ p;\ S\ j\ \Omega\ \ (L)\ > = \sum_{\Lambda} C\ (S\ L\ j\ |\ \Omega - \Lambda\ ,\ \Lambda\ ,\ \Omega).\ |J\ M\ p;(L)\ S\ \Omega\ \Lambda\ >$$

or alternatively (using the orthogonality property of the Clebsch-Gordon coefficients),

$$|J\ M\ p;\ (L)\ S\ \Omega\ \Lambda\ > = \sum_{j} C\ (S\ L\ j|\ \Omega - \Lambda\ ,\ \Lambda\ ,\ \Omega).\ |\ J\ M\ p\ ;\ S\ (L)\ j\ \Omega\ > \qquad (2\text{-}1)$$

Thus for the excited $L = 1$ states, using equation (2-1),

$$\begin{aligned} |\ B\ ^2\Sigma_{1/2}> &= \sqrt{1/3}\ \ |1/2\ \ 1/2\ > + \sqrt{2/3}\ \ |\ 3/2\ 1/2\ > \\ |\ A\ ^2\Pi_{1/2}> &= \sqrt{2/3}\ \ |1/2\ \ 1/2\ > - \sqrt{1/3}\ \ |\ 3/2\ \ 1/2\ > \\ |\ A\ ^2\Pi_{3/2}> &= |3/2\ \ 3/2\ > \end{aligned} \qquad (2\text{-}2)$$

B. ARGUMENT BASED ON NO ADDITIONAL MIXINGS OR CURVE CROSSINGS (NaHe MOLECULAR POTENTIALS)

1. BLUE WING EXCITATION

From the Franck-Condon principle, for positive detuning, laser absorption occurs at small internuclear separation, where Hund (a) coupling is valid, so that the Na-rare gas molecule is excited into the $B^2\Sigma_{1/2}$ state. If the Born-Oppenheimer potentials have no additional curve crossings or any further mixing of states we have the following probabilities of finishing in the $|j = 3/2 , \Omega = 1/2 \rangle$ or $|j = 1/2 , \Omega = 1/2 \rangle$ states:

$$\begin{aligned} |\langle B^2\Sigma_{1/2} | 3/2 \quad 1/2 \rangle|^2 &= 2/3 \\ |\langle B^2\Sigma_{1/2} | 1/2 \quad 1/2 \rangle|^2 &= 1/3 \end{aligned} \qquad (2\text{-}3)$$

so that the ratio of the D1 ($^2P_{1/2}$)/D2 ($^2P_{3/2}$) lines is given by

$$\frac{D1}{D2} = \frac{|\langle B^2\Sigma_{1/2} | 1/2 \quad 1/2 \rangle|^2}{|\langle B^2\Sigma_{1/2} | 3/2 \quad 1/2 \rangle|^2} = 1/2 \qquad (2\text{-}4)$$

2. RED WING EXCITATION

In red wing excitation (i.e. negative detuning), we

have equal probability of finishing in the $A^2\pi_{3/2}$ or in the $A^2\pi_{1/2}$ states after photon absorption. The wave function ψ can be constructed using equation (2-2):

$$\psi> = (1/\sqrt{2}\,)\,[\,|A^2\pi_{1/2}> + |A^2\pi_{3/2}>\,] =$$
$$(1/\sqrt{2}\,)\,[\,\sqrt{2/3}\,)\,|1/2\ \ 1/2\ > -$$
$$(\sqrt{1/3}\,)\,|3/2\ \ 1/2\ > + |3/2\ \ 3/2\ >\,] \qquad (2\text{-}5)$$

Thus the probabilities of finishing in the $|j\ \Omega\ >$ - states are

$$|<\ \psi\ |1/2\ 1/2>|^2 = 1/3$$
$$|<\ \psi\ |3/2\ 1/2>|^2 = 1/6 \qquad (2\text{-}6)$$
$$|<\ \psi\ |3/2\ 3/2>|^2 = 1/2$$

If we sum up the probabilities incoherently for finishing in the j= 3/2 state, then the line intensity ratio

$$I(D1)\ /\ I(D2) = (1/3)\ /\ (2/3) = 1/2 \qquad (2\text{-}7)$$

This situtation is expected to occur for the Na-He atom-atom collision since the $B^2\Sigma_{1/2}$ Born-Oppenheimer potential stays above the $A^2\pi_{1/2}$ state as a function of the internuclear separation i.e. there are no curve crossings.

C. ARGUMENT BASED ON STRONG CORRELATIONS BETWEEN $B^2\Sigma_{1/2}$ AND $A^2\pi_{1/2}$ ADIABATIC POTENTIAL CURVES

1. BLUE WING EXCITATION

For blue wing excitation by photon absorption from $X^2\Sigma_{1/2}$ to the $B^2\Sigma_{1/2}$ we find that as the Na-rare gas moleular internuclear separation increase there is a strong crossing with the $A^2\pi_{1/2}$ potential curve, so that, using the sudden approximation (Landau-Zener model [44]), we assume that the probability of switching from $|B^2\Sigma_{1/2}>$ into $|A^2\pi_{1/2}>$ is unity. Thus from equation (2-2)

$$\frac{I\ (D1)}{I\ (D2)} = \frac{\left|\langle A^2\pi_{1/2}\right|\ 1/2\quad 1/2\ \rangle\right|^2}{\left|\langle A^2\pi_{1/2}\right|\ 3/2\quad 1/2\ \rangle\right|^2} = \frac{2/3}{1/3} = 2 \qquad (2\text{-}8)$$

2. RED WING EXCITATION

For red wing excitation, we again can finish in the $|A^2\pi_{3/2}>$ or $|A^2\pi_{1/2}>$ states with equal probability. Thus for small R internuclear separations

$$|\Psi> = (1/2)\ \left[\ |A^2\pi_{1/2}> + |A^2\pi_{3/2}>\ \right]$$

But the strong curve crossing zone between $|A^2\pi_{1/2}>$ and $|B^2\Sigma_{1/2}>$ states implies, on using the sudden approximation that $|A^2\pi_{1/2}>$ (suddenly) $\longrightarrow$ $|B^2\Sigma_{1/2}>$ so that the wave function becomes

$$|\psi> = \sqrt{(1/2)}\ [\ \ |B\,^2\Sigma_{1/2}> + \ \ |A\,^2\Pi_{3/2}>\ ]$$

For large internuclear separations, we now switch from cylindrical to spherical symmetry i.e. from Hund (a) to Hund (c) representation. From from equation (2-2)

$$|\psi> = \sqrt{(1/2)}\ [\sqrt{(1/3)}\ \ |1/2\ 1/2> + \sqrt{(2/3)}\ \ |3/2\ 1/2> + |3/2\ 3/2>].$$

Assuming an incoherent probability sum for the j= 3/2 state, we have for the intensity ratio of the D1 to D2 lines

$$\frac{I\ (D1)}{I\ (D2)} = \frac{|<\psi\ |1/2\ \ 1/2>|^2}{|<\psi\ |3/2\ \ 1/2>|^2 + |<\psi\ 3/2\ \ 3/2>|^2} = 0.2 \qquad (2\text{-}9)$$

D. OTHER EFFECTS

We have ignored rotational mixing and the related phenomena of quantum interference. We thus expect the arguments given in sections (A) and (B) to give upper and lower bounds in the sudden approximation to the relative intensities i.e.

Blue wing excitation $0.5 < I(D1)/I(D2) < 2.0$

Red wing excitation $0.2 < I(D1)/I(D2) < 0.5$ (2-10)

E. CORIOLIS MIXING

We impose the effects of Coriolis mixing heuristically by stipulating the following two assumptions (i) Coriolis mixing two occurs after we switch from Hund case (a) to Hund case (c), and (ii) the Coriolis mixing probability, P_c , to switch from $^2P_{1/2}$ to $^2P_{3/2}$ is equal to the probability of switching from $^2P_{3/2}$ to $^2P_{1/2}$.

1.BLUE WING EXCITATION

From equation (2-8) without Coriolis mixing, the probability of finishing on the D1 line is 2/3 while that of finishing on the D2 line is 1/3. However, assuming the probability effects of Coriolis mixing to be P_c , we have

$$\frac{I(D1)}{I(D2)} = \frac{Pro\ (D1)}{Pro\ (D2)} = \frac{2/3(1-P_c) + (1/3)P_c}{(1/3)(1-P_c) + (2/3)P_c} = \frac{2-P_c}{1+P_c} \qquad (2\text{-}11)$$

We now choose P_c such that equation (2-11) agrees with experiment. i.e.

$$(2-P_c)/(1+P_c) = 1.6 ,$$

$$\text{i.e. } P_c = .154 \qquad (2\text{-}12)$$

2. RED WING EXCITATION

Proceeding similarly to the blue wing calculations, we find from equation (2-9) and probability Coriolis mixing after switching from Hund (a) to Hund (c) and using a value of $P = 0.154$

$$\frac{I(D1)}{I(D2)} = \frac{(1/6)(1-P_c) + (5/6)\ P_c}{(5/6)(1-P_c) + (1/6)\ P_c} = \frac{(1+4P_c)}{(5-4P_c)} = .37 \quad (2\text{-}13)$$

It is also possible for Coriolis mixing to occur before the switching from Hund (a) to Hund (c) occurs. In that case

$$\begin{aligned} |B^2\Sigma_{1/2}> &= [(2/3)\cdot(1-\alpha)]^{1/2} |3/2\ \ 1/2> + \\ &\quad [(1/3)\cdot(1+2\alpha)]^{1/2} |1/2\ \ 1/2> \\ |A^2\pi_{1/2}> &= -[(1/3)\cdot(1+2\alpha)]^{1/2} |3/2\ \ 1/2> + \\ &\quad [(2/3)\cdot(1-\alpha)]^{1/2} |1/2\ \ 1/2> \end{aligned} \quad (2\text{-}14)$$

Hence for blue wing we determine α by forcing the intensity ratio to be equal to the experimental value, i.e.

$$\frac{I(D1)}{I(D2)} = \frac{(2/3)(1-\alpha)}{(1/3)(1+2\alpha)} \Longrightarrow$$

mixing coefficient $\alpha = 0.077$.

Thus for the red wing

$$\frac{I(D1)}{I(D2)} = \frac{(1/2)\,[\,(1/3)\,(1+2\alpha)\,]}{(1/2)\,[1 + (2/3)\,(1-2\alpha)]} = \frac{(1+2\alpha)}{(5-2\alpha)}$$

$$= 0.24 \qquad (2\text{-}15)$$

which is not in as good agreement with experiment as equation (2-13).

Later we shall present the full quantum mechanical treatment of these adiabatic transitions and comment on these heuristic arguments.

CHAPTER 3

HAMILTONIANS AND LASER INTERACTIONS

Our discussion on the relevant Hamiltonians is based on a recent review by Mies [10] and a paper by Julienne [16]. However, in contrast to these calculations, we need to extend their work to systems with spin. We will be concerned with the laser-induced collision between an excited state sodium atom and a rare gas atom in its ground state. The total Hamiltonian for the system is

$$H = H_{AB} + H_{rad} + V_{rad} \tag{3-1}$$

where H_{AB} is the Hamiltonian for the isolated molecule AB, H_{rad} is the free radiation-field Hamiltonian, and V_{rad} is the dipole interaction term which gives the coupling between the radiation field and the molecule.

If we were considering the molecular collision in the absence of a radiation field, the total Hamiltonian for the system, H_{AB}, would be rotationally invariant. Thus the total molecular angular momentum $\vec{J}$ and its space-fixed projection M along an arbitrary axis are

conserved, together with the parity operator with respect to space-fixed spatial inversion of all coordinates. If we introduce a laser field with intensity $\mathcal{I} < \mathcal{I}_o$, where $\mathcal{I}_o$ is some threshold intensity, then the interaction V_{rad} between the molecule AB and the radiation field can be treated as a small perturbation on the zeroth order free molecular Hamiltonian H_{AB}. Thus, by standard pertubation theory we can express the transition cross section for the laser-induced absorption process in terms of the free-free matrix elements of conventional line profile theory. As the laser intensity is increased so that $\mathcal{I} > \mathcal{I}_o$ then we must resort to a non-perturbative formulation which treats both H_{AB} and V_{rad} on the same footing. This introduces the following complications. If we assume a linearly polarized radiation field (e.g. along the space-fixed Z-axis) and the absorption of one photon, then the final molecular angular momentum $\vec{J}_f$ can take on any value in the set

$$J_f \in [\,|J-1|\,,\ J,\ J+1\,] \qquad (3\text{-}2)$$

in which non-distinct elements of this set are to be automatically eliminated. Because the radiation field is linearly polarized, $M_f = M$. The coupling of JMp-state to J_f Mp-state , $J_f \in [\,|J-1|\,, J, J+1\,]$, greatly complicates the computation effort in finding the transition cross sections of interest.

A. FIELD-FREE HAMILTONIAN H

The field-free molecular Hamiltonian

$$H_{AB} = H_A(\vec{R}_A, \vec{r}_A) + H(\vec{R}_B, \vec{r}_B) + V_{AB}(\vec{R}_A - \vec{R}_B, \vec{r}_A, \vec{r}_B) \qquad (3\text{-}3)$$

where H_A and H_B are the isolated atomic Hamiltonians for atoms A and B respectively, and V_{AB} is the total (field-free) interaction between these atoms. $\vec{R}_A$ is the center-of-mass position of atom A, while $\vec{r}_A$ represents collectively all the spatial positions of the atomic electrons of A. Now

$$H_A(\vec{R}_A, \vec{r}_A) = -\frac{\hbar^2}{2\mu_A}\nabla^2_{R_A} + H_A^{el}(\vec{r}_A) \qquad (3\text{-}4)$$

where $-\hbar^2 \nabla^2_{R_A}/2\mu_A$ is the center-of-mass kinetic energy operator for atom A (with reduced mass μ_A) and H_A^{el} is the translationally invariant electronic Hamiltonian. Since H_A, by itself, is rotationally invariant the total electronic angular momentum $\vec{j}_A$ and its space-fixed projection $\hat{Z}\cdot\vec{j}_A$ commute with H_A so that, on representing the eigenstates of H_A^{el} by $|\alpha\rangle$,

$$H_A^{el}|\alpha\rangle = E_\alpha|\alpha\rangle, \qquad (3\text{-}5)$$

we have

$$\vec{J}_A^2 |\alpha\rangle = j_A(j_A+1) |\alpha\rangle$$
$$j_{z_A} |\alpha\rangle = m_\alpha |\alpha\rangle . \qquad (3\text{-}6)$$

The isolated atomic energy E_α is $(2j_\alpha + 1)$-fold degenerate. Since atom B will always represent the rare gas atom which remains in its initial ground state after the molecular collision, we do not need to explicitly discuss the analogous atom B Hamiltonian H_B. Introducing

$$\vec{R} = \vec{R}_A - \vec{R}_B \qquad (3\text{-}7)$$

as the interatomic coordinate we immediately note that as $R \to \infty$, the interatomic interaction $V_{AB} \to 0$. Thus, asymptotically, the molecular Hamiltonian H_{AB} becomes separable.

It is convenient to introduce the electronic molecular Hamiltonian H_{AB}^{el} by

$$H_{AB}^{el}(\vec{R},\vec{r}) = H_A^{el}(\vec{r}_A) + H_B^{el}(\vec{r}_B) + V_{AB}(\vec{R},\vec{r}) \qquad (3\text{-}8)$$

where $\vec{r} = (\vec{r}_A, \vec{r}_B)$ now stands for all the spatial electronic coodinates of the quasimolecule AB. Thus the total molecular field-free Hamiltonian H_{AB}

$$H_{AB} = -\frac{\hbar^2}{2(\mu_A+\mu_B)}\nabla_{R_{CM}}^2 - \frac{\hbar^2}{2\mu_{AB}}\nabla_R^2 + H_{AB}^{el}(r,R) \qquad (3\text{-}9)$$

where $\vec{R}_{CM} = (\mu_A\vec{R}_A + \mu_B\vec{R}_B)/(\mu_A+\mu_B)$ is the position of the

center-of-mass of the quasimolecule which has reduced $\mu_{AB}=\mu_A\mu_B/(\mu_A+\mu_B)$. The first two operators on the right hand side of equation (3-9) are just the kinetic energy operators with continuum eigenvalues which are uniquely determined from the given initial asymptotic conditions. It is convenient to work in the barycentric coordinate system in which the quasimolecule center-of-mass is fixed so that the corresponding center-of-mass kinetic energy eigenvalue is zero. Thus, the center-of-mass kinetic energy operator $-\hbar^2\nabla^2_{R_{CM}}/(2\mu_A+2\mu_B)$ can be dropped from equation (3-9). The total initial energy E, assuming initial atomic state $|\alpha\rangle$ and $|\beta\rangle$ for atoms A and B with corresponding energies E_α and E_β, is given by

$$E = E_\alpha + E_\beta + \epsilon \qquad (3\text{-}10)$$

where ϵ is the relative kinetic energy eigenvalue corresponding to the kinetic energy operator $-\hbar^2\nabla^2_R/2\mu_{AB}$ in equation (3-9).

We shall return later to discuss the molecular field-free Hamiltonian H_{AB} and its matrix elements in Hund case (a) representation.

B. FREE-RADIATION FIELD HAMILTONIAN H_{rad}

We neglect vacuum field contributions, and represent

the Hamltonian for the free-radiation field by creation a_λ^+ and annihilation a_λ operators for mode λ with photon energy $h\nu_\lambda$ which satisfy the commutation relation

$$[a_\lambda, a_{\lambda'}^+] = \delta_{\lambda,\lambda'}, \tag{3-11}$$

i.e.,

$$H_{rad} = \sum_\lambda h\nu_\lambda \cdot a_\lambda^+ a_\lambda \tag{3-12}$$

The scattering experiment is performed by focusing a ring laser into a localized region within a spherical volume $\mathcal{V}$ containing a mixture of atoms A and B. The vector potential operator $\vec{A}(\vec{r})$ at any point $\vec{r}$ in $\mathcal{V}$ can be represented by an orthogonal basis set of functions $\vec{U}_\lambda(\vec{r})$ which characterize the mode λ

$$\vec{A}(\vec{r}) = \sum_\lambda \sqrt{\frac{2\pi\hbar^2 c^2}{h\nu_\lambda}} \cdot [\vec{U}_\lambda(\vec{r}) a_\lambda + \vec{U}_\lambda^*(\vec{r}) a_\lambda^+] \tag{3-13}$$

with $\nabla \cdot \vec{A} = 0$.

A simplifying assumption commonly made for collisionally-induced transitions in the presence of strong laser fields is that the laser can be idealized as being monochromatic, with frequency ν_0 and polarization vector $\hat{e}_o$, which for a linearly polarized laser can be taken to be in

the $\hat{Z}$-direction. It is also usually assumed that only one state of the laser is populated, with eigenstate

$$|n_o\rangle = \frac{1}{[n_o!]^{1/2}} [a_o^+]^{n_o} |\text{vac.}\rangle \qquad (3\text{-}14)$$

where $a_o^+ a_o |n_o\rangle = n_o |n_o\rangle$. The total radiation energy = $n\,h\nu$ and photon density $\rho_o = n_o/\mathcal{V}$. It should be noted that knowing the state $|n_o\rangle$ exactly would violate the uncertainty principle [25]. Nevertheless, the approximation is very commonly made (and here also) although there are still many unresolved questions concerning it [10].

For laser-induced processes in a ring laser, an appropriate basis for $\vec{U}_o(\vec{r})$ is the traveling wave representation

$$\vec{U}_o(\vec{r}) = \exp(i\vec{k}_o \cdot \vec{r})\ \hat{e}_o / \mathcal{V}^{1/2} \qquad (3\text{-}15)$$

with the Coulomb guage $\nabla \cdot \vec{A} = 0$ requiring $\hat{e}_o \cdot \vec{k} = 0$. This is just the standard transversality condition for electromagnetic fields. In the Schrodinger representation, the electric field operator is given by

$$\vec{E}(\vec{r}) = i\sqrt{\frac{2\pi h\nu_o}{\mathcal{V}}}\,\hat{e}_o\,[\exp(i\vec{k}_o \cdot \vec{r})\ a_o - \exp(-i\vec{k}_o \cdot \vec{r})\ a_o^+] \qquad (3\text{-}16)$$

while the magnetic field operator is given by

$$\vec{B}(\vec{r}) = i\sqrt{\frac{2\pi h\nu_o}{\mathcal{V}}}\,(\hat{k}_o \times \hat{e}_o)[\exp(i\vec{k}_o \cdot \vec{r})\ a_o - \exp(-i\vec{k}_o \cdot \vec{r})\ a_o^+]. \qquad (3\text{-}17)$$

C. RADIATIVE INTERACTION HAMILTONIAN V_{rad}

The nonrelativistic Hamiltonian for the interaction of the radiation field with a single electron [26] (since in the AB quasimolecule there is only one active electron) is given by

$$V_{rad} = \frac{e}{2m_e c}\left\{[\vec{p}\cdot\vec{A}(\vec{r}_e) + \vec{A}(\vec{r}_e)\cdot\vec{p}] + \frac{e}{c}\vec{A}^2(\vec{r}_e) + \hbar\vec{\sigma}\cdot\nabla\times\vec{A}(\vec{r}_e)\right\} \quad (3\text{-}18)$$

where $\vec{r}_e$ is the position of the electron, $\vec{p}=-i\hbar\nabla_e$ is the conjugate momentum, m_e its mass and $\vec{\sigma}$ is the Pauli spin operator. For the laser intensities of interest here, we can neglect both the diamagnetic interaction $\vec{A}^2$ as well as the interaction of the spin magnetic moment with the radiation magnetic field $\vec{\sigma}\cdot\vec{B}$, with $\vec{B}=\nabla\times\vec{A}$. Since $\nabla\cdot\vec{A}=0$ and $\vec{p}=-i\hbar\nabla_e$, the operator $\vec{p}\cdot\vec{A}=\vec{A}\cdot\vec{p}$. Thus V_{rad} can be approximated by

$$V_{rad} = \frac{e}{m_e c}\vec{p}\cdot\vec{A}(r_e) \quad . \quad (3\text{-}19)$$

In passing we note that the $\vec{A}^2$ diamagnetic effect in equation (3-18) does not contribute to one-photon processes since the bilinear combinations of the photon annihilation a_o and creation a_o^+ operators

$$\langle n_o + 1 | a_o^+ | n_o \rangle = \sqrt{n_o + 1} \quad (3\text{-}20)$$
$$\langle n_o - 1 | a_o | n_o \rangle = \sqrt{n_o}$$

results in the change of photon population of either 0 or 2. It should also be noted that V_{rad}, equation (3-19), is referred to laboratory-fixed coordinates.

The dipole approximation is valid for slowly varying potentials so that $\vec{k}_o \cdot (\vec{r}-\vec{R}_{cM}) \ll 1$, i.e.

$$\vec{U}_o(\vec{r}) = \frac{e^{i\vec{k}_o\cdot\vec{r}}}{\vartheta^{1/2}}\hat{e}_o = \exp[i\vec{k}_o\cdot\vec{R}_{cM}]\,\hat{e}_o/\vartheta^{1/2} \equiv \vec{U}_o(\vec{R}_{cM}) \qquad (3\text{-}21)$$

In the barycentric coordinate system $\vec{k}_o\cdot\vec{R}_{cM}$ =const. One set of non-zero matrix elements is given by

$$\langle n_o|\, V_{rad}\,|n_o+1\rangle = \langle n_o|\frac{e}{m_e c}\vec{p}\cdot\{\vec{U}(\vec{R}_{cM})a_o + \vec{U}_o^*(\vec{R}_{cM})a_o^+\}|\, n_o+1\rangle \cdot \sqrt{\frac{2\pi\hbar^2c^2}{\hbar\omega_o}}$$

$$= \langle n_o|\, a_o\,|\, n_o+1\rangle \frac{e}{m_e\omega_o}\vec{p}\cdot\hat{e}_o \exp(i\vec{k}_o\cdot\vec{R}_{cM}) \sqrt{\frac{2\pi\hbar^2\omega_o^2}{\hbar\omega_o\cdot\vartheta}}$$

$$= \vec{\mu}^o\cdot\hat{e}_o\ \mathcal{E}_o\ \exp(i\vec{k}_o\cdot\vec{R}_{cM}) \qquad (3\text{-}22)$$

where the operator $\vec{\mu}^o$ has the dimensions of an electric dipole -- i.e. charge*distance = $\sqrt{\text{energy*volume}}$

$$\vec{\mu}^o = \frac{e}{m_e\omega_o}\vec{p} \qquad (3\text{-}23)$$

and the scalar quantity $\mathcal{E}_o$ has the dimensions of an electric field-- i.e. the dimensions of $\sqrt{\text{energy/volume}}$, c.f. equation (3-16)

$$\mathcal{E}_o = \sqrt{\frac{2\pi\hbar\omega_o\,(n_o+1)}{\mathcal{V}}} \tag{3-24}$$

Similarly, the other set of non-zero matrix elements is given by

$$\langle n_o + 1 \left| V_{rad} \right| n_o \rangle = \vec{\mu}^o \cdot \hat{e}_o^* \, \mathcal{E}_o \;\; \exp(-i\vec{k}_o \cdot \vec{R}_{cm}) \tag{3-25}$$

Thus the complete set of matrix elements for V_{rad}, including not only the photon field contribution $|n_o\rangle$ but also the direct product with the particular molecular wave function basis we shall work in (and here denoted collectively by $R,\gamma\rangle$ where R is the interatomic distance), is given by

$$\langle R\gamma, n_o \left| V_{rad} \right| R\,\gamma', n_o' \rangle = \delta_{n_o - n_o' \pm 1} \cdot e^{\pm i\vec{k}_o \cdot \vec{R}_{cm}} \langle R\gamma \left| \vec{\mu}^o \right| R\,\gamma' \rangle \cdot \hat{e}_o \, \mathcal{E}_o \tag{3-26}$$

Since we are working in the barycentric coordinate system, the center of mass momentum $\hbar\vec{k}_{cm} = 0$. Moreover the sum of all the momentum operators (in the general case of many active electrons) in equation (3-23) is just the total molecular momentum $-i\hbar\nabla_{R_{cm}}$ and the molecular basis is translationally invariant so that $\nabla_{R_{cm}} |R\gamma\rangle = 0$. This justifies the removal of $\exp[\pm i\vec{k}_o \cdot \vec{R}_{cm}]$ from the inner product $\langle R\gamma \left| \vec{\mu}^o \right| R\,\gamma' \rangle$ in equation (3-26). We now introduce the electric dipole operator $\vec{\mu}(\vec{r},\vec{R})$

$$\vec{\mu}(\vec{r},\vec{R}) = -\sum_{A,B} e\vec{r} + e\,\frac{m_B Z_A - m_A Z_B}{m_A + m_B}\,\vec{R} \qquad (3\text{-}27)$$

where $(\vec{r}_A - \vec{R}_{CM}, \vec{r}_B - \vec{R}_{CM}) \equiv \vec{r}$. Thus $\vec{\mu}^o$ can be expressed in terms of the commutator of the total molecular Hamiltonian H_{AB}, equation (3-9), with the electric dipole operator $\vec{\mu}$, equation (3-27):

$$\vec{\mu}^o(\vec{r},\vec{R}) = \sum_j \frac{eZ_j}{m_j\omega_o}\vec{p}_j = \frac{i}{\hbar\omega_o}[H_{AB}(\vec{r},\vec{R}), \vec{\mu}(\vec{r},\vec{R})] \qquad (3\text{-}28)$$

where $\sum_j$ runs over each (active) particle in the quasimolecule AB. Since we can evaluate $H_{AB}|R\gamma\rangle$, we have thus reduced the non-zero matrix elements of $\langle R\gamma, n_o | V_{rad} | R\gamma', n_o'\rangle$ into the form

$$\langle R\gamma, n_o | V_{rad} | R\gamma', n_o'\rangle \approx \langle R\gamma | \vec{\mu} | R\gamma'\rangle \cdot \hat{e}_o \ . \qquad (3\text{-}29)$$

In using the time independent Schrodinger theory, i.e., the stationary state representation for the total Hamiltonian $H = H_{AB} + H_{rad} + V_{rad}$, we are implicitly assuming that both the initial and final asymptotic atomic states do not interact with the externally applied photon frequency ν_o and that these asymptotic atomic states are sufficiently long-lived so that we can disregard the effects of spontaneous decay from the excited final states.

D. CONSERVATION LAWS IN MOLECULAR COLLISIONS IN A LASER FIELD

1. Conservation of Energy and Linear Momentum

In considering the conservation of energy in the presence of a laser field we must be more careful than when we consider energy conservation for molecular collisions in the absence of a radiation field. In particular, in the space-fixed frame, the molecular channel states $|R\gamma\rangle$ should be multiplied by the center of mass (volume normalized) eigenstate $\exp[i\vec{k}_{CM}\cdot\vec{R}_{CM}]/\mathcal{V}^{1/2}$ so that the total initial energy (in the space-fixed frame)

$$E=E_A+E_B+n_o h\nu_o + \epsilon + \hbar^2 k_{CM}^2/2(\mu_A+\mu_B) \qquad (3\text{-}30)$$

where ϵ is the relative kinetic energy of atoms A and B, and the last term in equation (3-30) arises from the center of mass motion. The final energy (using the fact that the rare gas atom B remains in its ground state) on absorption of one photon is given by

$$E'=E_{A'}+E_B+\epsilon'+(n_o-1)h\nu_o+\hbar^2 k_{CM}'^2/2(\mu_A+\mu_B) \qquad (3\text{-}31)$$

where ϵ' is the final relative kinetic energy and $\hbar\vec{k}'_{CM}$ is the final center of mass momentum. These last two terms in equations (3-30) and (3-31) can only be of some importance if we are considering laser induced collisions since for

pure atomic scattering n_o is effectively zero and so from momentum conservation $\vec{k}'_{cm} = \vec{k}_{cm}$. Thus for pure atomic scattering we can immediately transform to the barycentric coordinate system in which $\vec{k}_{cm} = 0$. However, for molecular collisions in the presence of a laser field (with wavenumber $\vec{k}_o$), we immediately find from conservation of linear momentum that

$$\vec{k}'_{cm} = \vec{k}_{cm} - \vec{k}_o \quad . \tag{3-32}$$

Thus, from equations (3-30) and (3-31)

$$\epsilon' = \epsilon + (E_A - E'_{A'}) + h\nu_o + \frac{\hbar^2 k_{cm}^2}{2(\mu_A + \mu_B)} \left[1 - \frac{k'^2_{cm}}{k^2_{cm}} \right]$$

$$= \epsilon + (E_A - E'_{A'}) + h\nu_o + \frac{\hbar^2 k_{cm}^2}{2(\mu_A + \mu_B)} \left[\frac{2k_o}{k_{cm}} \hat{k}_o \cdot \hat{k}_{cm} - \left(\frac{k_o}{k_{cm}} \right)^2 \right] \tag{3-33}$$

The last term in equation (3-33) arises from the Doppler shift associated with the non-zero center-of-mass motion in the space-fixed frame. Typically $k_o / k_{cm} << 1$, so that

$$\epsilon' = \epsilon + (E_A - E'_{A'}) + h\nu_o \tag{3-34}$$

which is just the barycentric result ($\vec{k}_{cm} = 0$). Note that E = E' , since we are using a time-independent Schrodinger representation. Note also that we are making a tacit assumption that the effect of the molecular collision on the

photon field itself can be ignored--i.e., the photon field is being treated as an infinite reservoir of linear momentum, $n_o \gg 1$.

From equation (3-31), upon dropping the last term, we can introduce the total molecular energy $E_{AB}(n_o')$ available to the outgoing atoms

$$E_{AB}(n_o') = E_A' + E_B + \epsilon' = E - (n_o - 1)h\nu_o \qquad (3\text{-}35)$$

If $\epsilon' > 0$ the asymptotic channel, as $R \to \infty$, is susceptible to direct experimental observation and the channel is said to be open. If $\epsilon' < 0$, the channel cannot be directly observed experimentally, but it can give rise to resonant structure in the scattering amplitudes of the open channels. For $\epsilon' < 0$, the channels are said to be closed .

2. Parity and Angular Momentum Conservation

To discuss parity and the conservation of angular momentum, it is convenient to outline here the derivation of the close-coupled theory in the presence of a radiation field.

Let $\Phi_{\gamma n_o}(E)$ be the total wavefunction for the whole system, i.e. the quasimolecule AB as well as the radiation field. Thus, in time-independent theory

$$(H - E)\,\Phi_{\gamma n_o}(E) = 0 \qquad (3\text{-}36)$$

where the total Hamiltonian $H=H_{AB}+H_{rad}+V_{rad}$, equation (3-1). We now choose some appropriate basis in which to expand $\Phi_{\gamma n_o}$. Denoting this basis by $|R\gamma'', n_o''>$ we have

$$\Phi_{\gamma n_o}(E) = \sum_{\gamma'', n_o''} |R\gamma'', n_o''> \frac{F^{\gamma n_o}_{\gamma'' n_o''}(E,R)}{R} \qquad (3\text{-}37)$$

where the matrix F(E,R)/R are the coupling coefficients to be determined. On substituting equation (3-37) into (3-36) and taking the inner product with $<R\gamma', n_o'|$,

$$\sum_{\gamma'', n_o''} <R\gamma', n_o'| H-E | R\gamma'', n_o''> \frac{F^{\gamma n_o}_{\gamma'' n_o''}(E,R)}{R} = 0 \qquad (3\text{-}38)$$

Now

$$<R\gamma', n_o'| H_{rad} | R\gamma'', n_o''> = n_o' h\nu_o \cdot \delta_{n_o' n_o''} \cdot \delta_{\gamma',\gamma''} \qquad (3\text{-}39)$$

while the molecular Hamiltonian

$$\begin{aligned} H_{AB} &= -\frac{\hbar^2 \nabla_R^2}{2\mu_{AB}} + H^{el}_{AB} \\ &= -\frac{\hbar^2}{2\mu_{AB}} \cdot \frac{1}{R} \cdot \frac{\partial^2}{\partial R^2} + \left(\frac{\hbar^2}{2\mu_{AB}} \frac{\vec{L}_R^2}{R^2} + H^{el}_{AB} \right) \end{aligned} \qquad (3\text{-}40)$$

(where $\vec{L}_R = -i\vec{R}x\nabla_R$ is the angular momentum operator conjugate to the interatomic coordinate $\vec{R}$), has matrix elements given by

$$R<R\gamma' n_o'| H_{AB} | R\gamma'' n_o''> \frac{F^{\gamma n_o}_{\gamma'' n_o''}}{R}$$

$$= \left[\left(-\frac{\hbar^2}{2\mu_{AB}} \cdot \frac{\partial^2}{\partial R^2} \right) \delta_{\gamma'\gamma''} + W_{\gamma'\gamma''}(R) \right] F^{\gamma n_o}_{\gamma'' n_o''} \cdot \delta_{n_o' n_o''} \qquad (3\text{-}41)$$

The $\underline{\underline{W}}(R)$ matrix is associated with the operator $\hbar^2 \vec{L}_R^2 / 2\mu_{AB} R^2 + H^{el}_{AB}$ in equation (3-40). Since the interatomic interaction V_{AB} between atoms A and B decays to zero as $R \to \infty$, the $\underline{\underline{W}}$ matrix becomes diagonal, to leading order, i.e.

$$W_{\gamma'\gamma''}(R) \underset{R\to\infty}{\sim} \left[E'_A + E_B + \frac{\hbar^2 \ell'(\ell'+1)}{2\mu_{AB} R^2} \right] \qquad (3\text{-}42)$$

with $\ell'(\ell'+1)$ being the angular momentum eigenvalue for the spherical harmonic eigenfunctions of $\vec{L}_R^2$. Thus,

$$R\langle R\gamma', n_o' \left| H_{AB} + H_{rad} - E \right| R\gamma'', n_o'' \rangle \frac{F^{\gamma n_o}_{\gamma'' n_o''}(E,R)}{R}$$

$$= \left[\left\{ -\frac{\hbar^2}{2\mu_{AB}} \frac{\partial^2}{\partial R^2} - E_{AB}(n_o') \right\} \delta_{\gamma'\gamma''} + W_{\gamma'\gamma''} \right] F^{\gamma n_o}_{\gamma'' n_o''} \cdot \delta_{n_o', n_o''} \qquad (3\text{-}43)$$

with $E_{AB}(n_o') = E - n_o' h\nu_o$, equation (3-35). It should be also noted than the $\underline{\underline{W}}$ matrix will, in general, contain the radial derivatives $\partial/\partial R$ and $\partial^2/\partial R^2$. These radial operators will be present in $\underline{\underline{W}}$ because of the radial variations of the molecular electronic states.

Since the molecular Hamiltonian H_{AB} is rotationally-invariant in the space-fixed frame, the total molecular angular momentum quantum numbers J and M, its space-fixed projection, are good quantum numbers, i.e. they

are conserved by H_{AB}. In particular, from equation (3-41), the molecular interaction matrix $\underline{\underline{W}}$ does not only not mix different J's and M's, but is itself independent of M.

Thus, from equations (3-38), (3-1), (3-26), (3-29), and (3-43), with $\gamma = (J,M)$

$$0 = R \sum_{\gamma'',n_o''} \langle R\gamma' n_o' \left| H-E \right| R\gamma'' n_o'' \rangle \frac{F^{\gamma n_o}_{\gamma'' n_o''}}{R} =$$

$$\sum_{\gamma'',n_o''} \left\{ -\frac{\hbar^2}{2\mu_{AB}} \cdot \frac{\partial^2}{\partial R^2} - E_{AB}(n_o') \right\} \cdot \delta_{\gamma'\gamma''} \cdot \delta_{n_o' n_o''} \cdot F^{\gamma n_o}_{\gamma'' n_o''} + \sum_{\gamma'',n_o''} W^{J'}_{\gamma'\gamma''}(R) \cdot \delta_{n_o' n_o''} \cdot F^{\gamma n_o}_{\gamma'' n_o''}$$

$$+ \sum_{\gamma'',n_o''} \frac{\hbar}{2} \delta_{n_o'', n_o' \pm 1} \cdot \mathcal{R}^{\pm}_{\gamma'\gamma''}(R) \cdot F^{\gamma n_o}_{\gamma'' n_o''}$$

where we define the so called Rabi frequency matrix $\mathcal{R}(R)$ [with units of sec^{-1}] by

$$\langle R\gamma' n_o' \left| V_{rad} \right| R\gamma'' n_o'' \rangle = \delta_{n_o'', n_o' \pm 1} \cdot \frac{\hbar}{2} \cdot \mathcal{R}^{\pm}_{\gamma'\gamma''}(R) \qquad (3\text{-}44)$$

Thus the close-coupled equations are

$$\left[-\frac{\hbar^2}{2\mu_{AB}} \frac{\partial^2}{\partial R^2} - E_{AB}(n_o') \right] F^{\gamma n_o}_{\gamma' n_o'} + \sum_{\gamma''} W^{J'}_{\gamma'\gamma''}(R) F^{\gamma n_o}_{\gamma'' n_o'} =$$

$$-\frac{\hbar}{2} \sum_{\gamma''} \sum_{n_o'' = n_o' \pm 1} \mathcal{R}^{\pm}_{\gamma'\gamma''}(R) F^{\gamma n_o}_{\gamma'' n_o''} \qquad (3\text{-}45)$$

with $\gamma = \gamma(J,M)$, $\gamma' = \gamma'(J',M')$, $\gamma'' = \gamma''(J'',M'')$ besides their dependence on other quantum numbers which are connected to the specific angular momentum representation chosen. This will be discussed in considerable detail in the following

chapters. However it should be noted that the $\underline{\underline{W}}$-matrix only couples states which have the same J, i.e. only $J''=J'=J$ states are coupled. The right-hand side of equation (3-45) deals with the radiative coupling of the laser field with the molecule AB. Since the photon carries with it one unit of angular momentum, we find from angular momentum conservation that the radiation coupling matrix couples states with $J''=J', J'\pm 1$. Since we will be interested only in linearly polarized light $M''=M'$.

Having now outlined the derivation of the close-coupled equations (3-45), we now return to consider the parity of the coupled states. Since H_{AB} is invariant under inversion in the space-fixed center of mass system,

$$\mathcal{I} H_{AB}(\vec{r},\vec{R}) = H_{AB}(-\vec{r},-\vec{R}) ,$$

the total angular momentum molecular channel states $|R\gamma\rangle = |R,\gamma(JMP)\rangle$ have a well-defined parity eigenvalue P, with $P=\pm 1$; i.e.

$$\mathcal{I}|R,\gamma(P)\rangle = P|R,\gamma(P)\rangle \qquad (3\text{-}46)$$

$P=\pm 1$, since $\mathcal{I}^2|R,\gamma(P)\rangle = |R,\gamma(P)\rangle$. Consider the matrix element $\langle R\gamma' n_\sigma' \,|\, H|R\gamma'' n_\sigma''\rangle$ in equation (3-38). The two types of terms of interest are (i) molecular interaction matrix elements $W^{J'}_{\gamma'\gamma''}(R)$, and (ii) the Rabi frequency matrix elements $\mathcal{R}_{\gamma'\gamma''}(R)$. Now for $W^{J'}_{\gamma'\gamma''}$ we have $n_\sigma' = n_\sigma''$ so that the

molecular interaction matrix preserves parity: $P'=P''$. However, the Rabi matrix involves the radiation coupling operator V_{rad}, equations (3-26) and (3-27), which have non-zero matrix elements only if $n_o'' = n_o' \pm 1$. From equation (3-27), we see that the electric dipole operator $\sim \vec{r}$, which has negative parity eigenvalue under inversion. Thus in the dipole approximation, for radiative coupling, we require $-P' = P''$. Combining these two results (i) and (ii) together, we have

$$\langle R, \gamma'(P'), n_o' | H | R, \gamma''(P''), n_o'' \rangle$$

$$= [P' x P(-1)^{n_o' + n_o''} + 1] \langle R \gamma' n_o' | H | R \gamma'' n_o'' \rangle \qquad (3\text{-}47)$$

i.e. for $n_o' = n_o''$, then $P' x P'' = +1$; while for $n_o'' = n_o' \pm 1$, nonzero matrix elements have $P' x P'' = -1$.

The molecular channel states $|R\gamma\rangle = |RJMj\ell\rangle$, where for rare gas B atoms $j = j_A$, and ℓ is the eigenvalue associated with the interatomic angular momentum operator $\vec{L}_R^2$. The parity of each channel is also determined by the j and ℓ values: $P = P(j,\ell)$. Now for the radiation-free molecular interaction matrix $\underline{\underline{W}}^J(R)$, not only are J and M conserved, but $\underline{\underline{W}}^J$ is independent of the space-fixed projection M.

On the other hand, using the Wigner-Eckart Theorem we have for the transition operator in the Rabi frequency matrix (see also Mies [10] for more algebraic details)

$$\langle RJMj\ell|\vec{\mu}^{o}\cdot\hat{e}_{o}|RJ'M'j'\ell'\rangle = C(J'1J|M'OM)\,\langle RJj\ell\|\mu^{o}\|RJ'j'\ell'\rangle \quad (3\text{-}48)$$

for linearly polarized light. Thus the Rabi frequency matrix $\mathcal{R}$ has explicit dependence on M in the Clebsch-Gordon coefficient in equation (3-48).

CHAPTER 4

ELECTRONIC-ROTATIONAL HAMILTONIAN MATRIX ELEMENTS

We now derive the Hund (a) matrix elements for the molecular Hamiltonian H_{AB}

$$H_{AB} = H_e(\vec{r},R) + B(R)\vec{L}_R^2 + H_{so} - \frac{\hbar^2}{2\mu R^2}\frac{\partial}{\partial R}\left(R^2\frac{\partial}{\partial R}\right) \qquad (4-1)$$

where $H_e(\vec{r},R)$ is the electronic Hamiltonian whose eigenvalues give the familiar Born-Oppenheimer potential energy curves

$$H_e(\vec{r},R).\psi_\Lambda(\vec{r},R) = W_\Lambda(R).\psi_\Lambda(\vec{r},R) \qquad (4-2)$$

with Λ being the (positive) projection of the total orbital angular momentum $\vec{L}$ onto the (moving) internuclear axis. The internuclear separation R is a parameter in equation (4-2). $\vec{L}_R = iR\times\nabla_R$ is the nuclear angular momentum operator and is directed perpendicular to the internuclear axis, i.e. $\vec{R}\cdot\vec{L}_R = 0$. $\vec{L}_R$ is related to the total angular momentum $\vec{J}$ of the molecular system by

$$\vec{L}_R = \vec{J} - \vec{L} - \vec{S} \tag{4-3}$$

where $\vec{S}$ is the total spin angular momentum. $B(R) = \hbar^2/2\mu R^2$, where μ is the reduced mass. $H_{rot} = B(R)\vec{L}_R^2$ is the rotational Hamiltonian and in the moving molecular frame is given by

$$\begin{aligned} H_{rot} &= B(R)\,\vec{L}_R^2 = (\hbar^2/2\mu R^2)\,[\vec{J} - \vec{L} - \vec{S}]^2 \\ &= B(R)\,[\vec{J}^2 - J_z^2 + \vec{L}^2 - L_z^2 + \vec{S}^2 - S_z^2 + (L_+S_- + L_-S_+) \\ &\quad -(J_+L_- + J_-L_+) - (J_+S_- + J_-S_+) \end{aligned} \tag{4-4}$$

while the spin-orbit Hamiltonian

$$H_{so} = A(R)\vec{L}\cdot\vec{S} = A(R)[L_zS_z + \tfrac{1}{2}(L_+S_- + L_-S_+)] \tag{4-5}$$

The coefficient A(R) in H_{so}, as well as the Born-Oppenheimer potentials $W_\Lambda(R)$ may be determined by experiment or by 'ab initio' or other types of calculations (see e.g.Saxon, Olson, and Liu[27]; Duren et. al. [28]; Loskowski et. al. [29]). In writing down the molecular Hamiltonian H_{AB}, equation (4-1), we have neglected any relativistic corrections to the kinetic energy as well as the interaction of the spin magnetic moment with the external (laser) magnetic field.

The matrix elements of H_{AB} will be evaluated in the Hund (a) representation $|\Lambda S\Sigma ;\Omega JM\rangle$ where Λ, Σ and Ω are the projections of $\vec{L}$, $\vec{S}$, and $\vec{J}$ onto the moving internuclear axis. M is the projection of $\vec{J}$ onto the space-fixed axis. Since the parity operator commutes with the molecular Hamiltonian H_{AB}, it is convenient to introduce the Hund (a) wavefunctions with definite parity. From Appendix 3, we see that under the inversion operator

$$i_{sp}\,|\Lambda S\Sigma;\Omega JM,P_{\pm}\rangle = i_{sp}\,\frac{1}{\sqrt{2}}\,[\,|\Lambda\, S\Sigma;\Omega JM\rangle \pm |-\Lambda,S,-\Sigma;-\Omega JM\rangle]$$

$$= \pm(-1)^{J-1/2}\;|\Lambda S\Sigma;\; JM,p_{\pm}\rangle \qquad (4\text{-}6)$$

i.e. the inversion operator i_{sp} has eigenvalues $p_{+}=(-1)^{J-1/2}$ and $p_{-}=(-1)^{J+1/2}$, since we work with sodium and rare gas atoms which yields $S=\frac{1}{2}$.

Using the convention that Λ, Σ, and Ω are non-negative we have the following Hund (a) representations for the ground and excited states:

$$|X\Sigma^{+}_{1/2},p_{\pm}\rangle = \frac{1}{\sqrt{2}}\,[\,|0\;\tfrac{1}{2}\;\tfrac{1}{2}\;;\tfrac{1}{2}\;J_i\;M_i\rangle \pm |0,\tfrac{1}{2},-\tfrac{1}{2};-\tfrac{1}{2}\;J_i\;M_i\rangle] \qquad (4\text{-}7)$$

$$|B\Sigma^{+}_{1/2},p_{\pm}\rangle = \frac{1}{\sqrt{2}}\,[\,|\;0\tfrac{1}{2}\;\tfrac{1}{2}\;;\tfrac{1}{2}\;J_f\;M_f\rangle \pm |\;0,\tfrac{1}{2},-\tfrac{1}{2};-\tfrac{1}{2}\;J_f\;M_f\rangle]$$

$$|A\Pi_{1/2},p_{\pm}\rangle = \frac{1}{\sqrt{2}}\,[\,|\;1,\tfrac{1}{2},-\tfrac{1}{2};\tfrac{1}{2}\;J_f\;M_f\rangle \pm |\;-1,\tfrac{1}{2},\tfrac{1}{2};-\tfrac{1}{2}\;J_f\;M_f\rangle] \qquad (4\text{-}8)$$

$$\left| A\pi_{3/2}, p_{\pm} \right\rangle = \frac{1}{\sqrt{2}} \left[\left| 1\ \tfrac{1}{2}\ \tfrac{1}{2}; \tfrac{3}{2}\ J_f\ M_f \right\rangle \pm \left| -1, \tfrac{1}{2}, -\tfrac{1}{2}; -\tfrac{3}{2}, J_f\ M_f \right\rangle \right]$$

We now make the customary (Hougen [30]) but unavoidable approximation: in the Hund (a) representation $\vec{L}^2$ does not commute with H_{AB} so that L(L+1) is not a good quantum number. Thus the matrix elements of $\vec{L}^2$ in equations (4-4) and (4-5) cannot be evaluated analytically, but must be computed numerically using the electronic wavefunctions $\psi_\Lambda(r)$.

Since we will be concerned specifically with the alkali-rare-gas atom interactions which are of the weak van-der-Waal type (Hougen [30]), it is a good approximation, following Julienne [16], to treat the orbital angular momentum $\vec{L}$ as a "good" observable even for finite R, and assign to its associated quantum number L its asymptotic final atomic orbital value. Of course, the final asymptotic ($R\to\infty$) atomic value is a good quantum number. Thus for the ground state $X^2\Sigma^+_{1/2}$ we have L=0 while for the 3 excited molecular states $B\,^2\Sigma^+_{1/2}$, $A\pi_{1/2}$, $A\pi_{3/2}$ (which dissociate as $R\to\infty$ into the atomic ^2P state) we assign L=1.

We introduce the following phase conventions so that the raising/lowering operators $S_\pm$, $J_\pm$ and $L_\pm$ have matrix elements

$$\langle S,\Sigma\pm1\,|\,S_{\pm}\,|\,S,\Sigma\rangle = +\sqrt{S(S+1)-\Sigma(\Sigma\pm1)} \qquad (4\text{-}9)$$

$$\langle J,\Omega\pm1\,|\,J_{\mp}\,|\,J,\Omega\rangle = +\sqrt{J(J+1)-\Omega(\Omega\pm1)} \qquad (4\text{-}10)$$

$$\langle L,\Lambda\pm1\,|\,L_{\pm}\,|\,L,\Lambda\rangle = +\sqrt{L(L+1)-\Lambda(\Lambda\pm1)} \qquad (4\text{-}11)$$

with $S_{\pm}=S_x\pm iS_y$, $J_{\mp}=J_x\mp iJ_y$, $L_{\pm}=L_x\pm iL_y$. In Appendix 2, it is shown explicitly why J_- (rather than J_+) is the raising operator in the non-inertial reference frame of the Hund (a) representation.

Now $S_-\,|\Sigma=-\frac{1}{2}, S=\frac{1}{2}\rangle = 0 = S_+\,|\Sigma=+\frac{1}{2}, S=\frac{1}{2}\rangle$ and $L_-\,|\Lambda=-1\rangle = 0 = L_+\,|\Lambda=+1\rangle$ so that we have the following non-zero states after applying the raising/lowering operators in equations (4-4) and (4-5) on the four allowed states:

(i) $X\Sigma^+_{1/2}$ $(L=0)$

$$J_+ S_-\,|\,0\ \tfrac{1}{2}\ \tfrac{1}{2}\ ;\tfrac{1}{2}\ JM\rangle = \sqrt{X+\tfrac{1}{4}}\ \,|\,0,\tfrac{1}{2},-\tfrac{1}{2}\ ;-\tfrac{1}{2}\ JM\rangle \qquad (4\text{-}12)$$

$$J_- S_+\,|\,0,\tfrac{1}{2},-\tfrac{1}{2}\ ;-\tfrac{1}{2}\ JM\rangle = \sqrt{X+\tfrac{1}{4}}\ \,|\,0\ \tfrac{1}{2}\ \tfrac{1}{2}\ ;\tfrac{1}{2}\ JM\rangle$$

where

$$X=J(J+1) \qquad (4\text{-}13)$$

(ii) $B\Sigma^+_{1/2}$ $(L=1)$

$$L_+ S_-\,|\,0\ \tfrac{1}{2}\ \tfrac{1}{2}\ ;\tfrac{1}{2}\ J_f\ M_f\rangle = \sqrt{2}\ \,|\,1\ \tfrac{1}{2}\ -\tfrac{1}{2}\ ;\tfrac{1}{2}\ J_f\ M_f\rangle$$
$$L_- S_+\,|\,0\ \tfrac{1}{2}\ -\tfrac{1}{2}\ ;-\tfrac{1}{2}\ J_f\ M_f\rangle = \sqrt{2}\ \,|\,-1,\tfrac{1}{2},\tfrac{1}{2}\ ;-\tfrac{1}{2}\ J_f\ M_f\rangle, \qquad (4\text{-}14)$$

$$L_+ J_- \left| 0\ \tfrac{1}{2}\ \tfrac{1}{2}\ ;\tfrac{1}{2}\ J_f\ M_f \right\rangle = \sqrt{2}.\ \sqrt{X_f - \tfrac{3}{4}}\ \left| 1\ \tfrac{1}{2}\ \tfrac{1}{2}\ ;\tfrac{3}{2}\ J_f\ M_f \right\rangle$$

$$L_+ J_- \left| 0\ \tfrac{1}{2}\ -\tfrac{1}{2}\ ;-\tfrac{1}{2}\ J_f\ M_f \right\rangle = \sqrt{2}.\ \sqrt{X_f + \tfrac{1}{4}}\ \left| 1\ \tfrac{1}{2}\ -\tfrac{1}{2}\ ;\tfrac{1}{2}\ J_f\ M_f \right\rangle$$

$$L_- J_+ \left| 0\ \tfrac{1}{2}\ -\tfrac{1}{2}\ ;-\tfrac{1}{2}\ J_f\ M_f \right\rangle = \sqrt{2}.\sqrt{X_f - \tfrac{3}{4}}\ \left| -1\ \tfrac{1}{2}\ -\tfrac{1}{2}\ ;-\tfrac{3}{2}\ J_f\ M_f \right\rangle$$

$$L_- J_+ \left| 0\ \tfrac{1}{2}\ \tfrac{1}{2}\ ;\tfrac{1}{2}\ J_f\ M_f \right\rangle = \sqrt{2}\ \sqrt{X_f + \tfrac{1}{4}}\ \left| -1\ \tfrac{1}{2}\ \tfrac{1}{2}\ ;-\tfrac{1}{2}\ J_f\ M_f \right\rangle \qquad (4\text{-}15)$$

$$J_+ S_- \left| 0\ \tfrac{1}{2}\ \tfrac{1}{2}\ ;\tfrac{1}{2}\ J_f\ M_f \right\rangle = \sqrt{X_f + \tfrac{1}{4}}\ \left| 0\ \tfrac{1}{2}\ -\tfrac{1}{2}\ ;-\tfrac{1}{2}\ J_f\ M_f \right\rangle$$

$$J_- S_+ \left| 0\ \tfrac{1}{2}\ -\tfrac{1}{2}\ ;-\tfrac{1}{2}\ J_f\ M_f \right\rangle = \sqrt{X_f + \tfrac{1}{4}}\ \left| 0\ \tfrac{1}{2}\ \tfrac{1}{2}\ ;\tfrac{1}{2}\ J_f\ M_f \right\rangle \qquad (4\text{-}16)$$

with

$$X_f = J_f\ (J_f + 1), \qquad \sqrt{2} = \sqrt{L(L+1)} \qquad (4\text{-}17)$$

(iii) $^2\Pi_{1/2}$ (L=1)

$$L_+ S_- \left| -1\ \tfrac{1}{2}\ \tfrac{1}{2}\ ;-\tfrac{1}{2}\ J_f\ M_f \right\rangle = \sqrt{2}\ \left| 0\ \tfrac{1}{2}\ -\tfrac{1}{2}\ ;-\tfrac{1}{2}\ J_f\ M_f \right\rangle$$

$$L_- S_+ \left| 1\ \tfrac{1}{2}\ -\tfrac{1}{2}\ ;\tfrac{1}{2}\ J_f\ M_f \right\rangle = \sqrt{2}\ \left| 0\ \tfrac{1}{2}\ \tfrac{1}{2}\ ;\tfrac{1}{2}\ J_f\ M_f \right\rangle \qquad (4\text{-}18)$$

$$L_+ J_- \left| -1\ \tfrac{1}{2}\ \tfrac{1}{2}\ ;-\tfrac{1}{2}\ J_f\ M_f \right\rangle = \sqrt{2}\ \sqrt{X_f + \tfrac{1}{4}}\ \left| 0\ \tfrac{1}{2}\ \tfrac{1}{2}\ ;\tfrac{1}{2}\ J_f\ M_f \right\rangle$$

$$L_- J_+ \left| 1\ \tfrac{1}{2}\ -\tfrac{1}{2}\ ;\tfrac{1}{2}\ J_f\ M_f \right\rangle = \sqrt{2}\ \sqrt{X_f + \tfrac{1}{4}}\ \left| 0\ \tfrac{1}{2}\ -\tfrac{1}{2}\ ;-\tfrac{1}{2}\ J_f\ M_f \right\rangle, \qquad (4\text{-}19)$$

$$J_+ S_- \left| -1\ \tfrac{1}{2}\ \tfrac{1}{2}\ ;-\tfrac{1}{2}\ J_f\ M_f \right\rangle = \sqrt{X_f - \tfrac{3}{4}}\ \left| -1,\ \tfrac{1}{2}\ ,-\tfrac{1}{2}\ ;-\tfrac{3}{2}\ J_f\ M_f \right\rangle$$

$$J_- S_+ \left| 1\ \tfrac{1}{2}\ -\tfrac{1}{2}\ ;\ \tfrac{1}{2}\ J_f\ M_f \right\rangle = \sqrt{X_f - \tfrac{3}{4}}\ \left| 1\ \tfrac{1}{2}\ \tfrac{1}{2}\ ;\ \tfrac{3}{2}\ J_f\ M_f \right\rangle \qquad (4\text{-}20)$$

(iv) $^2\Pi_{3/2}$ (L=1)

$$L\ J \left| -1, \tfrac{1}{2}, -\tfrac{1}{2}\ ;-\tfrac{3}{2}\ J_f\ M_f \right\rangle = \sqrt{2}\ \sqrt{X_f - \tfrac{3}{4}}\ \left| 0, \tfrac{1}{2}, -\tfrac{1}{2}\ ;-\tfrac{1}{2}\ J_f\ M_f \right\rangle$$

$$L\ J \left| 1\ \tfrac{1}{2}\ \tfrac{1}{2}\ ;\ \tfrac{3}{2}\ J_f\ M_f \right\rangle = \sqrt{2}\ \sqrt{X_f - \tfrac{3}{4}}\ \left| 0\ \tfrac{1}{2}\ \tfrac{1}{2}\ ;\ \tfrac{1}{2}\ J_f\ M_f \right\rangle \qquad (4\text{-}21)$$

$$J\ S \left| 1\ \tfrac{1}{2}\ \tfrac{1}{2}\ ;\tfrac{3}{2}\ J_f\ M_f \right\rangle = \sqrt{X_f - \tfrac{3}{4}}\ \left| 1\ \tfrac{1}{2}\ -\tfrac{1}{2}\ ;\tfrac{1}{2}\ J_f\ M_f \right\rangle$$

$$J\ S \left| -1, \tfrac{1}{2}, -\tfrac{1}{2}\ ;-\tfrac{3}{2}\ J_f\ M_f \right\rangle = \sqrt{X_f - \tfrac{3}{4}}\ \left| -1, \tfrac{1}{2}, \tfrac{1}{2}\ ;-\tfrac{1}{2}\ J_f\ M_f \right\rangle, \qquad (4\text{-}22)$$

A. ELECTRONIC-ROTATIONAL MATRIX ELEMENTS

We now consider the matrix elements of the Hamiltonian $H_e + H_{so} + H_{rot}$. Since the parity operator commutes with this Hamiltonian, the bra- and ket- states must have the same parity. Because $X\Sigma$ has L=0 asymptotically while the final states have L=1 (asymptotically), there will be no asymptotic coupling of $X\Sigma$ with any of the three final states $\{B\Sigma\ ,\ A\Pi_{1/2}\ ,\ A\Pi_{3/2}\}$ by the electronic-rotational Hamiltonian $H_e + H_{so} + H_{rot}$.

$$\left\langle X\ \Sigma^+_{1/2}\ , p\pm \right| H_{AB} \left| X\ \Sigma^+_{1/2}\ , p\pm \right\rangle$$

Since L=0=Λ, we have

$$\langle X\,\Sigma^+_{1/2}, p+ \left| H_{rot} \right| X\,\Sigma^+_{1/2}, p+\rangle = \tfrac{1}{2} B(R)\left[\langle 0\,\tfrac{1}{2}\,\tfrac{1}{2};\tfrac{1}{2}\,JM\right| + \langle 0\,\tfrac{1}{2}\,-\tfrac{1}{2};-\tfrac{1}{2}\,JM\left|\right]. \left[\vec{J}^2 - J_z^2 + \vec{S}^2 - S_z^2 - (J_+ S_- + J_- S_+)\right] .$$

$$\left[\left|0\,\tfrac{1}{2}\,\tfrac{1}{2};\tfrac{1}{2}\,JM\right\rangle + \left|0\,\tfrac{1}{2}\,-\tfrac{1}{2};-\tfrac{1}{2}\,JM\right\rangle\right]$$

$$= B(R)\left[X - \tfrac{1}{4} + \tfrac{1}{2}\cdot\tfrac{3}{2} - \tfrac{1}{4} - \sqrt{X + \tfrac{1}{4}} \right]$$

$$= B(R)\left[X + \tfrac{1}{4} - \sqrt{X + \tfrac{1}{4}} \right] \qquad (4\text{-}23)$$

Similarly,

$$\langle X\,\Sigma^+_{1/2}, P_- \left| H_{rot} \right| X\,\Sigma^+_{1/2}, P_- \rangle = B(R)\left[X + \tfrac{1}{4} + \sqrt{X+\tfrac{1}{4}}\right] \qquad (4\text{-}24)$$

There is no contribution from H_{so} while the diagonal element of H_e yields the Born-Oppenheimer potential $W_{oi}(R)$.

Proceeding in like fashion, we obtain the following symmetric matrices

Atomic $^2S_{1/2}$, $P_+ = (-1)^{J-1/2}$

$$X\,^2\Sigma^+_{1/2}: \quad \left[W_{oi}(R) + B(R)\left\{X + \tfrac{1}{4} - \sqrt{X+\tfrac{1}{4}}\right\}\right] \qquad (4\text{-}25)$$

Atomic ^2P, $P_+ = (-1)^{J_f - 1/2}$

$$B\Sigma: \quad a_{11}$$

$$A\Pi_{1/2}: \quad \begin{pmatrix} a_{11} & \\ a_{21} & a_{22} \end{pmatrix}$$

$$A\Pi_{3/2}: \quad \begin{pmatrix} a_{11} & & \\ a_{21} & a_{22} & \\ a_{31} & a_{32} & a_{33} \end{pmatrix}$$

where

$$a_{11} = W_{of}(R) + B(R)\left\{ X_f + \tfrac{9}{4} - \sqrt{X_f + \tfrac{1}{4}} \right\}$$

$$a_{22} = W_{1f}(R) + B(R)\left\{X_f + \tfrac{5}{4}\right\} - A(R)/2$$
$$a_{33} = W_{1f}(R) + B(R)\left\{X_f - \tfrac{3}{4}\right\} + A(R)/2$$
$$a_{21} = \sqrt{2}\,B(R)\left\{1 - \sqrt{X_f + \tfrac{1}{4}}\right\} + A(R)/\sqrt{2}$$
$$a_{31} = -\sqrt{2}\,B(R)\sqrt{X_f - \tfrac{3}{4}}$$
$$a_{32} = -B(R)\sqrt{X_f - \tfrac{3}{4}} \qquad (4\text{-}26)$$

while for the negative parity states p_- we find

Atomic $^2S_{1/2}$, $p_- = (-1)^{J+1/2}$

$$X\,^2\Sigma^+_{1/2}: [W_{0i}(R) + B(R)\left\{X + \tfrac{1}{4} + \sqrt{X + \tfrac{1}{4}}\right\}] \qquad (4\text{-}27)$$

Atomic ^2P, $p_- = (-1)^{J_f+1/2}$

$$\begin{array}{ll} B\Sigma: & \begin{pmatrix} b_{11} & & \\ b_{21} & b_{22} & \\ b_{31} & b_{32} & b_{33} \end{pmatrix} \\ A\Pi_{1/2}: & \\ A\Pi_{3/2}: & \end{array} \qquad (4\text{-}28)$$

where

$$b_{11} = W_{0f}(R) + B(R)\left\{X_f + \tfrac{9}{4} + \sqrt{X_f + \tfrac{1}{4}}\right\}$$
$$b_{22} = W_{1f}(R) + B(R)\left\{X_f + \tfrac{5}{4}\right\} - A(R)/2$$
$$b_{33} = W_{1f}(R) + B(R)\left\{X_f - \tfrac{3}{4}\right\} + A(R)/2$$
$$b_{21} = \sqrt{2}\,B(R)\left\{1 + \sqrt{X_f + \tfrac{1}{4}}\right\} + A(R)/\sqrt{2}$$
$$b_{31} = -\sqrt{2}\,B(R)\sqrt{X_f - \tfrac{3}{4}}$$
$$b_{32} = -B(R)\sqrt{X_f - \tfrac{3}{4}}$$

B. DERIVATION OF RADIATIVE COUPLING MATRIX ELEMENTS IN HUND (a) REPRESENTATION

The V_{rad} operator gives the interaction between the quasimolecule AB and the laser field. It is convenient to work out the V_{rad} matrix elements in the Hund (a) representation, so that the space- fixed projection of the dipole operator μ_o^{sp} is given in the moving molecule-fixed projection by

$$\mu_o^{sp} = \sum_{k=-1}^{1} D_{ok}^{1*} \cdot \mu_k \qquad (4\text{-}29)$$

where the vector transition dipole operator (in molecule-fixed frame) is defined

$$\mu_o = ez, \quad \mu_{+1} = -e(x+iy)/\sqrt{2}, \quad \mu_{-1} = +e(x-iy)/\sqrt{2} \qquad (4\text{-}30)$$

since there is only one active electron in the Na-rare gas quasi- molecule. $D^{J*}(\varphi,\theta,o)$ is the Wigner rotation matrix [26,31,32], with θ and φ being the Euler angles giving the orientation of the (moving) internuclear axis with respect to the space-fixed coordinate system.

We now turn to the explicit derivation of the matrix element $\langle X\Sigma, p_+ | V_{rad} | f, p_\pm \rangle$ where $|f\rangle$ stands for one of the excited states, equation (4-8). On introducing the nuclear rotation matrices $D_{M\Omega}^{J*}$ for these states, we have

$$\langle X\Sigma, p_+ | \mu_o^{sp} | f, p \rangle = \sqrt{(2J_i+1)(2J_f+1)/8\pi} \sum_{k=-1}^{1} \int d^2\hat{R} \left\{ D^{J_i}_{M_i,1/2} \langle \Lambda_i \tfrac{1}{2} \Sigma_i | \right.$$

$$\left. + D^{J_i}_{M_i,-\frac{1}{2}} \langle -\Lambda_i \tfrac{1}{2} -\Sigma_i | \right\} \cdot D'^{*}_{ok} \mu_k \cdot \left\{ D^{J_f *}_{M_f,\Omega_f} | \Lambda_f \tfrac{1}{2} \Sigma_f \rangle \pm D^{J_f *}_{M_f,-\Omega_k} | -\Lambda_f \tfrac{1}{2} \; -\Sigma_f \rangle \right\} \quad (4\text{-}31)$$

Since one of the Euler angles is zero, $D^{J*}_{M\Omega} = D^{J*}_{M\Omega}(\varphi, \theta, o)$, the angular integration $\int d^2\hat{R}$ is two-dimensional so that $\int d^2\hat{R}\, 1 = 4\pi$. Thus, since the Clebsch-Gordon coefficients are real,

$$\int d^2\hat{R} D^{J_i}_{M_i\Omega_i} \cdot D'^{*}_{ok} \cdot D^{J_f *}_{M_f\Omega_f} = \frac{4\pi}{2J_i+1} C(J_f\, 1 J_i |\, M_f\, 0 M_i) \cdot C(J_f\, 1 J_i |\, \Omega_f\, k\, \Omega_i). \quad (4\text{-}32)$$

Now the Clebsch-Gordon coefficient is zero unless

$$M_f = M_i \equiv M \quad (4\text{-}33)$$

$$\Omega_f + k = \Omega_i \quad , \quad k = -1 \text{ or } 0 \text{ or } +1 \quad (4\text{-}34)$$

Equation (4-33) arises from the fact that the laser radiation is linearly polarized. Using equation (4-32) in (4-31) we immediately find, on letting $M = M_i = M_f$,

$$\langle X\Sigma, p_+ | \mu_o^{sp} | f, p_\pm \rangle = (1/2) \sqrt{(2J_f+1)/(2J_i+1)} \cdot C(J_f\, 1 J_i |\, M 0 M)$$

$$\sum_{k=-1}^{1} [\langle \Lambda_i \tfrac{1}{2} \Sigma_i \| \mu_k \| \Lambda_f \tfrac{1}{2} \Sigma_f \rangle C(J_f\, 1 J_i |\, \Omega_f, k, -\tfrac{1}{2})$$
$$+ \langle -\Lambda_i, \tfrac{1}{2}, -\Sigma_i \| \mu_k \| \Lambda_f \tfrac{1}{2} \Sigma_f \rangle C(J_f\, 1 J_i |\, \Omega_f, k, -\tfrac{1}{2})$$
$$\pm \langle \Lambda_i \; \tfrac{1}{2} \; \Sigma_i \| \mu_k \| -\Lambda_f, \tfrac{1}{2}, -\Sigma_f \rangle C(J_f\, 1 J_i |\, -\Omega_f, k, \tfrac{1}{2})$$
$$\pm \langle -\Lambda_i, \tfrac{1}{2}, -\Sigma_i \| \mu_k \| -\Lambda_f, \tfrac{1}{2}, -\Sigma_f \rangle C(J_f\, 1 J_i |\, -\Omega_f, k, -\tfrac{1}{2}) \quad (4\text{-}35)$$

where $\langle \ldots \| \mu_k \| \ldots \rangle$ is the reduced transition dipole matrix since the explicit M-dependence has been factored out (c.f. Wigner-Eckart Theorem).

We now substitute in the explicit final excited state for $f, p_{\pm}\rangle$, equation (4-8), into equation (4-35) and using the properties for Clebsch-Gordon coefficients to be non-zero:

(i) $\langle X\Sigma, p_+ | \mu_o^{sp} | B\Sigma, p_{\pm}\rangle$

Proceeding from equation (4-35) and noting that here $\Lambda_i = 0 = \Lambda_f$,

$$\langle X\Sigma, p_+ \left| \mu_o^{sp} \right| B\Sigma, p_{\pm}\rangle = (1/2)\sqrt{(2J_f+1)/(2J_i+1)}\, C(J_f\ 1\ J_i \mid MOM)$$

$$\left[\langle 0\ \tfrac{1}{2}\ \tfrac{1}{2} \| \mu_o \| 0\ \tfrac{1}{2}\ \tfrac{1}{2}\rangle \cdot C(J_f\ 1\ J_i \mid \tfrac{1}{2}\ 0\ \tfrac{1}{2}) + \langle 0, \tfrac{1}{2}, -\tfrac{1}{2} \| \mu_{-1} \| 0\ \tfrac{1}{2}\ \tfrac{1}{2}\rangle C(J_f\ 1\ J_i \mid \tfrac{1}{2}, -1, -\tfrac{1}{2}) \right.$$

$$\pm \langle 0\ \tfrac{1}{2}\ \tfrac{1}{2} \| \mu_1 \| 0\ \tfrac{1}{2}\ -\tfrac{1}{2}\rangle C(J_f\ 1\ J_i \mid -\tfrac{1}{2}, 1, \tfrac{1}{2})$$

$$\left. \pm \langle 0\ \tfrac{1}{2}\ -\tfrac{1}{2} \| \mu_o \| 0, \tfrac{1}{2}, -\tfrac{1}{2}\rangle C(J_f\ 1\ J_i \mid -\tfrac{1}{2}, 0, -\tfrac{1}{2})\right], \qquad (4\text{-}36)$$

where μ_o, $\mu_{\pm 1}$ are the components of the transition dipole operator, equation (4-30). Since

$$C(J_f\ 1\ J_i \mid M_1\ M_2\ M_3) = (-1)^{J_f+1-J_i}\ C(J_f\ 1\ J_i \mid -M_1\ -M_2\ -M_3),$$

equation (4-36) can be simplified to

$$\langle X\Sigma, p_+ \left| \mu_o^{sp} \right| B\Sigma, p_\pm \rangle = (1/2)\sqrt{(2J_f+1)/(2J_i+1)}\, C(J_f\, 1\, J_i \mid M0M)$$

$$\left[C(J_f\, 1\, J_i \mid \tfrac{1}{2}\, 0\, \tfrac{1}{2})\, \langle 0\, \tfrac{1}{2}\, \tfrac{1}{2} \left\| \mu_o \right\| 0\, \tfrac{1}{2}\, \tfrac{1}{2} \rangle \pm (-1)^{J_f+1-J_i} \cdot \langle 0\, \tfrac{1}{2}\, -\tfrac{1}{2} \left\| \mu_o \right\| 0\, \tfrac{1}{2}\, -\tfrac{1}{2} \rangle \right.$$

$$\left. \mp C(J_f\, 1 J_i \mid \tfrac{1}{2}, -1, -\tfrac{1}{2})\, \langle 0, \tfrac{1}{2}, -\tfrac{1}{2} \left\| \mu_{-1} \right\| 0\, \tfrac{1}{2}\, \tfrac{1}{2} \rangle \right.$$

$$\left. \pm (-1)^{J_f+1-J_i} \langle 0\, \tfrac{1}{2}\, \tfrac{1}{2} \left\| \mu_{+1} \right\| 0\, \tfrac{1}{2}\, -\tfrac{1}{2} \rangle \right] \qquad (4\text{-}37)$$

Consider the angular integration in the reduced matrix inner products. Since $\mu_o = ez = \sqrt{4\pi/3}\, er\, Y_{10}$, and from the integration of the product of three spherical harmonics

$$\int d^2\phi\, Y^*_{\ell m}\, Y_{\ell_1 m_1} Y_{\ell_2 m_2} = \sqrt{(2\ell_1+1)(2\ell_2+1)/(4\pi(2\ell+1))}\; C(\ell_1 \ell_2 \ell_3 \mid 000)\; C(\ell_1 \ell_2 \ell \mid m_1\, m_2\, m) \qquad (4\text{-}38)$$

so that non-zero inner products must have $m_1 + m_2 = m$,

$$\langle X\Sigma \left\| \mu_o \right\| B\Sigma \rangle \Big|_{ang} = \langle 0\, \tfrac{1}{2}\, \tfrac{1}{2} \left\| \mu_o \right\| 0\, \tfrac{1}{2}\, \tfrac{1}{2} \rangle \Big|_{ang} =$$

$$\int d^2\phi\, Y^*_{00} \cdot Y_{10} \cdot \sqrt{\tfrac{4\pi}{3}}\, Y_{10} = \sqrt{3}\, C^2(110 \mid 000) = 1/\sqrt{3}$$

$$= \langle 0\, \tfrac{1}{2}\, -\tfrac{1}{2} \left\| \mu_o \right\| 0\, \tfrac{1}{2}\, -\tfrac{1}{2} \rangle \Big|_{ang}$$

Thus a non-zero electronic transition dipole moment is

$$\tau_o(R) = \langle X\Sigma \left\| \mu_o \right\| B\Sigma \rangle \qquad (4\text{-}39)$$

But

$$\langle 0\ \tfrac{1}{2}\ -\tfrac{1}{2}\left|\mu_{-1}\right|0\ \tfrac{1}{2}\ \tfrac{1}{2}\rangle\Big|_{ang} = \int d^2\phi\ Y^*_{00}\ Y_{1,-1}\ .\ Y_{10}\ \sqrt{4\pi/3} = 0$$
$$= \langle 0\ \tfrac{1}{2}\ \tfrac{1}{2}\left|\mu_{+1}\right|0\ \tfrac{1}{2}\ -\tfrac{1}{2}\rangle\Big|_{ang},$$

since $C(110\,|\,\mp 100)=0$, $\mu_{-1}=e(x-iy)/\sqrt{2} = \sqrt{\frac{4\pi}{3}}\,er.Y_{1,-1}$, and $\mu_{+1}=-e(x+iy)/\sqrt{2} = \sqrt{\frac{4\pi}{3}}\,er.Y_{1,+1}$.

Thus

$$\langle X\Sigma, p_+\left\|\mu_o^{sp}\right\|B\Sigma, p_\pm\rangle = (1/2)\sqrt{(2J_f+1)/(2J_i+1)}.$$

$$C(J_f\ 1\ J_i\,|\,\tfrac{1}{2}\ 0\ \tfrac{1}{2}).[1\pm(-1)^{J_f+1-J_i}].\tau_o \qquad (4\text{-}40)$$

(ii) $\langle X\Sigma,\ p_+\ \ \mu^{sp}\ \ \pi_{1/2}, p_\pm\rangle$

From equation (4-35), with $\Lambda_i=0$, $\Lambda_f=1$,

$$\langle X\Sigma\ , p_+\ |\mu|\ \pi_{1/2}, p_\pm\rangle = (1/2)$$
$$\sqrt{(2J_f+1)\ /(2J_i+1)}.\ [\langle 0\ \tfrac{1}{2}\ \tfrac{1}{2}\left\|\mu_o\right\|1\ \tfrac{1}{2}\ -\tfrac{1}{2}\rangle\ C(J_f\ 1J_i|\tfrac{1}{2}0\tfrac{1}{2})$$

$$+\langle 0\ \tfrac{1}{2}\ -\tfrac{1}{2}\left\|\mu_{-1}\right\|1\ \tfrac{1}{2}\ -\tfrac{1}{2}\rangle C(J_f\ 1J_i\ |\ \tfrac{1}{2}-1\ \ -\tfrac{1}{2})$$

$$\pm\langle 0\ \tfrac{1}{2}\ \tfrac{1}{2}\left\|\mu_{+1}\right\|-1\ \tfrac{1}{2}\ +\tfrac{1}{2}\rangle C(J_f\ 1J_i\ |-\tfrac{1}{2}\ 1\ \tfrac{1}{2})$$

$$\pm\langle 0\ \tfrac{1}{2}\ -\tfrac{1}{2}\left\|\mu_o\right\|-1\ \tfrac{1}{2}\ +\tfrac{1}{2}\rangle\ C(J_f\ 1J_i\ \ -\tfrac{1}{2}\ 0-\tfrac{1}{2})] \qquad (4\text{-}41)$$

Now the angular integration for the reduced matrix elements involving μ_o are zero:

$$\langle 0\ \tfrac{1}{2}\ \tfrac{1}{2}\ \|\mu_0\|\ 1\ \tfrac{1}{2}\ -\tfrac{1}{2}\rangle\Big|_{ang} = \int d^2\phi\ Y^*_{00}\ Y_{10}\ Y_{11}\sqrt{4\pi/3} = 0$$

$$= \langle 0\ \tfrac{1}{2}\ -\tfrac{1}{2}\ \|\mu_0\|\ -1\ \tfrac{1}{2}\ -\tfrac{1}{2}\rangle\Big|_{ang} \qquad (4\text{-}42)$$

since $C(110|0,+1,0)=0$, and using equation (4-38). However

$$\langle 0\ \tfrac{1}{2}\ -\tfrac{1}{2}\ \|\mu_{-1}\|\ 1\ \tfrac{1}{2}\ -\tfrac{1}{2}\rangle\Big|_{ang} = \int d^2\phi\ Y^*_{00}\ Y_{1,-1}\ Y_{11}\sqrt{4\pi/3} = -1/\sqrt{3}$$

$$= \int d^2\phi\ Y^*_{00}\ Y_{11}\ Y_{1,-1}\sqrt{4\pi/3} = \langle 0\ \tfrac{1}{2}\ \tfrac{1}{2}\ \|\mu_{+1}\|\ -1\ \tfrac{1}{2}\ \tfrac{1}{2}\rangle\Big|_{ang} \qquad (4\text{-}43)$$

so that on introducing the electronic transition dipole moment

$$\tau_1(R) = \langle X\Sigma\ \|\mu_{+1}\|\pi^{(-1)}_{1/2}\rangle = \langle X\Sigma\ \|\mu_{-1}\|\pi^{(+1)}_{1/2}\rangle, \qquad (4\text{-}44)$$

where the superscript (-1) or (+1) on the π-state indicates the sign of $\Lambda_f = 1$. Thus

$$\langle X\Sigma,\ p_+\ \|\mu_o^{sp}\|\ \pi_{1/2}\ p_\pm\rangle = (1/2)\ \sqrt{(2J_f+1)/(2J_i+1)}$$
$$C(J_f\ 1\ J_i\ |\ \tfrac{1}{2}\ -1\ \ -\tfrac{1}{2})$$
$$[1\pm(-1)^{J_f+1-J_i}\ ]\ .\ \tau_1 \qquad (4\text{-}45)$$

(iii) $\langle X\Sigma\ ,p_+\ \|\mu_o^{sp}\|\ \pi_{3/2},p_\pm\rangle$

Proceeding as in (ii) on noting that $C(J_f\ 1\ J_i\ |\pm\frac{3}{2}\ k\ -\frac{1}{2})=0$ for k restricted to the set $\{-1,0,1\}$,

$$\langle X\Sigma\ ,p_+\ \|\mu_o^{sp}\|\ \pi_{3/2},p_\pm\rangle = (1/2)\ \sqrt{(2J_f+1)/(2J_i+1)}$$

$$[\langle 0\ \tfrac{1}{2}\ \tfrac{1}{2} \| \mu_{-1} \| 1\ \tfrac{1}{2}\ \tfrac{1}{2}\rangle$$

$$C(J_f\ 1 J_i \mid \tfrac{3}{2}\ -1\ \tfrac{1}{2}) \pm \langle 0\ \tfrac{1}{2}\ -\tfrac{1}{2} \| \mu_{+1} \| -1\ \tfrac{1}{2}\ -\tfrac{1}{2}\rangle\, C(J_f\ 1 J_i \mid -\tfrac{3}{2}\ 1\ -\tfrac{1}{2})]$$

$$= \tfrac{1}{2}\, C(J_f\ 1 J_i \mid \tfrac{3}{2}\ -1\ \tfrac{1}{2})[1 \pm (-1)^{J_f + 1 - J_i}]\sqrt{2J_f+1 \,/\, 2J_i+1} \qquad (4\text{-}46)$$

We now consider the $\langle X\Sigma, p_- \| \mu_o^{sp} \| f, p_\pm \rangle$ matrix elements. Proceeding as for the $\langle X\Sigma, p_+$ state, we find

$$\langle X\Sigma, p_- \| \mu_o^{sp} \| f, p_\pm \rangle = C(J_f\ 1 J_i \mid \mathrm{MOM})\ \langle X\Sigma, p_- \| \mu_o^{sp} \| f, p_\pm \rangle \qquad (4\text{-}47)$$

where the reduced matrix elements

$$\langle X\Sigma, p_- \| \mu_o^{sp} \| f, p_\pm \rangle = (1/2)\ \sqrt{(2J_f + 1)/(2J_i + 1)}$$

$$\sum_{k=-1}^{1} [\langle \Lambda_i\ \tfrac{1}{2}\ \Sigma_i \| \mu_k \| \Lambda_f\ \tfrac{1}{2}\ \Sigma_f\rangle\, C(J_f\ 1 J_i \mid \Omega_f\ k\ \tfrac{1}{2})$$

$$- \langle -\Lambda_i\ \tfrac{1}{2}\ -\Sigma_i \| \mu_k \| \Lambda_f\ \tfrac{1}{2}\ \Sigma_f\rangle\, C(J_f\ 1 J_i \mid \Omega_f\ k\ -\tfrac{1}{2})$$

$$\pm \langle \Lambda_i\ \tfrac{1}{2}\ \Sigma_i \| \mu_k \| -\Lambda_f\ \tfrac{1}{2}\ -\Sigma_f\rangle\, C(J_f\ 1 J_i \mid -\Omega_f\ k\ \tfrac{1}{2})$$

$$\mp \langle -\Lambda_i\ \tfrac{1}{2}\ -\Sigma_i \| \mu_k \| -\Lambda_f\ \tfrac{1}{2}\ -\Sigma_f\rangle\, C(J_f\ 1 J_i \mid -\Omega_f\ k\ -\tfrac{1}{2})] \qquad (4\text{-}48)$$

It should be noticed that the right hand side of equation (4-48) is identical to equation (4-35) except for the reversal of signs in the 2nd and 4th terms. Thus, with $\tau_0(R)$ and $\tau_1(R)$ defined by equations (4-39) and (4-44), we

immediately find from equations (4-40), (4-45) and (4-46),

$$\langle X\Sigma, p_- \| \mu_o^{sp} \| B\Sigma, p_\pm \rangle = (1/2)\sqrt{(2J_f+1)/(2J_i+1)} \cdot C(J_f\ 1\ J_i\ \tfrac{1}{2}\ 0\ \tfrac{1}{2}) \cdot [1 \mp (-1)^{J_f+1-J_i}] \cdot \tau_o \qquad (4\text{-}49)$$

$$\langle X\Sigma, p_- \| \mu_o^{sp} \| \pi_{1/2}, p_\pm \rangle = (-1/2)\sqrt{(2J_f+1)/(2J_i+1)} \cdot C(J_f\ 1\ J_i\ \tfrac{1}{2}\ -1\ -\tfrac{1}{2}) \cdot [1 \mp (-1)^{J_f+1-J_i}] \cdot \tau_1 \qquad (4\text{-}50)$$

$$\langle X\Sigma, p_- \| \mu_o^{sp} \| \pi_{3/2}, p_\pm \rangle = (1/2)\sqrt{(2J_f+1)/(2J_i+1)} \cdot C(J_f\ 1\ J_i\ \tfrac{3}{2}\ -1\ \tfrac{1}{2}) \cdot [1 \mp (-1)^{J_f+1-J_i}] \cdot \tau_1 \qquad (4\text{-}51)$$

Consider the radiative coupling matrix elements for the parity $p_+ = (-1)^{J-1/2}$ for the $X\Sigma$ state with $J_i = J$.

$X\Sigma, p_+ \longrightarrow B\Sigma$

Since both the initial and final states are Σ-terms and $\vec{\mu} = e\vec{r}$ is an ordinary (polar) vector whose component μ_o along the internuclear axis remains unchanged in sign with respect to a reflection in a plane passing through the internuclear axis, we can immediately conclude that μ_o can only couple terms of the same parity--i.e. the only non-zero matrix elements will be $\langle X\Sigma, p_+ \| \mu_o \| B\Sigma, p_+ \rangle$ and $\langle X\Sigma, p_- \| \mu_o \| B\Sigma, p_- \rangle$, while $\langle X\Sigma, p_+ \| \mu_o \| B\Sigma, p_- \rangle = 0 = \langle X\Sigma, p_- \| \mu_o \| B\Sigma, p_+ \rangle$,

Q-branch ($J_f = J$)

From equation (4-40), for $J_f = J_i = J$, we immediately have

$$\langle X\Sigma, p_+ \| \mu \| B\Sigma, p_+ \rangle_Q = 0 = \langle X\Sigma, p_+ \| \mu \| B\Sigma, p_- \rangle_Q \qquad (4\text{-}52)$$

R-branch ($J_f = J+1$)

$$\langle X\Sigma, p_+ \| \mu \| B\Sigma, p_+ \rangle_R = (1/2)\sqrt{(2J_f + 1)/(2J + 1)} \cdot [(J+1-1/2)(J+1+1/2)/((J+1)(2J+3))]^{1/2} \cdot 2\tau_o$$

$$= -(\tau_o/2)\sqrt{(2J+3)/(J+1)} \quad , \qquad (4\text{-}53)$$

P-branch ($J_f = J-1$)

$$\langle X\Sigma, p_+ \| \mu \| B\Sigma, p_+ \rangle_P = (1/2)\sqrt{(2J-1)/(2J+1)} \cdot [(J-1/2)(J+1/2)/(J(2J-1))]^{1/2} \cdot 2\tau_o$$

$$= (\tau_o/2)\sqrt{(2J-1)/J} \qquad (4\text{-}54)$$

The radiative coupling matrix elements for the other transitions are obtained similarly. The results are collected in Table 1.

C. FULL CLOSE-COUPLED EQUATIONS

We now combine the electronic-rotational matrix elements of H_{AB}, equations (4-25)-(4-28) with the radiative coupling matrix given in Table 1. We immediately find that for $X\Sigma$ of parity P_+ we have the following 10x10 matrix, where a * represents a non-zero matrix element

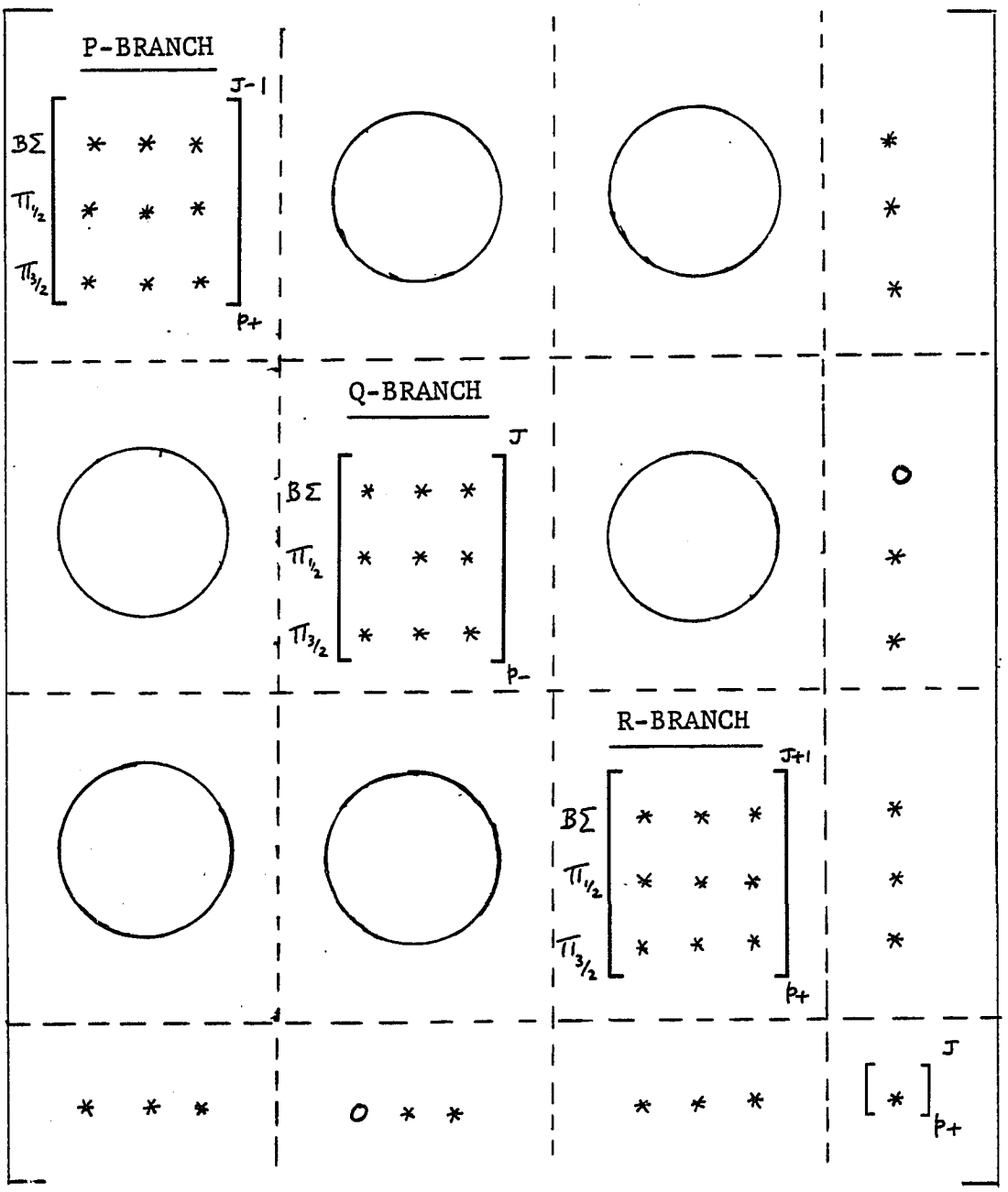

(4-55)

TABLE 1

Radiative coupling matrix elements evaluated in Hund (a) basis

HUND (A) REPRESENTATION OF V

PARITY	BRANCH	$\langle X\Sigma \Vert \mu \Vert B\Sigma \rangle$	$\langle X\Sigma \Vert \mu \Vert \pi_{1/2} \rangle$	$\langle X\Sigma \Vert \mu \Vert \pi_{3/2} \rangle$
$p_+ \rightarrow p_-$	Q	0	$\sqrt{\frac{(2J+1)^2}{8J(J+1)}}\cdot\tau_1$	$\sqrt{\frac{(2J-1)(2J+3)}{8J(J+1)}}\cdot\tau_1$
$p_+ \rightarrow p_+$	P	$\sqrt{\frac{2J-1}{4J}}\cdot\tau_0$	$\sqrt{\frac{2J-1}{8J}}\cdot\tau_1$	$\sqrt{\frac{(2J-1)(2J-3)}{8J(2J+1)}}\cdot\tau_1$
$p_+ \rightarrow p_+$	R	$-\sqrt{\frac{2J+3}{4(J+1)}}\cdot\tau_0$	$\sqrt{\frac{2J+3}{8(J+1)}}\cdot\tau_1$	$\sqrt{\frac{(2J+3)(2J+5)}{8(J+1)(2J+1)}}\tau_1$
$p_- \rightarrow p_+$	Q	0	$-\sqrt{\frac{(2J+1)^2}{8J(J+1)}}\tau_1$	$\sqrt{\frac{(2J-1)(2J+3)}{8J(J+1)}}\cdot\tau_1$
$p_- \rightarrow p_-$	P	$\sqrt{\frac{2J-1}{4J}}\cdot\tau_0$	$-\sqrt{\frac{2J-1}{8J}}\tau_1$	$\sqrt{\frac{(2J-1)(2J-3)}{8J(2J+1)}}\cdot\tau_1$
$p_- \rightarrow p_-$	R	$-\sqrt{\frac{2J+3}{4(J+1)}}\cdot\tau_0$	$\sqrt{\frac{2J+3}{8(J+1)}}\tau_1$	$\sqrt{\frac{(2J+3)(2J+5)}{8(J+1)(2J+1)}}\cdot\tau_1$

which simplifies into three uncoupled blocks of 4x4 matrices corresponding to the P-, Q-, and R-branches. Thus, incorporating both parities, we have

P-branch, $p_{\pm}=(-1)^{J\mp 1/2}$ for $X\Sigma$

$$\begin{array}{c} \\ B\Sigma \\ \Pi_{1/2} \\ \Pi_{3/2} \\ X\Sigma \end{array} \begin{bmatrix} ap_{11} & & & \\ ap_{21} & ap_{22} & & \\ ap_{31} & ap_{32} & ap_{33} & \\ ap_{41} & ap_{42} & ap_{43} & ap_{44} \end{bmatrix} \qquad (4\text{-}56)$$

where

$$\begin{aligned}
ap_{11} &= W_{of} + B(R)\left\{X_f + \tfrac{9}{4} \mp \sqrt{X_f + \tfrac{1}{4}}\right\} \\
ap_{22} &= W_{1f} + B(R)\left\{X_f + \tfrac{5}{4}\right\} - A/2 \\
ap_{33} &= W_{1f} + B(R)\left\{X_f - \tfrac{3}{4}\right\} + A/2 \\
ap_{44} &= W_{oi} + B(R)\left\{X + \tfrac{1}{4} \mp \sqrt{X + \tfrac{1}{4}}\right\} \\
ap_{21} &= \sqrt{2}\, B(R)\left\{1 \mp \sqrt{X_f + \tfrac{1}{4}}\right\} + A/\sqrt{2} \\
ap_{31} &= -\sqrt{2}\, B(R)\sqrt{X_f - \tfrac{3}{4}} \\
ap_{41} &= \sqrt{(2J-1)/4J}\ \cdot \tau_0 \\
ap_{32} &= -B(R)\sqrt{X_f - 3/4} \\
ap_{42} &= \pm\sqrt{(2J-1)/8J}\ \cdot \tau_1 \\
ap_{43} &= \sqrt{(2J-1)(2J-3)/8J(2J+1)}\ \cdot \tau_1
\end{aligned} \qquad (4\text{-}57)$$

with $X=J(J+1)$, $X_f=J_f(J_f+1)=J(J-1)$ since $J_f=J-1$.

Q-branch, $p_{\pm}=(-1)^{J\mp 1/2}$ for $X\Sigma$

$$\begin{array}{c} \\ B \\ \Pi_{1/2} \\ \Pi_{3/2} \\ X\Sigma \end{array} \begin{bmatrix} aq & & & \\ aq & aq & & \\ aq & aq & aq & \\ 0 & aq & aq & aq \end{bmatrix}$$

where

$$aq_{11} = W_{of} + B(R)\left\{X + \tfrac{9}{4} \pm \sqrt{X + \tfrac{1}{4}}\right\}$$

$$aq_{22} = W_{1f} + B(R)\left\{X + \tfrac{5}{4}\right\} - A/2$$

$$aq_{33} = W_{1f} + B(R)\left\{X - \tfrac{3}{4}\right\} + A/2$$

$$aq_{44} = W_{oi} + B(R)\left\{X + \tfrac{1}{4} \mp \sqrt{X + \tfrac{1}{4}}\right\}$$

$$aq_{21} = \sqrt{2}\, B(R)\left\{1 \pm \sqrt{X + \tfrac{1}{4}}\right\} + A/\sqrt{2}$$

$$aq_{31} = -\sqrt{2}\, B(R)\sqrt{X - \tfrac{3}{4}}$$

$$aq_{42} = \pm (2J+1)/\sqrt{8J(J+1)}\ .\tau_1$$

$$aq_{32} = -B(R)\sqrt{X - \tfrac{3}{4}}$$

$$aq_{43} = +\sqrt{(2J-1)(2J+3)/8J(J+1)}\ .\tau_1 \qquad (4\text{-}58)$$

since $X_f = X$, with $J_f = J$.

R-branch, $p_{\pm} = (-1)^{J \mp 1/2}$ for $X\Sigma$

$$\begin{array}{ll} B\Sigma & \left[\begin{array}{cccc} ar_{11} & & & \\ ar_{21} & ar_{22} & & \\ ar_{31} & ar_{32} & ar_{33} & \\ ar_{41} & ar_{42} & ar_{43} & ar_{44} \end{array}\right. \\ {}^2\Pi_{1/2} & \\ {}^2\Pi_{3/2} & \\ X\Sigma & \end{array}$$

where

$$ar_{11} = W_{of} + B(R)\left\{X_f + \tfrac{9}{4} \mp \sqrt{X_f + \tfrac{1}{4}}\right\}$$

$$ar_{22} = W_{1f} + B(R)\left\{X_f + \tfrac{5}{4}\right\} - A/2$$

$$ar_{33} = W_{1f} + B(R)\left\{X_f - \tfrac{3}{4}\right\} + A/2$$

$$ar_{44} = W_{oi} + B(R)\left\{X + \tfrac{1}{4} \mp \sqrt{X + \tfrac{1}{4}}\right\}$$

$$ar_{21} = \sqrt{2}\, B(R)\left\{1 \mp \sqrt{X_f + \tfrac{1}{4}}\right\} + A/\sqrt{2}$$

$$ar_{31} = -\sqrt{2}\, B(R)\sqrt{X_f - \tfrac{3}{4}}$$

$$ar_{41} = -\sqrt{(2J+3)/4(J+1)}\ .\tau_0$$

$$ar_{32} = -B(R)\sqrt{X_f - \tfrac{3}{4}}$$

$$ar_{+2} = \pm\sqrt{(2J+3)/8(J+1)}\ .\ \tau_1$$
$$ar_{+3} = \sqrt{(2J+3)(2J+5)/8(J+1)(2J+1)}\ .\ \tau_1 \qquad (4\text{-}59)$$

with $X_f = (J+1)(J+2)$, since $J_f = J+1$.

D. V_{rad} MATRIX ELEMENTS IN HUND (e) REPRESENTATION

The reduced electric dipole radiation interaction matrix has been derived in Section B for Hund case (a) representation. We now wish to transform this matrix into Hund(e) representation. For convenience we relist in Table 2, the Hund(a) representation for V_{rad}.

1. Initial Parity State $P_i = (-1)^{J+1/2}$

Now the initial parity $P_i = (-1)^{\ell+1}$ so that the initial orbital interatomic angular momentum $\ell_i = J - \frac{1}{2}$.

We thus obtain the following Hund(e) V_{rad} matrix elements. Since the radiation interaction operator is evaluated in the dipole approximation, the nonzero matrix elements for V_{rad} must have final parity $P_f = (-1)^{J-\frac{1}{2}} = (-1)^{\ell_f+1}$, i.e. $\ell_f = J + \frac{1}{2} \pmod 2$.

For the Q-branch $J_f = J$. Moreover the initial state, in Hund (e) representation is given by [see Appendix 3].

$$|i\rangle_{(e)} = \sqrt{2}\ (-1)\ C(J\ \tfrac{1}{2}\ J-\tfrac{1}{2}\ \ -\tfrac{1}{2}\ \tfrac{1}{2}\ 0)\ C(\tfrac{1}{2}\ 0\ \tfrac{1}{2}\ \ \tfrac{1}{2}\ 0\ \tfrac{1}{2})X\Sigma_{1/2} \qquad (4\text{-}60)$$

so that

TABLE 2

Radiative coupling matrix elements evaluated in a Hund (a) basis with parity information on each branch

HUND (A) REPRESENTATION OF V

PARITY of X	BRANCH	$\langle X\Sigma \Vert \mu \Vert B\Sigma \rangle$	$\langle X\Sigma \Vert \mu \Vert \pi_{1/2} \rangle$	$\langle X\Sigma \Vert \mu \Vert \pi_{3/2} \rangle$
$(-1)^{J-\frac{1}{2}}$	Q	0	$\sqrt{\frac{(2J+1)^2}{8J(J+1)}}\cdot\tau_1$	$\sqrt{\frac{(2J-1)(2J+3)}{8J(J+1)}}\cdot\tau_1$
	P	$\sqrt{\frac{2J-1}{4J}}\cdot\tau_0$	$\sqrt{\frac{2J-1}{8J}}\cdot\tau_1$	$\sqrt{\frac{(2J-1)(2J-3)}{8J(2J+1)}}\cdot\tau_1$
	R	$-\sqrt{\frac{2J+3}{4(J+1)}}\cdot\tau_0$	$\sqrt{\frac{2J+3}{8(J+1)}}\cdot\tau_1$	$\sqrt{\frac{(2J+3)(2J+5)}{8(J+1)(2J+1)}}\tau_1$
$(-1)^{J+\frac{1}{2}}$	Q	0	$-\sqrt{\frac{(2J+1)^2}{8J(J+1)}}\tau_1$	$\sqrt{\frac{(2J-1)(2J+3)}{8J(J+1)}}\cdot\tau_1$
	P	$\sqrt{\frac{2J-1}{4J}}\cdot\tau_0$	$-\sqrt{\frac{2J-1}{8J}}\tau_1$	$\sqrt{\frac{(2J-1)(2J-3)}{8J(2J+1)}}\cdot\tau_1$
	R	$-\sqrt{\frac{2J+3}{4(J+1)}}\cdot\tau_0$	$\sqrt{\frac{2J+3}{8(J+1)}}\tau_1$	$\sqrt{\frac{(2J+3)(2J+5)}{8(J+1)(2J+1)}}\cdot\tau_1$

$$|i\rangle_{@} = +X\Sigma_{1/2} \qquad (4\text{-}61)$$

Thus, from the Hund(a) → Hund(e) transformation Table 10.

$$\langle i \| \mu \| j=\tfrac{3}{2}, \ell=J+\tfrac{1}{2} \rangle = \langle X\Sigma_{1/2} \| \mu \| \Big\{ -\sqrt{(2J+3)/12J}\, B\Sigma$$

$$- \sqrt{(2J+3)/24J}\, T\pi_{1/2} + \sqrt{3(2J-1)/8J}\, \pi_{3/2} \Big\rangle$$

$$= \frac{J-1}{2J}\sqrt{\frac{2J+3}{3(J+1)}}\cdot \tau_1 \qquad (4\text{-}62)$$

on using the above Table 2.

The other matrix elements for this initial parity are evaluated in this same fashion.

2. Initial Parity State $P_i = (-1)^{J-1/2}$

Now the initial state has $\ell = J+1/2$, so that for this parity

$$|i\rangle_{@} = \sqrt{2}\,(-1)\, C(J\tfrac{1}{2}\, J+\tfrac{1}{2} \mid -\tfrac{1}{2}\, \tfrac{1}{2}\, 0) X\Sigma_{1/2} = -X\Sigma_{1/2} \qquad (4\text{-}63)$$

Thus, for example, for the R-branch $J_f = J+1$. For nonzero matrix elements for V_{rad}, we must have $P_f = (-1)^{J+1/2} = (-1)^{\ell_f+1}$, i.e. $\ell_f = J+3/2 \pmod 2 = J_f + 1/2 \pmod 2$. Consider the matrix element

$$\langle i \| \mu \| j=\tfrac{3}{2}, l_f = J_f + \tfrac{1}{2} \rangle = -\langle X\Sigma_{1/2} \| \mu \| \left\{ - (2J+5)/12(J+1)\ B\Sigma_{1/2} \right.$$

$$\left. - \quad (2J+5)/24(J+1).\pi_{1/2} + \ 3(2J+1)/8(J+1).\pi_{3/2} \right\} \rangle$$

$$= - \frac{\sqrt{(2J+3)(2J+5)}}{4.\sqrt{3}\ (J+1)} \left[\tau_0 + 2\tau_1 \right] \qquad (4\text{-}64)$$

The transition moments in the Hund (e) representation are given in Table 3.

TABLE 3

Radiative coupling matrix elements evaluated in a Hund (e) basis

$\langle i \Vert \mu \Vert j, 1 \rangle$	Q-branch, $P=(-1)^{J+1/2}$	P-branch, $P=(-1)^{J-1/2}$	R-branch, $P=(-1)^{J-1/2}$
$\langle i \Vert \mu \Vert 3/2, J+1/2 \rangle$	$\frac{J-1}{2J}\left[\frac{2J+3}{3(J+1)}\right]^{1/2}\tau_1$	$\sqrt{\frac{(2J-1)(2J+1)}{3J(J-1)}}\left[\frac{\tau_0}{4} - \frac{(J-1)}{2J+1}\tau_1\right]$	$-\sqrt{\frac{(2J+3)(2J+5)}{48(J+1)}}\left[\tau_0 + 2\tau_1\right]$
$\langle i \Vert \mu \Vert 1/2, J+1/2 \rangle$	$\frac{1}{2J}\sqrt{(2J-1)(J+1)}\,\tau_1$	$-\sqrt{\frac{(2J-3)(2J-1)}{J(J-1)}}\,\frac{\tau_0}{4}$	$\sqrt{\frac{2J+3}{2J+1}}\left[\frac{(J+1/2)\tau_0 - \tau_1}{2(J+1)}\right]$
$\langle i \Vert \mu \Vert 1/2, J+1/2 \rangle$	$\sqrt{\frac{(2J-1)(2J+3)}{12J(J+1)}}\,\tau_1$	$\sqrt{\frac{(2J-1)}{12J}}\left[\tau_0 + \tau_1\right]$	$-\sqrt{\frac{2J+3}{12(J+1)}}\left[\tau_0 - \tau_1\right]$
$\langle i \Vert \mu \Vert 3/2, J+3/2 \rangle$	$\frac{\sqrt{J(2J+3)}\,\tau_1}{2(J+1)}$	$\sqrt{\frac{2J-1}{2J+1}}\left[\frac{(2J+1)\tau_0 + 2\tau_1}{4J}\right]$	$-\sqrt{\frac{(2J+3)(2J+5)}{(J+1)(J+2)}}\,\frac{\tau_0}{4}$
$\langle i \Vert \mu \Vert 3/2, J-1/2 \rangle$	$\sqrt{\frac{2J-1}{3J}}\cdot\frac{(J+2)}{2(J+1)}\,\tau_1$	$-\sqrt{\frac{(2J-3)(2J-1)}{48J^2}}\left[\tau_0 + 2\tau_1\right]$	$\sqrt{\frac{(2J+1)(2J+3)}{3(J+1)(J+2)}}\left[\frac{\tau_0}{4} - \frac{(J+2)\tau_1}{(2J+1)}\right]$
$\langle i \Vert \mu \Vert 1/2, J-1/2 \rangle$	$-\frac{(2J+1)}{\sqrt{12J(J+1)}}\,\tau_1$	$\sqrt{\frac{(2J-1)}{12J}}\left[\tau_0 - \tau_1\right]$	$-\sqrt{\frac{2J+3}{12(J+1)}}\left[\tau_0 + \tau_1\right]$

CHAPTER 5

GORDON'S NUMERICAL TECHNIQUE

The close-coupled linear second order ordinary differential equations are solved by using Gordon's algorithm [33] which specifically avoids the usual numerical instabilities which arise when one is considering wavefunction behavior in classically forbidden regions. The basic idea is to subdivide the interatomic distance R into sufficiently small subintervals so that within these intervals we can approximate the given potential energy function to the desired accuracy by an appropriate polynomial which we call the "reference potential". Within each of these subintervals, the wavefunctions corresponding to the polynomial approximation can be found analytically. These subinterval eigenfunctions are then matched to each other at the subinterval end points. Thus this eigenfunction over the whole interatomic separation range R is piecewise analytic for our reference potential.

It is convenient to first describe Gordon's numerical method for the case of the uncoupled Schrodinger equation before turning to its extension to our close-coupled equations.

A. UNCOUPLED RADIAL EQUATION

Consider the one dimensional Schrodinger equation which in appropriate units can be written

$$\frac{d^2\psi}{dR^2}+[E-U(R)]\psi = 0 \qquad (5\text{-}1)$$

for a given potential U(R). We now partition the radial interval $[0,\infty)$ and within each of these subintervals a sufficiently simple "reference potential" $U_o(R)$ which not only approximates the given potential U(R) in this subinterval, but which allows an analytic solution to the Schrodinger equation (5-1). For example, in Figure 4a, we have chosen the reference potential $U_o(R)$ to be constant throughout each subinterval, the constant in the case shown in Figure 4a has been chosen to be the value of the given potential U(R) at the mid-point of each subinterval. Of course, more sophisticated choices of the values of this piecewise constant reference potential can be made, but we can immediately write down the analytic solution for this reference problem: In the "classicially allowed" region the reference wavefunction has oscillating trigonometric solutions, while in the "classically forbidden" regions the reference solutions are exponential functions. Another choice of reference potential is shown in Figure 4b. In this case we have a piecewise linear fit which in Figure 4b has been chosen to be the line tangent passing through the midpoint of each subinterval. Again, there is considerable

FIGURE 4

Simple choices of reference potentials for use in Gordon's algorithm
(a) piecewise constant potential
(b) piecewise linear potential

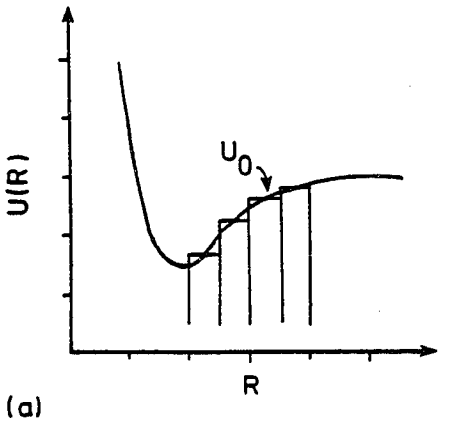

(a)

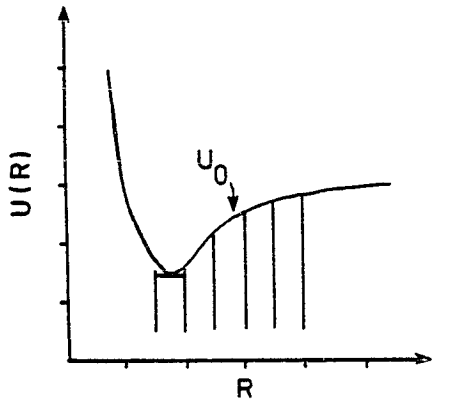

(b)

flexibility in the choice of this piecewise linear reference potential. The resulting Schrodinger equation is exactly soluable in terms of Airy functions.

In any case, we choose a particular reference potential $U_o(R)$ such that analytically we can determine the two linearly independent (exact) reference solutions A(R) and B(R):

$$A''(R)+[E-U_o(R)]A(R)=0$$

$$B''(R)+[E-U_o(R)]B(R)=0 \qquad (5\text{-}2)$$

where primes denote differentiation with respect to R. The Wronskian W of these reference solutions is a non-zero constant since A(R) and B(R) are linearly independent

$$W = \begin{vmatrix} A(R) & B(R) \\ A'(R) & B'(R) \end{vmatrix} = \text{constant, for all R} \qquad (5\text{-}3)$$

(This can be easily shown by evaluating W'(R), and eliminating A"(R) and B"(R) by using equation (5-2).)

Consider the following "mixed" Wronskians

$$b(R) = 1/W \begin{vmatrix} A(R) & \psi(R) \\ A'(R) & \psi'(R) \end{vmatrix}$$

$$a(R) = 1/W \begin{vmatrix} B(R) & \psi(R) \\ B'(R) & \psi'(R) \end{vmatrix} \qquad (5\text{-}4)$$

which for convenience are normalized by W from equation (5-3). Since ψ satisfies equation (5-1) while A and B satisfy equation (5-2), these mixed Wronskians b(R) and a(R), will be slowly varying functions of R, and they will have slower and slower radial variation as the reference potential $U_o(R)$ gets more and more accurate in its representation of the given potential U(R). This can be easily seen algebraically by differentiating equation (5-4) to give

$$b'(R) = (A(R)/W)\,[U(R)-U_o(R)]\psi(R)$$

$$a'(R) = -(B(R)/W)\,[U(R)-U_o(R)]\psi(R) \qquad (5\text{-}5)$$

From equations (5-4) and (5-5) we can immediately write the required eigenfunctions and its derivative in terms of these reference solutions and slowly varying Wronskians

$$\psi(R)=A(R)a(R)+B(R)b(R)$$
$$\psi'(R)=A'(R)a(R)+B'(R)b(R), \qquad (5\text{-}6)$$

It can be seen these mixed Wronskians, a(R) and b(R), are just the expansion coefficients for the representation of the required "exact" eigenfunction ψ (R) in terms of the approximate reference solution basis A(R), B(R). These expansion coefficients can be determined from the closed pair of coupled linear first-order differential equations

$$a'(R)= -(B(R)/W)\ [U(R)-U_o(R)][A(R)a(R)+B(R)b(R)]$$
$$b'(r)=(A(R)/W)\ [U(R)-U_o(R)][A(R)a(R)+B(R)b(R)], \qquad (5\text{-}7)$$

which result from substituting equation (5-6) for ψ in equation (5-5).

The beauty of Gordon's idea lies in the fact that the expansion coefficients a(R) and b(R) are slowly varying functions of R. Indeed, if the reference potential $U_o(R)$ is chosen to coincide with the given potential U(R) at the mid-point $\bar{R}$ of each subinterval, as in Figure 4a, then from equation (5-7), we see that

$$a'(\bar{R}) = 0 = b'(\bar{R}) \qquad (5\text{-}8)$$

For sufficiently small subintervals a(R), b(R) should be slowly varying. Such behavior is in sharp contrast to the original Schrodinger equation, equation (5-1), which typically has rapidly oscillating wavelike solutions which are notoriously difficult to handle accurately on the computer.

B. SYSTEM OF COUPLED RADIAL EQUATIONS

Consider a system of N coupled radial equations of the form

$$\sum_{n=1}^{N} [(\frac{d^2}{dR^2} + E)\delta_{mn} - U_{mn}(R)]\psi_n(R) = 0, \quad m=1,\ldots,N \qquad (5\text{-}9)$$

These equations can be put in matrix form for the "channel" wavefunction vector

$$\underline{\underline{\psi}}(R) = \begin{bmatrix} \psi_1(R) \\ \psi_2(R) \\ \vdots \\ \psi_N(R) \end{bmatrix}$$

$$[(\frac{d^2}{dR^2} + E)\underline{\underline{1}} - \underline{\underline{U}}(R)]\underline{\underline{\psi}}(R) = 0, \qquad (5\text{-}10)$$

a form totally analogous to the scalar problem of section (A), equation (1). Thus proceeding analogously to section (A) we will generate an eigenvector $\underline{\underline{\psi}}$. Since we are dealing

only with scattering states, we can introduce a diagonal matrix of real wave vectors representing the asymptotic atomic channels

$$\underline{\underline{k}}=(k_{ij}\,\delta_{ij}), \quad i,j=1,\ldots,N, \quad k_{ii}=\sqrt{E-U_{ii}\,(R\to\infty)}, \quad (5\text{-}11)$$

$$k_{ii}^2 > 0, \text{for each } i=1,\ldots,N$$

The boundary conditions on the scattering wavefunction are regularity at the origin,

$$\underline{\underline{\psi}}\,(R=0)=0 \quad (5\text{-}12)$$

and asymptotically, as $R\to\infty$

$$\underline{\underline{\psi}} \longrightarrow \underline{\underline{J}}-\underline{\underline{N}}k^{-1/2}\,\underline{\underline{R}}k^{1/2} \quad (5\text{-}13)$$

whose $\underline{\underline{J}}$ and $\underline{\underline{N}}$ diagonal matrices, whose diagonal elements are the spherical Bessel (regular) and Neumann (irregular) functions, respectively. $\underline{\underline{R}}$ is the reactance matrix to be determined.

The usual numerical technique to determine the reactance matrix $\underline{\underline{R}}$ and the $\underline{\underline{S}}$ matrix is to integrate N solution vectors, all of which satisfy equation (5-12) near the origin but have N linearly independent initial derivative vectors. The initial radial integration point is so chosen that the channel wave number $k_{ii}^2\,(R)=E-U_{ii}\,(R)$

first becomes non-negative (it should be remembered that $U_{ii} >> 1$ as $R \to 0$). Typically, this initial radial point varies with i as i=1,...,N. After integrating these N solution vectors into the far asymptotic region R>>1 we obtain a wavefunction matrix with the general asymptotic form

$$\underline{\underline{\psi_o}} = \underline{\underline{J}}\,\underline{\underline{X}} - \underline{\underline{N}}\,\underline{\underline{Y}}, \tag{5-14}$$

for some constant matrices $\underline{\underline{X}}$ and $\underline{\underline{Y}}$. These constant matrices are determined from equation (5-14) and its derivative:

$$\begin{aligned} \underline{\underline{X}} &= [\underline{\underline{J}}\,\underline{\underline{N}}' - \underline{\underline{N}}\,\underline{\underline{J}}']^{-1} [\underline{\underline{N}}'\underline{\underline{\psi_o}} - \underline{\underline{N}}\,\underline{\underline{\psi_o}}'] \\ \underline{\underline{Y}} &= [\underline{\underline{J}}\,\underline{\underline{N}}' - \underline{\underline{N}}\,\underline{\underline{J}}']^{-1} [\underline{\underline{J}}'\underline{\underline{\psi_o}} - \underline{\underline{J}}\,\underline{\underline{\psi_o}}'] \end{aligned} \tag{5-15}$$

Now from equation (5-14), multiplying on the right by $\underline{\underline{X}}^{-1}$, we obtain

$$\underline{\underline{\psi_o}}\,\underline{\underline{X}}^{-1} = \underline{\underline{J}} - \underline{\underline{N}}\,\underline{\underline{Y}}\,\underline{\underline{X}}^{-1} \tag{5-16}$$

Comparing equations (5-13) and (5-16), we immediately find $\underline{\underline{N}}\underline{\underline{k}}^{-1/2}\,\underline{\underline{R}}\underline{\underline{k}}^{1/2} = \underline{\underline{N}}\,\underline{\underline{Y}}\,\underline{\underline{X}}^{-1}$, i.e.

$$(\underline{\underline{k}}^{1/2}\,\underline{\underline{X}})^{T}\,\underline{\underline{R}}=(\underline{\underline{k}}^{1/2}\,\underline{\underline{Y}}) \qquad (5\text{-}17)$$

with T denoting the matrix transpose. The scattering matrix $\underline{\underline{S}}$ is related to the $\underline{\underline{R}}$ matrix by

$$\underline{\underline{S}}=(\underline{\underline{1}}+i\underline{\underline{R}})(\underline{\underline{1}}-i\underline{\underline{R}}) \qquad (5\text{-}18)$$

CHAPTER 6

CROSS SECTIONS

We now consider the cross sections for the laser induced collisions

$$Na(^2S_{1/2})+Ar+n_o\,h\nu \rightarrow Na(^2P_{1/2,3/2})+Ar+(n_o-1)h\nu \qquad (6\text{-}1)$$

assuming that the time-independent Schrodinger equation

$$H_{tot}\,\Psi = E\,\Psi \qquad (6\text{-}2)$$

can be invoked, with the total Hamiltonian

$$H_{tot} = -\frac{1}{2\mu}\nabla_R^2 + H_a + H_{rad} + V_{rad}\,. \qquad (6\text{-}3)$$

In equation (6-3), H_a is the atomic sodium Hamiltonian with space-fixed eigenfunction $|jm_j\rangle$

$$H_a\,|jm_j\rangle = \epsilon_j\,|jm_j\rangle\,. \qquad (6\text{-}4)$$

As discussed earlier , $H_{tot} - V_{rad}$ is separable asymptotically as $R \to \infty$. On separating out the radial and angular parts of the kinetic energy operator ∇_R^2 , we have

$$\nabla_R^2 = \frac{\partial^2}{\partial R^2} + \frac{2}{R}\frac{\partial}{\partial R} - \frac{1}{R^2}\vec{L}_R^2 \quad . \tag{6-5}$$

It is customary to designate the eigenstates of the nuclear angular momentum, $\vec{L}_R^2$, and the sodium atom Hamiltonian, H_a, as the channel states (Mies[2]). In particular, it is convenient to introduce the partial-wave representation $|JMj\ell\rangle$, where $\ell(\ell+1)$ is the eigenvalue of $\vec{L}_R^2$, since asymptotically $H_{tot} - V_{rad}$ commutes with $\vec{L}_R^2$. $\vec{j}$ is the total electronic sodium angular momentum. We can represent the total wavefunction in the channel representation by

$$\Psi = \Psi_{j\ell n_o}^{JME} = \sum_{\substack{J'M' \\ j'\ell' n_o'}} |\vec{R}, J'M'j'\ell', n_o'\rangle \frac{i}{R} F_{J'M'j'\ell' n_o'}^{JMj\ell n_o}(R) \tag{6-6}$$

The close-coupled equations take the form

$$\langle R, \alpha' | H - E | \Psi_{j\ell n_o}^{JME} \rangle = 0 \tag{6-7}$$

where we introduce the abbreviation

$$|\alpha\rangle = |JMj\ell, n_o\rangle . \tag{6-8}$$

Thus, from equation (6-6),

$$\sum_{\alpha''} \langle R,\alpha' \left| -\frac{1}{2\mu}\nabla^2 + H_a + H_{rad} + V_{rad} - E \right| R,\alpha'' \rangle \frac{1}{R} F^{\alpha}_{\alpha''}(R) = 0 \qquad (6\text{-}9)$$

While the radiation field H_{rad} is diagonal in this representation, the nuclear kinetic energy operator $-\nabla_R^2/2\mu$ acts on both $|\vec{R},\alpha\rangle$ as well as on the close-coupling coefficients $F^{\alpha}_{\alpha''}(R)$. Because of the low (room temperature) energies involved it is expected (DeVries and George [8], Mies[10]) that the important radial dependence occurs in the coupling coefficients $F^{\alpha}_{\alpha''}(R)$ rather than in the radial change of the actual wavefunction $|R,\alpha\rangle$. Thus

$$\langle \vec{R},\alpha' \left| -\frac{1}{2\mu}\nabla_R^2 \right| \vec{R},\alpha'' \rangle \frac{F^{\alpha}_{\alpha''}(R)}{R} = -\left[\frac{d^2}{dR^2} + \frac{2}{R}\frac{d}{dR} - \frac{l''(l''+1)}{R^2}\right] \frac{F^{\alpha}_{\alpha''}(R)}{2\mu R} \cdot \delta_{\alpha'\alpha''} \qquad (6\text{-}10)$$

Asymptotically, as $R \to \infty$,

$$\delta_{\alpha'\alpha''}\left[\frac{d^2}{dR^2} + \frac{2}{R}\frac{d}{dR} - \frac{l''(l''+1)}{R^2} + k_j^2\right] \frac{F^{\alpha}_{\alpha''}(R)}{R} = 0 \qquad (6\text{-}11)$$

where k_j^2, the wavenumber squared, is given by

$$k_j^2 = 2\mu[E - \epsilon_j - n_0 h\nu]. \qquad (6\text{-}12)$$

If $k_j^2 > 0$ then equation (6-11) yields a spherical Bessel function solution with real argument, i.e. scattering boundary conditions can be imposed so that asymptotically

one can deduce the $\underline{\underline{T}}$-matrix from the radial coefficients $F^{\alpha}_{\alpha''}$:

$$\frac{1}{R} F^{JM_j \ell n_0}_{J''M_j'' \ell'' n_0''}(R) \xrightarrow[R\to\infty]{} \delta_{\alpha''\alpha} j_\ell(k_j R) - \frac{i}{2}\left(\frac{k_{j''}}{k_j}\right)^{1/2} T^{\alpha}_{\alpha''} h_{\ell''}(k_{j''} R) \qquad (6\text{-}13)$$

where the spherical Bessel functions have the asymptotic property

$$j_\ell(k_j R) \xrightarrow[R\to\infty]{} \sin(k_j R - \frac{\ell\pi}{2}) \frac{1}{k_j R} \qquad (6\text{-}14)$$

$$h_{\ell''}(k_{j''} R) \xrightarrow[R\to\infty]{} \frac{-i}{k_{j''} R} \exp[i(k_{j''} R - \frac{\ell''\pi}{2})] \qquad (6\text{-}15)$$

Channels with $k_j^2 > 0$ are called open channels and these channels directly affect the $\underline{\underline{T}}$-matrix. Channels with $k_j^2 < 0$ are called closed channels, and because of irregular asymptotic behavior, they do not contribute directly to the scattering matrix $\underline{\underline{S}} = \underline{\underline{1}} - \underline{\underline{T}}$. Nevertheless, they can indirectly effect the $\underline{\underline{S}}$-matrix and Mies [10] has extended the close-coupling theory to allow for these effects. This extension is discussed in Ref. [10]. But for the NaAr problem we need deal only with open channels.

A. SCATTERING AMPLITUDE

Working in an atomic basis, we express the wave-function as a superposition of Hund (e) basis wave functions

$$\Psi_{j m_j n_0} = \sum_{JMl} \Psi^{JME}_{jl n_0} \cdot \mathcal{C}^{j m_j n_0}_{JMl} \qquad (6\text{-}16)$$

where the coefficients $\mathcal{C}$ are so chosen so that asymptotically

$$\Psi_{j m_j n_0} \xrightarrow[R\to\infty]{} \exp[i\vec{k}_j \cdot \vec{R}] \left| R j m_j, n_0 \right\rangle$$

$$+ \sum_{j' m_j' n_0'} f^{j m_j n_0}_{j' m_j' n_0'} \left(\frac{k_j}{k_{j'}}\right)^{1/2} \frac{e^{i k_{j'} R}}{R} \left| R j' m_j' \right\rangle, \qquad (6\text{-}17)$$

i.e. asymptotically Ψ has a contribution from the incident plane wave $\exp[i\vec{k}_j \cdot \vec{R}]$ and a contribution coming from the spherically outgoing wave $\exp[ik_{j'}R]/R$. The extra factor $(k_j/k_{j'})^{1/2}$ and the summation Σ arises since the scattering is inelastic. f is the familiar scattering amplitude.

We now detemine the coefficients $\mathcal{C}^{j m_j n_0}_{JME}$ such that equation (6-16) asymptotically tends to equation (6-17). Consider, in particular, the incident plane wave and expand it as an identity in terms of spherical harmonics

$$\exp[i\vec{k}_j \cdot \vec{R}] = 4\pi \sum_{l=0}^{\infty} \sum_{m_l=-l}^{l} i^l j_l(k_j R) . Y_{l m_l}(\hat{R}) . Y^*_{l m_l}(\hat{k}) \qquad (6\text{-}18)$$

where $\vec{R}=(R,\hat{R})$ and $\vec{k}=(k,\hat{k})$--i.e. $\hat{R}$ and $\hat{k}$ are the respective angles for the vectors $\vec{R}$ and $\vec{k}$ in spherical polar coordinates. From equations (6-6), (6-16) and (6-17) we have

$$4\pi \sum_{l=0}^{\infty} \sum_{m_j=-l}^{l} i^l j_l(k_j R) Y_{l m_l}(\hat{R}) Y^*_{l m_l}(\hat{k}) \left| R j m_j n_o \right\rangle = \sum_{JM l} \sum_{J' M' l' j' n_o'} C^{j m_j n_o}_{JM l}$$

$$\cdot \delta_{JJ'} \cdot \delta_{MM'} \cdot \delta_{ll'} \cdot \delta_{jj'} \cdot \delta_{n_o n_o'} \cdot j_l(k_j R) \left| R J' M' j' l' n_o' \right\rangle$$

$$= \sum_{\substack{JMl \\ m_j'}} C^{j m_j n_o}_{JM l'} \cdot j_l(k_j R) C(l j J | M - m_j', m_j', M)\, Y_{l, M-m_j'}(\hat{R}) \left| R j m_j' n_o \right\rangle, \qquad (6\text{-}19)$$

where we have expanded the channel state in terms of the spherical harmonic eigenfunctions of $\vec{L}_R^2$ and the atomic state $|jm_j\rangle$

$$\left| R J' M' j' l', n_o \right\rangle = \sum_{m_l, m_j'} C(l j J | m_l m_j', M) Y_{l m_l}(\hat{R}) \left| R j m_j' n_o \right\rangle \qquad (6\text{-}20)$$

Here $C(l j J | m_l m_j' M)$ is the usual Clebsch-Gordon coefficient. In equation (6-19), the orthogonality of the states $|Rjm_j, n_o\rangle$ requires $m_j = m_j'$, with $M - m_j = m_l$. From the orthogonality of the spherical harmonics $Y_{l m_l}(\hat{R})$ we get

$$4\pi i^l Y^*_{l m_l}(\hat{k}_j) = \sum_{JM} C^{j m_j n_o}_{JM l} C(l j J | M - m_j, m_j, M). \qquad (6\text{-}21)$$

Since

$$\sum_{j,M} C(l j J | m_l m_j' M) C(l j J | M - m_j, m_l, M) = \delta_{m_l, M - m_j} \cdot \delta_{m_j m_j'}, \qquad (6\text{-}22)$$

we can finally determine the coefficient $C^{j m_j n_o}_{JM l}$ from equation (6-21)

$$\mathcal{C}^{j m_j n_0}_{J M \ell} = 4\pi i^{\ell} \cdot Y^{*}_{\ell, M-m_j}(\hat{k}_j)\, C(\ell j J \,|\, M-m_j, m_j, M) \qquad (6\text{-}23)$$

We now turn to the scattering spherical wave part of the wavefunction $\Psi_{j m_j n_0}$. From equations (6-6), (6-13), (6-16) and (6-17) we have

$$\sum_{j' m_j' n_0'} f^{j m_j n_0}_{j' m_j' n_0'} \left(\frac{k_j}{k_{j'}}\right)^{1/2} \frac{e^{i k_{j'} R}}{R} \,|R j' m_j'\rangle = \sum_{J M \ell} \sum_{J' M' \ell' j' n_0'} \mathcal{C}^{j m_j n_0}_{J M \ell} \,(-1/2).\left(\frac{k_{j'}}{k_j}\right)^{1/2}$$

$$T^{\alpha}_{\alpha'} (-i)^{\ell'+1} \frac{e^{i k_{j'} R}}{k_{j'} R} \sum_{m_j'} C(\ell' j' J' \,|\, M'-m_j', m_j', M')$$

$$Y_{\ell', M'-m_j'}(\hat{R}) \,|R j' m_j'\rangle .$$

Since the set $|R j' m_j', n_0\rangle$ is orthogonal, we have

$$f^{j m_j n_0}_{j' m_j' n_0'} \left(\frac{k_j}{k_{j'}}\right)^{1/2} = -\frac{1}{2} \sum_{\substack{J M \ell \\ J' M' \ell'}} \mathcal{C}^{j m_j n_0}_{J M \ell} \left(\frac{k_{j'}}{k_j}\right)^{1/2} T^{\alpha}_{\alpha'} \,(+i)^{-\ell'-1} \frac{1}{k_{j'}}$$

$$C(\ell' j' J' \,|\, M'-m_j', m_j', M')\; Y_{\ell', M'-m_j'}(\hat{R})$$

Hence, from equation (6-23), the scattering amplitude is given by

$$f^{j m_j n_0}_{j' m_j' n_0'} = 2\pi i \sum_{\substack{J M \ell \\ J' M' \ell'}} \frac{i^{\ell-\ell'}}{k_j}\; C(\ell j J \,|\, M-m_j, m_j, M) \cdot C(\ell' j' J' \,|\, M'-m_j', m_j', M') \cdot$$

$$Y^{*}_{\ell, M-m_j}(\hat{k}_j) \cdot Y_{\ell', M'-m_j'}(\hat{R}) \cdot T^{J m_j \ell n_0}_{J' M' j' \ell' n_0'} \qquad (6\text{-}24)$$

B. CROSS SECTIONS

The differential scattering cross section is obtained

immediately from equation (6-24)

$$\frac{d\sigma}{d\Omega}(\hat{k}_j,\hat{R}) = \left|f^{j m_j n_0}_{j' m_j' n_0'}(\hat{k}_j,\hat{R})\right|^2$$

$$= \frac{(2\pi)^2}{k_j^2}\sum_{JM\ell} Y^*_{\ell,M-m_j}(\hat{k}_j)\cdot C(\ell jJ|M-m_j,m_j,M)\cdot \sum_{\tilde{J}\tilde{M}\tilde{\ell}}$$
$$Y_{\tilde{\ell},\tilde{M}-m_j}(\hat{k}_j)\cdot C(\tilde{\ell}\, j\tilde{J}|\tilde{M}-m_j,m_j,\tilde{M})\cdot \sum_{J'M'\ell'}$$

$$Y_{\ell',M'-m_j'}(\hat{R})\cdot C(\ell' j' J'|M'-m_j',m_j',M')\cdot \sum_{\tilde{J}'\tilde{M}'\tilde{\ell}'}$$
$$Y^*_{\tilde{\ell}',\tilde{M}'-m_j'}(\hat{R})\cdot C(\tilde{\ell}' j' \tilde{J}'|M'-m_j',m_j',M')$$

$$T^{JM_j\ell n_0}_{J'M_j'\ell' n_0'}\cdot T^{*\,\tilde{J}\tilde{M}\tilde{j}\tilde{\ell}n_0}_{\tilde{J}'\tilde{M}'\tilde{j}'\tilde{\ell}'\tilde{n}_0'} \qquad (6\text{-}25)$$

Equation (6-25) gives the differential scattering cross section for an incident beam initial angle $\hat{k}_j$ into the solid angle $\hat{R}$, $\hat{R}+d\hat{R}$.

1. Total Cross Section

The total cross section is obtained by integrating equation (6-25) over all final angles $\hat{R}$.

$$\sigma^{j m_j n_0}_{j' m_j' n_0'}(\hat{k}_j) = \int d\hat{R}\ \left|f^{j m_j n_0}_{j' m_j' n_0'}(\hat{k}_j,\hat{R})\right|^2 \qquad (6\text{-}26)$$

From equation (6-25) we see that the integration over the final angles $\hat{R}$ affects only the two spherical harmonic terms, giving the orthogonality condition

$$\int d\hat{R}\; Y_{\ell',M'-m_j'}(\hat{R}) \cdot Y^{*}_{\tilde{\ell}',\tilde{M}'-\tilde{m}_j'}(\hat{R}) = \delta_{\ell'\tilde{\ell}'} \cdot \delta_{M'\tilde{M}'} \qquad (6\text{-}27)$$

Thus, the total cross section becomes

$$\sigma^{jm_j n_0}_{j'm_j'n_0'}(\hat{k}_j) = \frac{(2\pi)^2}{k_j^2} \sum_{JM\ell} Y^{*}_{\ell,M-m_j}(\hat{k}_j) \cdot C(\ell jJ|M-m_j,m_j,M) \cdot \sum_{\tilde{J}\tilde{M}\tilde{\ell}}$$

$$Y_{\tilde{\ell},\tilde{M}-m_j}(\hat{k}_j) \cdot C(\tilde{\ell} j\tilde{J}|\tilde{M}-m\ ,m\ ,\tilde{M}) \cdot \sum_{\substack{J'M'\ell' \\ \tilde{J}'}} C(\ell' j' J'|M'-m_j',m_j',M') \cdot$$

$$C(\ell' j' \tilde{J}'|M'-m_j',m_j',M') \cdot T^{JMj\ell n_0}_{J'M'j'\ell'n_0'} \cdot T^{*\,\tilde{J}\tilde{M}j\tilde{\ell}n_0}_{\tilde{J}'\tilde{M}'j'\tilde{\ell}'n_0'} \qquad (6\text{-}28)$$

2. Average Cross Section

Since we are dealing with the experimental situation of a random beam interaction between the Na atom and the rare gas atom, we should also average over the initial incident angle $\hat{k}_j$:

$$\bar{\sigma}^{jm_j n_0}_{j'm_j'n_0'} = \int d\hat{k}_j\, \sigma^{jm_j n_0}_{j'm_j'n_0'}(\hat{k}_j) \qquad (6\text{-}29)$$

Again, the orthogonality condition of the spherical harmonics (this time over the incident angles $\hat{k}_j$) yields

$$\int d\hat{k}_j\; Y^{*}_{\ell,M-m_j}(\hat{k}_j) \cdot Y_{\tilde{\ell},\tilde{M}-m_j}(\hat{k}_j) = \delta_{\ell\tilde{\ell}} \cdot \delta_{M\tilde{M}} \qquad (6\text{-}30)$$

From equations (6-29) and (6-28) the average cross section can be written

$$\bar{\sigma}^{j m_j n_0}_{j' m_j' n_0'} = \frac{\pi}{k_j^2} \sum_{J M \ell \tilde{J}} C(\ell j J | M - m_j, m_j, M) \cdot C(\ell j \tilde{J} | M - m_j, m_j, M) \cdot$$

$$\sum_{\substack{J' M' \ell' \\ \tilde{J}'}} C(\ell' j' J' | M' - m_j', m_j', M') \cdot C(\ell' j' \tilde{J}' | M' - m_j', m_j', M') \cdot$$

$$T^{J M j \ell n_0}_{J' M' j' \ell' n_0'} \cdot T^{* \tilde{J} \tilde{M} j \tilde{\ell} n_0}_{\tilde{J}' \tilde{M}' j' \ell' n_0'} \qquad (6\text{-}31)$$

3. Degeneracy Averaged Cross Section

On averaging equation (6-31) over the initial degeneracy we have

$$\bar{\bar{\sigma}}^{j n_0}_{j' m_j' n_0'} = \frac{1}{2j+1} \sum_{m_j} \bar{\sigma}^{j m_j n_0}_{j' m_j' n_0'} \qquad (6\text{-}32)$$

We immediately obtain, from the orthogonality of the Clebsch-Gordon coefficients

$$\sum_{m_j} C(\ell j J | M - m_j, m_j, M) C(\ell j \tilde{J} | M - m_j, m_j, M) = \delta_{J \tilde{J}} \qquad (6\text{-}33)$$

Finally, on summing over the final m_j -states, we find

$$\sum_{m_j'} C(\ell' j' J' | M' - m_j', m_j', M') \cdot C(\ell' j' J' | M' - m_j', m_j', M') = \delta_{J' \tilde{J}'} \qquad (6\text{-}34)$$

From equations (6-32)-(6-34), the degeneracy averaged cross section becomes

$$\tilde{\sigma}^{j n_o}_{j' n_o'} = \sum_{m_j'} \bar{\bar{\sigma}}^{j n_o}_{j' m_j' n_o'}$$

$$= \frac{\pi}{k_j^2} \frac{1}{2j+1} \sum_{\substack{JM\ell \\ J'M'\ell'}} \left| T^{JMj\ell n_o}_{J'M'j'\ell' n_o'} \right|^2 \qquad (6\text{-}35)$$

C. NUMERICAL DETERMINATION OF CROSS SECTIONS

1. Degeneracy Averaged Cross Section

Since the molecular dipole operator μ_o^{sp} is a spherical tensor operator (Rose [32]) of rank 1 and since the basis set $|\alpha\rangle = |JMj\ell n_o\rangle$ is an eigenfunction of the molecular angular momentum $\vec{L}_R^2$, we can apply the Wigner- Eckart Theorem to $\langle \alpha | V_{rad} | \alpha' \rangle$. The Wigner-Eckart Theorem separates the generic aspects of an operator from its pecularities that relate to the physical measurement under study. The geometric aspects with their dependence on M, M' are separated from the "physics of the problem" carried in the reduced matrix elements which are independent of M,M' . Thus, from equation (6-25), the degeneracy averaged cross section for linear polarized radiation field is

$$\tilde{\sigma}^{jn_o}_{j'n_o'} = \frac{\pi}{k_j^2}\cdot\frac{1}{2j+1}\sum_{\substack{J\Pi\ell\\ J'\ell'}} C^2(J'1J\,|\,MOM)\left|T^{Jj\ell}_{J'j'\ell'}\right|^2 \qquad (6\text{-}36)$$

since for linearly polarized light the Clebsch-Gordon coefficient $C(J_f\,1J\,|\,M_f\,OM)$ is non-zero only if $M_f=M$. The reduced matrix is contained within $\left|T^{Jj\ell}_{J'j'\ell'}\right|^2$ which is numerically computed by the close-coupled code.

Consider an e-parity initial state, so that $\ell=J+\frac{1}{2}$. Since only one photon is absorbed, the Clebsch-Gordon coefficient in equation (6-36) is non-zero only if J'=J-1 (P branch),or J'=J (Q branch),or J'=J+1 (R branch). The allowed ' must satisfy

	P branch	Q branch	R branch	
$\ell'=$	$J-\frac{3}{2}$	$J+\frac{1}{2}$	$J+\frac{1}{2}$	$j'=\frac{1}{2}$
	$J-\frac{3}{2}$	$J-\frac{3}{2}$	$J+\frac{1}{2}$	
	$J+\frac{1}{2}$	$J+\frac{1}{2}$	$J+\frac{5}{2}$	$j'=\frac{3}{2}$

(6-37)

with $\ell=J+\frac{1}{2}$. Using equation (6-37) in (6-36) we can write the degeneracy averaged cros section as

$$\tilde{\sigma}\left(j=\tfrac{1}{2}\rightarrow j'=\tfrac{1}{2}\right) = \frac{\pi}{k_j^2}\cdot\frac{1}{2j+1}\sum_{J\Pi}\delta_{\ell,J+\frac{1}{2}}\Big[\,\delta_{\ell',J+\frac{1}{2}}\Big|$$

$$C^2(J+1,1,J\,|\,MOM)\cdot\left|T^{Jj\ell}_{J+1\;j'\ell'}(R)\right|^2 + C^2(J1J\,|\,MOM)\cdot\left|T^{Jj\ell}_{J\;j'\ell'}(Q)\right|^2\Big\}$$

$$+\; C^2(J-1,1,J\,|\,MOM)\cdot\delta_{\ell',J-\frac{3}{2}}\left|T^{Jj\ell}_{J-1\;j'\ell'}(P)\right|^2\Big]$$

From tables of Clebsch-Gordon coefficients, this equation simplifies to

$$\tilde{\sigma}(\tfrac{1}{2}\to\tfrac{1}{2}) = \frac{\pi}{k_j^2}\frac{1}{2j+1}\sum_J \delta_{\ell,J+\frac{1}{2}}\left\{\delta_{\ell',J+\frac{1}{2}}\left[\frac{|T(R)|^2}{(J+1)(2J+3)}\sum_{M=-J}^{J}[(J+1)^2-M^2]\right.\right.$$

$$\left.\left.+\frac{|T(Q)|^2}{J(J+1)}\sum_M M^2\right] + \delta_{\ell',J-\frac{1}{2}}\frac{|T(P)|^2}{J(2J-1)}\sum_M [J^2-M^2]\right\} \qquad (6\text{-}38)$$

since the only M-dependence arises from the Clebsch-Gordon coefficients. Now

$$\sum_{M=-J}^{J} M^2 = J(J+1)(2J+1)/3 \quad ,$$

so that

$$\sum_{M=-J}^{J}[(J+1)^2-M^2] = (J+1)(2J+1)(2J+3)/3$$

$$\sum_{M=-J}^{J}[J^2-M^2] = J(2J-1)(2J+1)/3 \quad .$$

Hence the degeneracy averaged cross section for the transition of $j=\frac{1}{2} \to j'=\frac{1}{2}$ is given by

$$\tilde{\sigma}(j=\tfrac{1}{2}\to j'=\tfrac{1}{2}) = \frac{1}{3}\cdot\frac{\pi}{k_j^2}\cdot\frac{1}{2j+1}\sum_J \delta_{\ell,J+\frac{1}{2}}\,(2J+1)\left\{\delta_{\ell',J+\frac{1}{2}}\left[\left|T^{J\,\frac{1}{2}\,\ell}_{J+1\;\frac{1}{2}\;\ell'}(R)\right|^2\right.\right.$$

$$+\left|T^{J\frac{1}{2}\ell}_{J\,\frac{1}{2}\ell'}(Q)\right|^2\Big] \quad + \delta_{\ell',J-3/2}\left|T^{J\frac{1}{2}\ell}_{J-1\,\frac{1}{2}\ell'}(P)\right|^2\Bigg\} \tag{6-39}$$

Now consider the degeneracy averaged cross section for the transition of $j=\frac{1}{2} \longrightarrow j'=\frac{3}{2}$. From equations (6-37) and (6-36),

$$\tilde{\sigma}\left(j=\tfrac{1}{2} \rightarrow j'=\tfrac{3}{2}\right) = \frac{\pi}{k_j^2}\frac{1}{2j+1}\sum_{J,M}\delta_{\ell,J+\frac{1}{2}}\Bigg\{\delta_{\ell',J-3/2}\cdot$$

$$\left[C^2(J1J|MOM)\cdot\left|T^{J\frac{1}{2}\ell}_{J\,\frac{3}{2}\ell'}(Q)\right|^2 + C^2(J-1,1,J|MOM)\left|T^{J\frac{1}{2}\ell}_{J-1\,\frac{3}{2}\ell'}(P)\right|^2\right]$$

$$+\delta_{\ell',J+\frac{1}{2}}\left[C^2(J1J|MOM)\cdot\left|T^{J\frac{1}{2}\ell}_{J\,\frac{3}{2}\ell'}(Q)\right|^2 + C^2(J-1,1,J|MOM)\cdot\left|T^{J\frac{1}{2}\ell}_{J-1\,\frac{3}{2}\ell'}(P)\right|^2\right.$$

$$\left. + C^2(J+1,1,J|MOM)\cdot\left|T^{J\frac{1}{2}\ell}_{J+1\,\frac{3}{2}\ell'}(R)\right|^2\right]$$

$$+\delta_{\ell',J+\frac{5}{2}}\cdot C^2(J+1,1,J|MOM)\cdot\left|T^{J\frac{1}{2}\ell}_{J+1\,\frac{3}{2}\ell'}(R)\right|^2\Bigg\}$$

$$= \frac{\pi}{k_j^2}\cdot\frac{1}{2j+1}\sum\delta_{\ell,J+\frac{1}{2}}\Bigg\{\delta_{\ell',J-3/2}\left[\frac{M^2}{J(J+1)}|T(Q)|^2 + \frac{J^2-M^2}{J(2J-1)}|T(P)|^2\right]$$

$$+\delta_{\ell',J+\frac{1}{2}}\left[\frac{M^2}{J(J+1)}|T(Q)|^2 + \frac{J^2-M^2}{J(2J-1)}|T(P)|^2 + \frac{(J+1)^2-M^2}{(J+1)(2J+3)}|T(R)|^2\right]$$

$$+\delta_{\ell',J+\frac{5}{2}}\cdot\frac{(J+1)^2-M^2}{(J+1)(2J+3)}|T(R)|^2\Bigg\} \tag{6-40}$$

Again, the M-summation can be performed immediately to give

$$\tilde{\sigma}\left(j=\tfrac{1}{2} \rightarrow j'=\tfrac{3}{2}\right) = \frac{1}{3}\frac{\pi}{k_j^2}\frac{1}{2j+1}\sum_J\delta_{\ell,J+\frac{1}{2}}\cdot(2J+1).$$

$$\cdot\left\{\delta_{\ell',J-3/2}\left|T^{J\frac{1}{2}\ell}_{J\,\frac{3}{2}\ell'}(Q)\right|^2+\left|T^{J\frac{1}{2}\ell}_{J-1\,\frac{3}{2}\ell'}(P)\right|^2\right\}$$

$$+\delta_{\ell',J+\frac{1}{2}}\left\{\left|T^{J\frac{1}{2}\ell}_{J\,\frac{3}{2}\ell'}(Q)\right|^2+\left|T^{J\frac{1}{2}\ell}_{J-1\,\frac{3}{2}\ell}(P)\right|^2+\left|T^{J\frac{1}{2}\ell}_{J+1\,\frac{3}{2}\ell'}(R)\right|^2\right\}$$

$$+\delta_{\ell',J+\frac{5}{2}}\left|T^{J\frac{1}{2}\ell}_{J+1\,\frac{3}{2}\ell'}(R)\right|^2\Bigg\} \qquad (6\text{-}41)$$

2. Cross Section for Transitions Averaged over the Initial Degeneracy

From equations (6-31) and (6-33), we have, for this initial degeneracy averaged cross section

$$\bar{\sigma}(j=\tfrac{1}{2}\rightarrow j'm'_j) = \frac{\pi}{k_j^2}\cdot\frac{1}{2j+1}\sum_{\substack{J\ell M\\ J'\ell'M'\tilde{J}'}} C(J'1J|MOM).C(\tilde{J}'1J|MOM).$$

$$C(\ell'j'J'|M-m'_j,m'_j,M).\ C(\ell'j'\tilde{J}'|M-m'_j,m'_j,M).\ T^{Jj\ell}_{J'j'\ell'}\ .\ T^{*\tilde{J}j\ell}_{\tilde{J}'j'\ell'} \qquad (6\text{-}42)$$

From the theory of angular momentum [Biedenharn and Louck [31], equation (3.269)], one can express the product of two Clebsch-Gordon coefficients via the Racah coefficients W(abcd|ef) which will then allow us to perform the M-summation explicitly. Now from Biedenharn and Louck[31],

$$C(\ell'j'J'|M-m'_j,m'_j,M).\ C(J'1J|MOM) = \sum_{\tilde{J}}\sqrt{(2J'+1)(2\tilde{J}+1)}$$

$$\cdot\, W(\ell' j' J 1 | J' \tilde{J}\,) \cdot C(j' 1 \tilde{J} | m_j' 0 m_j') \cdot C(\ell' \tilde{J} J | M - m_j', m_j', M) \qquad (6\text{-}43)$$

Thus, from equation (6-42)

$$\bar{\bar{\sigma}}(j \rightarrow j' m_j') = \frac{\pi}{k_j^2} \cdot \frac{1}{2j+1} \sum_{\substack{\mathcal{J}\ell\,\tilde{\mathcal{J}}\tilde{\ell} \\ \mathcal{J}'\ell'\,\tilde{\tilde{\mathcal{J}}}}} \sqrt{(2J'+1)(2\tilde{J}+1)} \cdot W(\ell' j' J 1 | J' \tilde{J}) \cdot$$

$$\cdot \sqrt{(2\tilde{J}'+1)(2\tilde{\tilde{J}}+1)} \cdot W(\ell' j' J 1 | \tilde{J}' \tilde{\tilde{J}}) \cdot T^{\mathcal{J} j \ell}_{\mathcal{J}' j' \ell'} \cdot T^{*\,\tilde{\mathcal{J}} j \ell}_{\tilde{\mathcal{J}}' j' \ell'} \cdot$$

$$\cdot\, C(j' 1 \tilde{J} | m_j' 0 m_j') \cdot C(j' 1 \tilde{\tilde{J}} | m_j' 0 m_j') \cdot \sum_M C(\ell' \tilde{J} J | M - m_j', m_j', M) \cdot C(\ell' \tilde{\tilde{J}} J | M - m_j', m_j', M) \qquad (6\text{-}44)$$

Now to use the property that the row product of Clebsch-Gordon coefficients are orthogonal, we must first rewrite the Clebsch-Gordon coefficient into the form

$$C(\ell' \tilde{J} J | M - m_j', m_j', M) = (-1)^{\ell' - M - m_j'} \sqrt{\frac{2J+1}{2\tilde{J}+1}}\; C(\ell' J \tilde{J} | M - m_j', -M, -m_j')$$

so that

$$C(\ell' \tilde{J} J | M - m_j', m_j', M) \cdot C(\ell' \tilde{\tilde{J}} J | M - m_j', m_j', M) =$$

$$\sum_{M}(-1)^{\ell'-M-m_j'}\sqrt{\frac{2J+1}{2\tilde{J}+1}}\; C(\ell' J \tilde{J}\,|\,M-m_j', -M, -m_j').$$

$$(-1)^{\ell'-M-m_j'}\sqrt{\frac{2J+1}{2\tilde{\tilde{J}}+1}}\; C(\ell' J \tilde{\tilde{J}}\,|\,M-m_j', -M, -m_j') \qquad (6\text{-}45)$$

Now both M and m_j' are of the form [odd integer/2], so that with ℓ' integer and $M-m_j'$ necessarily being an integer, we obtain

$$(-1)^{2(\ell'-M-m_j')} = +1 .$$

Hence, from the row-orthogonality of Clebsch-Gordon coefficients, equation (6-45) reduces to

$$\sum_{M} C(\ell' \tilde{J} J\; M-m_j', m_j', M)\; .C(\ell' \tilde{\tilde{J}} J\; M-m_j', m_j', M) = \frac{2J+1}{2\tilde{J}+1}.\delta_{\tilde{J}\tilde{\tilde{J}}} \qquad (6\text{-}46)$$

Using equation (6-46) in (6-44), we have our final expression for the initial state degeneracy averaged cross section

$$\bar{\sigma}(j \rightarrow j' m_j') = \frac{\pi}{k_j^2}\cdot\frac{1}{2j+1}\sum_{\substack{J\ell\tilde{J}\\ J'\ell'\tilde{J}'}}(2J+1).\sqrt{(2J'+1)(2\tilde{J}'+1)}.$$

$$W(\ell' j' J 1\,|\,J' \tilde{J})\; .W(\ell' j' J 1\,|\,\tilde{J}' \tilde{J})\; .C^2(j' 1 J\,|\,m_j' 0 m_j').$$

$$T^{J j \ell}_{J' j' \ell'}\; .\; T^{*\tilde{J} j \ell}_{\tilde{J}' j' \ell'} \qquad (6\text{-}47)$$

(a) Cross section $(j=\frac{1}{2} \rightarrow j'=\frac{3}{2}, m_j')$

We first note that

$$C^2(\tfrac{3}{2}1J|m_j'0m_j') = \begin{cases} (\frac{5}{2}-m_j')(\frac{5}{2}+m_j')/10, & \tilde{J}=5/2 \\ 4m_j'^2/15, & \tilde{J}=3/2 \\ (\frac{3}{2}-m_j')(\frac{3}{2}+m_j')/6, & \tilde{J}=1/2 \end{cases} \tag{6-48}$$

and rewrite equation (6-47) in the form

$$\bar{\sigma}(\tfrac{1}{2} \rightarrow \tfrac{3}{2}\ m_j') = \frac{\pi}{k_j^2}\frac{1}{2j+1}\sum_{\substack{J\ell\tilde{J} \\ J'\ell'\tilde{J}'}}(2J+1).\ (2J'+1)(2\tilde{J}'+1)\ .C^2(\tfrac{3}{2}1J|m_j'0m_j')$$

$$W(\ell'J\tfrac{3}{2}1|\tilde{J}J').W(\ell'J\tfrac{3}{2}\ 1|\tilde{J}\tilde{J}').\ T^{Jj\ell}_{J'j'\ell'}\ .T^{*Jj\ell}_{\tilde{J}'j'\ell'} \tag{6-49}$$

on using the symmetry properties of the Racah coefficients W. Now the Racah coefficient W is non-zero if the following triangularity conditions are satisfied

i.e., $W(\ell'J\frac{3}{2}1|\tilde{J}J') \neq 0$, providing

$$\begin{aligned} &\ell' \in [\tilde{J}+J,\ \tilde{J}+J=1,\ldots\ldots,|\tilde{J}-J|] \\ &\tilde{J} \in [\tfrac{5}{2}, \tfrac{3}{2}, \tfrac{1}{2}] \\ &J' \in [J+1, J, |J-1|] \wedge [\ell'+\tfrac{3}{2}, \ldots. |\ell'-\tfrac{3}{2}|] \end{aligned} \tag{6-50}$$

while $W(\ell'J\frac{3}{2}1|\tilde{J}\tilde{J}')\neq 0$ with the constraint

$$\tilde{J}' \in \{J+1, J, |J-1|\} \wedge \{\ell'+\tfrac{3}{2}, \ldots\ldots, |\ell'-\tfrac{3}{2}|\} \tag{6-51}$$

We now investigate the respective ranges of summation in equation (6-49). Consider, for example, P parity state with $\ell = J_i + \frac{1}{2}$. To compress the notation, let $J_i \equiv J$. For $\ell = J + \frac{1}{2}$, we find that

$$\ell' = \begin{cases} J+\frac{1}{2} \ , \ J-\frac{3}{2} \ , \ J+\frac{1}{2} & \text{-- Q branch} \\ J-\frac{3}{2} \ , \ J-\frac{3}{2} \ , \ J+\frac{1}{2} & \text{-- P branch} \\ J+\frac{1}{2} \ , \ \underbrace{J+\frac{1}{2} \ , \ J+\frac{5}{2}}_{j'=\frac{3}{2}} & \text{-- R branch} \end{cases} \qquad (6\text{-}52)$$

$$j' = \tfrac{1}{2}$$

Now

$$\tilde{J} = \begin{cases} \frac{1}{2} \Rightarrow \ell' = J \pm \frac{1}{2} & \Longrightarrow \ \ell' = J + \frac{1}{2} \\ \frac{3}{2} \Rightarrow \ell' = J \pm \frac{3}{2} \ , J \pm \frac{1}{2} & \Longrightarrow \ \ell' = J+\frac{1}{2}, J-\frac{3}{2}, \\ \frac{5}{2} \Rightarrow \ell' = J \pm \frac{5}{2} \ , J \pm \frac{3}{2} \ , \ J \pm \frac{1}{2} & \Longrightarrow \ \ell' = J+\frac{5}{2}, J+\frac{1}{2}, J-\frac{3}{2} \end{cases} \qquad (6\text{-}53)$$

since the further restriction on ℓ' is that $\ell' \in [\tilde{J}+J, \ldots, |\tilde{J}-J|]$ besides the restriction equation (6-52) for $j' = \frac{3}{2}$. Thus, for

$$\ell' = J - \tfrac{3}{2} \longrightarrow J', \tilde{J}' = J, \ J-1,$$

i.e., only 2 terms contribute for each J' and $\tilde{J}'$;

$$\ell' = J + \tfrac{1}{2} \longrightarrow J', \ \tilde{J}' = J+1, \ J, \ J-1,$$

i.e., 3 terms contribute for each J' and J';

while for

$$\ell' = J + \tfrac{5}{2} \longrightarrow J', \tilde{J}' = J+1, \qquad (6\text{-}54)$$

i.e., only 1 term contributes for each J' and J'.

Remembering that $J', \tilde{J}' = J-1$ for the P-branch; $J', \tilde{J}' = J$ for the Q-branch, and $J', \tilde{J}' = J+1$ for the R-branch, we thus have for the initially-averaged degeneracy cross section: ($j = \frac{1}{2}$)

$$\bar{\sigma}\left(\tfrac{1}{2} \to \tfrac{3}{2}\ m_j'\right) = \frac{\pi}{k_j^2}\frac{1}{2j+1}\sum_{J=3/2}^{\infty}(2J+1)\Bigg(C^2\left(\tfrac{3}{2}1\tfrac{1}{2}\middle|m_j' 0 m_j'\right).\delta_{\ell',J+\frac{1}{2}}.\sum_{\tilde{J}'=J-1}^{J+1}\sqrt{(2J'+1)(2\tilde{J}'+1)}\ .W\left(\ell'\ J\ \tfrac{3}{2}\ 1\middle|\tfrac{1}{2}\ J'\right).W\left(\ell'\ J\ \tfrac{3}{2}\middle|1\ \ \tilde{J}'\right).\ T(\alpha).T^*(\beta)$$

$$+C^2\left(\tfrac{3}{2}1\tfrac{3}{2}\middle|m_j' 0 m_j'\right).\Bigg\{\delta_{\ell',J+\frac{1}{2}}\sum_{\tilde{J}'=J-1}^{J+1}\sqrt{(2J'+1)(2\tilde{J}'+1)}\ .$$

$$W\left(\ell' J\ \tfrac{3}{2}\ 1\middle|\tfrac{3}{2}\ J'\right).W\left(\ell' J\ \tfrac{3}{2}\ 1\middle|\tfrac{3}{2}\ \tilde{J}'\right).\ T(\alpha).T^*(\beta)$$

$$+\delta_{\ell',J-\frac{3}{2}}\sum_{\tilde{J}'=J-1}^{J+1}\sqrt{(2J'+1)(2\tilde{J}'+1)}\ .$$

$$W\left(\ell' J\ \tfrac{3}{2}\ 1\middle|\tfrac{3}{2}\ J'\right).W\left(\ell' J\ \tfrac{3}{2}\ 1\middle|\tfrac{3}{2}\ \tilde{J}'\right).\ T(\alpha).T^*(\beta)\Bigg\}$$

$$+C^2\left(\tfrac{3}{2}1\tfrac{5}{2}\middle|m_j' 0 m_j'\right)\Bigg\{\delta_{\ell',J-3/2}\sum_{\tilde{J}'=J-1}^{J}\sqrt{(2J'+1)(2\tilde{J}'+1)}\ .$$

$$W\left(\ell' J\ \tfrac{3}{2}\ 1\middle|\tfrac{5}{2}\ J'\right).W\left(\ell' J\ \tfrac{3}{2}\ 1\middle|\tfrac{5}{2}\ \tilde{J}'\right).\ T(\alpha).T^*(\beta)$$

$$+\delta_{\ell',J+\frac{1}{2}}\sum_{\tilde{J}'=J-1}^{J+1}\sqrt{(2J'+1)(2\tilde{J}'+1)}\ .$$

$$W\left(\ell' J\ \tfrac{3}{2}\ 1\middle|\tfrac{5}{2}\ J'\right).W\left(\ell' J\ \tfrac{3}{2}\ 1\middle|\tfrac{5}{2}\ J'\right).\ T(\alpha).T^*(\beta)$$

$$+\ \delta_{\ell',J+\frac{5}{2}}\ (2J+3).W^2\left(\ell' J\ \tfrac{3}{2}\ 1\middle|\tfrac{5}{2}\ J+1\right).\left|T(R)\right|^2\Bigg\}\Bigg)$$

$$+\frac{\pi}{k_j^2}\cdot\frac{1}{2j+1}\,2\Bigg\{ C^2\left(\tfrac{3}{2}\,1\,\tfrac{1}{2}\,|\,m_j'\,0\,m_j'\right)\cdot\delta_{\ell',J+\frac{1}{2}}\sum_{J'=J-1}^{J+1}\frac{}{\sqrt{(2J'+1)(2\tilde{J}'+1)}}\cdot W(\ell'\,J\,\tfrac{3}{2}\,1|\tfrac{1}{2}\,J')\cdot W(\ell'\,J\,\tfrac{3}{2}\,1|\tfrac{1}{2}\,\tilde{J}')\cdot T(\alpha)\cdot T^*(\beta)$$

$$+C^2\left(\tfrac{3}{2}\,1\,\tfrac{3}{2}\,|\,m_j'\,0\,m_j'\right)\cdot\delta_{\ell',J+\frac{1}{2}}\sum_{J'=J-1}^{J+1}\sqrt{(2J'+1)(2\tilde{J}'+1)}\cdot$$

$$W(\ell'J\,\tfrac{3}{2}\,1|\tfrac{3}{2}\,J')\cdot W(\ell'J\,\tfrac{3}{2}\,1|\tfrac{3}{2}\,\tilde{J}')\cdot T(\alpha)\cdot T^*(\beta)$$

$$+C^2\left(\tfrac{3}{2}\,1\,\tfrac{5}{2}\,|\,m_j'\,0\,m_j'\right)\cdot\Bigg\{\delta_{\ell',J+\frac{1}{2}}\sum_{J'=J-1}^{J+1}\sqrt{(2J'+1)(2\tilde{J}'+1)}\cdot$$

$$W(\ell'J\,\tfrac{3}{2}\,1|\tfrac{5}{2}\,J')\cdot W(\ell'J\,\tfrac{3}{2}\,1|\tfrac{5}{2}\,J')\cdot T(\alpha)\cdot T^*(\beta)$$

$$+\,\delta_{\ell',J+\frac{5}{2}}(2J+3)\cdot W^2(\ell'J\,\tfrac{3}{2}\,1|\tfrac{5}{2}\,J+1)\cdot|T(R)|^2\Bigg\}\Bigg\} \qquad (6\text{-}55)$$

where α,β denote which particular branch, P, Q, or R, is being considered. The indices on the T-matrices are

$$T(\alpha) = T^{J\,\frac{1}{2}\,J+\frac{1}{2}}_{J'\,\frac{3}{2}\,\ell'}(\alpha). \qquad T^*(\beta) = T^{*\,J\,\frac{1}{2}\,J+\frac{1}{2}}_{J'\,\frac{3}{2}\,\ell'}(\beta).$$

(b) Cross Section $\bar{\bar{\sigma}}\,(j=\tfrac{1}{2}\rightarrow j'=\tfrac{1}{2}\,,m_j')$

The average over initial degenerate states cross section is given by [from equation (6-47)]

$$\bar{\bar{\sigma}}\,(j=\tfrac{1}{2}\rightarrow j'=\tfrac{1}{2},m_j') = \frac{\pi}{k_j^2}\cdot\frac{1}{2j+1}\sum_{J\ell\tilde{J},J'\ell'\tilde{J}'}\sqrt{(2J'+1)(2\tilde{J}'+1)}\cdot(2J+1)$$

$$C^2(\tfrac{1}{2}\,1\,\tilde{J}\,|\,m_j'\,0\,m_j')\cdot W(\ell'J\,\tfrac{1}{2}\,1|\tilde{J}J')\cdot W(\ell'J\,\tfrac{1}{2}\,1|\tilde{J}'J').$$

$$T^{\tau_j \ell}_{\tau'_j \ell'} \cdot T^{*\tau_j \ell}_{\tilde{\tau}'_j \ell'} \tag{6-56}$$

Now, from tables of Clebsch-Gordan coefficients

$$C^2(\tfrac{1}{2}1\tilde{J}|m'_j 0 m'_j) = \begin{cases} 1/3 & , \tilde{J}=\tfrac{1}{2} \\ 2/3 & , \tilde{J}=\tfrac{3}{2} \end{cases} \tag{6-57}$$

since $m'_j = \tfrac{1}{2}$. The Racah coefficients W are non-zero if

$$\begin{aligned} &\tilde{J} \in [\tfrac{1}{2}, \tfrac{3}{2}] \\ &\ell' \in [\tilde{J}+J, \ldots\ldots, |\tilde{J}-J|] \\ &\tau' \in [\ell'+\tfrac{1}{2}, \ell'-\tfrac{1}{2}] \wedge [J+1,\ J,\ J-1] \\ &\tilde{J}' \in [\ell'+\tfrac{1}{2}, \ell'-\tfrac{1}{2}] \wedge [\ +1,\ J,\ J-1] \end{aligned} \tag{6-58}$$

Again, considering e-parity with $\ell = J+\tfrac{1}{2}$, we have (equation (6-52)) $\ell' = J+\tfrac{1}{2}$ for the Q-branch and R-branch, while $\ell' = J-\tfrac{3}{2}$ for the P-branch. For $\tilde{J}=\tfrac{1}{2}$, $\ell' = J+\tfrac{1}{2}$ while for $\tilde{J}=\tfrac{3}{2}$, $\ell' = J+\tfrac{1}{2}$ or $J-\tfrac{3}{2}$. Thus

$$\begin{aligned} &\ell' = J+\tfrac{1}{2} \longrightarrow J', \tilde{J}' = J, J+1 \\ &\ell' = J-\tfrac{3}{2} \longrightarrow J', \tilde{J}' = J-1 \end{aligned} \tag{6-59}$$

Hence the desired cross section

$$\bar{\bar{\sigma}}\left(\tfrac{1}{2} \to \tfrac{1}{2}\, m_j'\right) = \frac{\pi}{k_j^2}\cdot\frac{1}{2j+1}\sum_{J=3/2}^{\infty}(2J+1)\Bigg(C^2\left(\tfrac{1}{2}1\tfrac{1}{2}\,|\,m_j' 0 m_j'\right).\delta_{\ell',J+\frac{1}{2}}\sum_{\tilde{J}'=J}^{J+1}\sqrt{(2J'+1)(2\tilde{J}'+1)}\;.W\left(\ell'\;J\;\tfrac{1}{2}\;1\,|\,\tfrac{1}{2}J'\right).W\left(\ell'\;J\;\tfrac{1}{2}\;1\,|\,\tfrac{1}{2}\tilde{J}'\right).\;T(\alpha).T^*(\beta)$$

$$+C^2\left(\tfrac{1}{2}1\tfrac{3}{2}\,|\,m_j' 0 m_j'\right).\Bigg\{\delta_{\ell',J+\frac{1}{2}}\sum_{\tilde{J}'=J}^{J+1}\sqrt{(2J'+1)(2\tilde{J}'+1)}\;.$$

$$W\left(\ell' J\;\tfrac{1}{2}\;1\,|\,\tfrac{3}{2}J'\right).W\left(\ell' J\;\tfrac{1}{2}\;1\,|\,\tfrac{3}{2}\tilde{J}'\right).\;T(\alpha).T^*(\beta)$$

$$+\delta_{\ell',J-\frac{3}{2}}.\delta_{J',J-1}.\delta_{\tilde{J}',J-1}(2J-1).W\left(\ell' J\;\tfrac{1}{2}\;1\,|\,\tfrac{3}{2}J'\right).W\left(\ell' J\;\tfrac{1}{2}\;1\,|\,\tfrac{3}{2}\tilde{J}'\right).$$

$$.T(P).T^*(P)\Bigg\}\Bigg)$$

$$+\frac{\pi}{k_j^2}\frac{1}{2j+1}2\Bigg(C^2\left(\tfrac{1}{2}1\tfrac{1}{2}\,|\,m_j' 0 m_j'\right).\delta_{\ell',1}.\sum_{\tilde{J}'=1/2}^{3/2}.\;\delta_{J,1/2}.$$

$$\sqrt{(2J'+1)(2\tilde{J}'+1)}\;.W\left(\ell'\;J\;\tfrac{1}{2}\;1\,|\,\tfrac{1}{2}J'\right).W\left(\ell'\;J\;\tfrac{1}{2}\;1\,|\,\tfrac{1}{2}\tilde{J}'\right).\;T(\alpha).T^*(\beta)$$

$$+C^2\left(\tfrac{1}{2}1\tfrac{3}{2}\,|\,m_j' 0 m_j'\right).\delta_{\ell',1}\sum_{J',\tilde{J}'=1/2}^{3/2}(2J'+1)(2\tilde{J}'+1)\;.\;\delta_{J,1/2}.$$

$$W\left(\ell' J\;\tfrac{1}{2}\;1\,|\,\tfrac{3}{2}J'\right).W\left(\ell' J\;\tfrac{1}{2}\;1\,|\,\tfrac{3}{2}\tilde{J}'\right).\;T(\alpha).T^*(\beta)\Bigg) \qquad (6\text{-}60)$$

D. POLARIZATION EFFECTS IN NaAr OPTICAL COLLISIONS

In the previous section on cross sections, we derived the probability of exciting the Na-atom from its ground state $3^2S_{1/2}$ into an excited state [either into (i) $3^2P_{3/2}$ with $m_j=\pm\frac{3}{2}$, or, (ii) $3^2P_{3/2}$ with $m_j=\pm\frac{1}{2}$, or (iii) $3^2P_{1/2}$ with

$m_j = \pm \frac{1}{2}$ states] by using the close- coupled stationary state theory. The excitation was performed by a non-resonant linearly polarized photon incident on the Na-rare gas molecule. A molecular excitation occurred at some internuclear separation R of the Na atom and rare gas atom. The molecule then disintegrated ($R \rightarrow \infty$) leaving the Na atom in an excited 3 P-state (see Figure 1). In this chapter, we examine the polarization of the emitted resonant photon as the Na atom decays from the excited 3 P-state into its ground state $3\,^2S_{1/2}$.

We shall first examine the resultant polarization of the resonant D2 and D1 photons, ignoring hyperfine depolarization effects. Following Fano and Macek [34], the emission can be treated by stationary state theory, treating the atomic Na state as one with well- defined angular momentum $\vec{j}_i$. However, there is a complication. The nuclear spin I of the Na atom is equal to the total (electronic) angular momentum j_a of the initial (and excited) P atom:

$$I = \frac{3}{2} = j_i$$

This will introduce hyperfine mixing within the $^2P_{3/2}$, $^2P_{1/2}$, and $^2S_{1/2}$ states so that $\vec{j}$ is no longer a good quantum number. We then work in the coupled representation $|F, m_F, I, j\rangle$, with $\vec{F} = \vec{I} + \vec{j}$. As both the original absorbed non-resonant laser photon [bandwidth 3GHz] and the detector for the resonant emitted photon have resolution which cannot

resolve the Na hyperfine structure [see Figure 5] we are forced into a time-dependent formulation. However, following Fano and Macek [34], this can be done quite readily and will basically introduce a multiplicative correction factor to the previous formulation when hyperfine effects were ignored. We will see that the strong coherent hyperfine effects will lead to considerable depolarization of the D1 and D2 lines.

1. ANGULAR DISTRIBUTION OF EMITTED RADIATION

It is convenient to introduce two different coordinate systems: the 'physical' reference frame (x,y,z) centered on the Na atom with the z-direction the axis of quantization (giving the quantum numbers $|j_i\, m_i>$), and a 'detector' frame(x',y',z') with the detector lying on the x'-axis. The detector frame is then free to rotate about the common origin of the two coordinate systems [which is centered on the Na-atom] to give the angular distribution of the emitted light. These frames are connected to each other through the three Euler angles (α,β,γ) and the rotation matrix $D^{(1)}(\alpha\beta\gamma)$.[See figure 6]

Since the detector lies on the x'-axis, the polarization vector of the emitted photon must lie in the y'-z' plane. It is convenient to introduce the angle θ so that the polarization direction is

FIGURE 5

Hyperfine energy levels for the $^2S_{1/2}$, $^2P_{1/2}$ and $^2P_{3/2}$ states of ^{23}Na. (Not to scale)

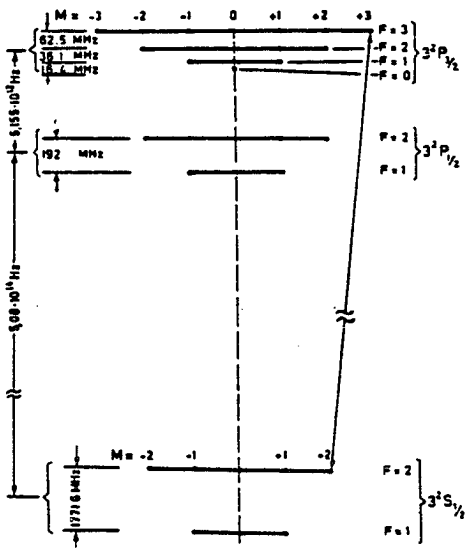

FIGURE 6

Illustration of the detector reference frame

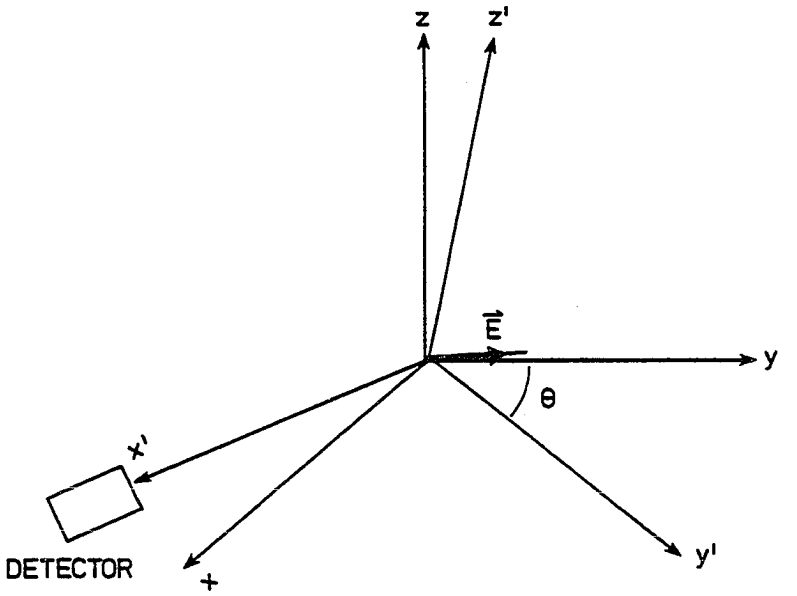

$$\hat{\epsilon} = \cos\theta \cdot y' + \sin\theta \cdot z' \qquad (6\text{-}61)$$

The intensity of light emitted into the detector with polarization vector $\hat{\epsilon}$ from an initial excited state $|i\rangle$ to the ground state $|f\rangle$ is given by

$$I = C_o \cdot \sum_{m_f} \left| \langle f | \hat{\epsilon}^* \cdot \vec{r} | i \rangle \right|^2_{av.} \qquad (6\text{-}62)$$

where $C_o = e^2 \omega_o^4 / 2\pi c^3 D^2$ is a constant depending on the emitted photon frequency ω_o and the distance D from the detector to the radiating Na atom. $\vec{r}$ is the transition dipole operator of the atom and one performs a sum Σ_{m_f} over all the final (ground) state magnetic quantum numbers m_f. The subscript "av." implies averaging over all the initial (excited) m_i. It should be noted that coherence effects are present in the averaging over the initial excited states. In this equation $|\ldots|^2_{av.}$ actually represents

$$I = C_o \sum_{m_f} \left(\frac{1}{2j_f + 1} \right) \cdot \sum_{m_i, m_i'} \langle i | \hat{\epsilon} \cdot \vec{r} | f \rangle \langle f | \hat{\epsilon}^* \cdot \vec{r} | i' \rangle \qquad (6\text{-}63)$$

with non-diagonal (coherent) terms in $\langle i | \ldots | i' \rangle$.

It is convenient to rewrite both the polarization vector $\hat{\epsilon}$ and the transition dipole operator $\vec{r}$ in terms of irreducible tensor operators of rank 1. For the transition dipole operator $\vec{r}$ we have $r_q^{(1)}$, with q=+1,0,-1

corresponding to the spherical components

$$r_{+1}^{(1)} = -\frac{1}{\sqrt{2}}(x+iy)$$

$$r_{o}^{(1)} = z$$

$$r_{-1}^{(1)} = \frac{1}{\sqrt{2}}(x-iy) \qquad (6\text{-}64)$$

However for the polarization vector $\hat{\epsilon}_{q}^{(1)}$ we have, in the detector frame [Figure 6]

$$\epsilon_{+1}^{(1)} = -(i/\sqrt{2})\cos\theta$$

$$\epsilon_{o}^{(1)} = \sin\theta$$

$$\epsilon_{-1}^{(1)} = -(i/\sqrt{2})\cos\theta \qquad (6\text{-}65)$$

which must be transformed to the physical coordinate system by the rotation matrix $D_{qk}^{(1)}$

$$\epsilon_{k}^{(1)} = \sum_{q=-1}^{1} D_{qk}^{(1)} \cdot \epsilon_{q}^{(1)} \qquad (6\text{-}66)$$

where $D_{qk}^{(1)}(-\gamma,-\beta,-\alpha) = D_{kq}^{(1)*}(\alpha\beta\gamma)$ and α,β,γ are the usual Euler angles that describe the rotation transformations from the physical coordinate system to the detector frame [see Appendix 2]. Thus, the intensity, from equation (6-62)

$$I = C_0 \sum_{m_f} \left| \sum_{k,q=-1}^{1} D^{(1)}_{qk} \, \epsilon^{(1)}_{q} \, \langle f | r^{(1)}_{k} | i \rangle \right|^2_{av.} \qquad (6\text{-}67)$$

We can now apply the Wigner-Eckart theorem to equation (6-67), where the final total angular momentum $|f\rangle = |\ldots j\ m\rangle$, where ... in the ket-vector represents all the other quantum numbers needed to totally specify the state. Now the initial excited ^2P Na-atomic states are actually created by non-resonant photon absorption of the Na-rare gas molecular state [see Figure 1]. The cross sections for the asymptotic formation of $^2P_{3/2}$ ($m_j = \pm 3/2$), $^2P_{3/2}$ ($m_j = \pm 1/2$), and $^2P_{1/2}$ ($m_j = \pm 1/2$) are determined numerically from the close-coupled formalism discussed in chapters 4 and 5. Thus the initial wave function $|i\rangle$ in the polarization of the emitted resonance D2 (or D1) lines is a weighted average of all the degenerate $^2P_{3/2}$ (or $^2P_{1/2}$) energy levels:

$$|i\rangle = \sum_{m_i} p(m_i) |\ldots j_i\ m_i\rangle, \qquad (6\text{-}68)$$

with $p = p(m_i)$. It is assumed that the detector can spectrally resolve the D2 from the D1 line. Thus

$$I = C_0 \sum_{m_f} \left[\sum_{k,k'} \sum_{m_i, m_i'} \epsilon^{(1)}_{k} \epsilon^{(1)*}_{k'} p^*(m_i) . p(m_i') . C(j_i\ 1\ j_f \,|\, m_i\ k\ m_f) . \right.$$

$$\left. . C(j_i\ 1\ j_f \,|\, m_i'\ k'\ m_f) \right] . \left[\langle \ldots j_f \| \vec{r}^{(1)} \| \ldots j_i \rangle \right]^2 . \qquad (6\text{-}69)$$

However, we must average this single collision intensity I over all initial directional angles and detector angles so as to include all such binary collisions that can contribute to the intensity. This averaging only affects $p^*(m_i).p\,(m_i')$ which is non-zero providing $m_i = m_i'$. The degree of polarization P is defined by

$$\begin{aligned} P &= [\, I(\theta=\pi/2) - I(\theta=0)\,]/[\, I(\theta=\pi/2) + I(\theta=0)\,] \\ &= [\, I_{\parallel} - I_{\perp}\,] \,/\, [\, I_{\parallel} + I_{\perp}\,] \end{aligned} \qquad (6\text{-}70)$$

where it is understood that we have already preformed the angular integration mentioned above. Since equation (6-70) involves ratios of intensities of certain angles, we can drop all constants in equation (6-69), -- in particular C_o and the reduced matrix element $[\langle \ldots j_f \| \vec{r}^{(1)} \| \ldots j_i \rangle]^2$.

2. POLARIZATION OF $^2P_{1/2} \longrightarrow {}^2S_{1/2}$

For $\theta = \pi/2$, from equation (6-65), the only nonzero component of the polarization vector occurs for k=0 with $\epsilon_o^{(1)} = 1$; while for $\theta = 0$, the non-zero components occur for $k = \pm 1$ with $\epsilon_{\pm 1}^{(1)} = -i/\sqrt{2}$. Thus, from equation (6-69) dropping unimportant constants, we obtain

$$\begin{aligned} I_{\parallel} &= I(\theta=\pi/2) \\ &= \sum_{\substack{m_i, m_f = \frac{1}{2} \\ m_i'}}^{1/2} \left| p(m_i) \right|^2 .[C(\tfrac{1}{2}\,1\,\tfrac{1}{2}\; m_i\, 0 m_f).C(\tfrac{1}{2}\,1\,\tfrac{1}{2}\; m_i'\, 0 m_f)].\delta_{m_i' m_i} \end{aligned} \qquad (6\text{-}71)$$

From the properties of Clebsch-Gordon coefficients $m_i = m_i' = m_f$, so that

$$I_{\parallel} = 2\,|p(1/2)|^2 \cdot C^2(\tfrac{1}{2}1\tfrac{1}{2}\,\tfrac{1}{2}0\tfrac{1}{2}) = 2\,|p(1/2)|^2/3$$
$$= \tfrac{2}{3}\bar{\sigma}(1/2 \rightarrow 1/2\ 1/2) \qquad (6\text{-}72)$$

on relating the averaged scattering amplitude squared to the cross section. For $I_{\perp}$, k, $k=\pm 1$ so that

$$I_{\perp} = I(\theta=0)$$
$$= \tfrac{1}{2}\sum_{\substack{m_i \\ m_i'}}^{1/2} |p(m_i)|^2 \cdot [\, C(\tfrac{1}{2}1\tfrac{1}{2}|m_i 1 m_f) \cdot C(\tfrac{1}{2}1\tfrac{1}{2}|m_i' 1 m_f)$$
$$+ C(\tfrac{1}{2}1\tfrac{1}{2}|m_i -1 m_f) \cdot C(\tfrac{1}{2}1\tfrac{1}{2}|m_i', -1 m_f) + C(\tfrac{1}{2}1\tfrac{1}{2}|m_i -1 m_f) \cdot C(\tfrac{1}{2}1\tfrac{1}{2}|m_i' 1 m_f)$$
$$+ C(\tfrac{1}{2}1\tfrac{1}{2}|m_i' -1 m_f)\,] \cdot \delta_{m_i m_i'}$$

for $m_f = 1/2$ only the first term can contribute, while for $m_f = -1/2$ only the fourth term contributes to $I_{\perp}$. In each case $m_i = m_i' = m_f$. Hence, on evaluating the Clebsch-Gordon coefficients we find

$$I_{\perp} = 2\,|p(1/2)|^2/3 = \tfrac{2}{3}\bar{\sigma}(1/2 \rightarrow 1/2\ 1/2) \qquad (6\text{-}73)$$

Thus for the degree of polarization P, equation (6-71), for transition $^2P_{1/2} \rightarrow {}^2S_{1/2}$

$$P = [\, I_{\parallel} - I_{\perp}] \,/\, [\, I_{\parallel} + I_{\perp}]$$
$$= 0, \qquad (6\text{-}74)$$

from equations (6-72) and (6-73).

3. POLARIZATION OF $^2P_{3/2} \longrightarrow {}^2S_{1/2}$

$$I_{\parallel} = I(\theta = 0)$$
$$= \sum_{m_f=-1/2}^{1/2} |p(m_i)|^2 \cdot C^2(\tfrac{3}{2}\,1\,\tfrac{1}{2}\,|\,m_f\,0\,m_f)$$
$$= 2\,|p(1/2)|^2/3\,, \qquad (6\text{-}75)$$

since $k=0$, $m_i = m_i' = m$.

$$I_{\perp} = I(\theta = \pi/2)$$
$$= \frac{1}{2} \sum_{m_f=-\frac{1}{2}}^{1/2} \sum_{m_i=-3/2}^{3/2} p^*(m_i).p(m_i').[\, C(\tfrac{3}{2}\,1\,\tfrac{1}{2}\,|\,m_i\,1\,m_f).C(\tfrac{3}{2}\,1\,\tfrac{1}{2}\,|\,m_i'\,1\,m_f)$$
$$+C(\tfrac{3}{2}\,1\,\tfrac{1}{2}\,|\,m_i\,1\,m_f).C(\tfrac{3}{2}\,1\,\tfrac{1}{2}\,|\,m_i'\,,-1\,,m_f) + C(\tfrac{3}{2}\,1\,\tfrac{1}{2}\,|\,m_i\,,-1\,,m_f).C(\tfrac{3}{2}\,1\,\tfrac{1}{2}\,|\,m_i'\,1\,m_f)$$
$$+ C(\tfrac{3}{2}\,1\,\tfrac{1}{2}\,|\,m_i\,,-1\,,m_f).C(\tfrac{3}{2}\,1\,\tfrac{1}{2}\,|\,m_i'\,,-1\,,m_f)] \cdot \delta_{m_i m_i'}$$

By symmetry $m_f = -\frac{1}{2}$ and $m_f = +\frac{1}{2}$ terms will give the same contributions, so that

$$I_{\perp} = p^*(m_i).p(m_i')\,[\, C^2(\tfrac{3}{2}\,1\,\tfrac{1}{2}\,|\,-\tfrac{1}{2}\,1\,\tfrac{1}{2}).\delta_{m_i,-1/2} \cdot \delta_{m_i m_i'}$$

$$+ C^2\left(\tfrac{3}{2}\,1\tfrac{1}{2}\,\middle|\,\tfrac{3}{2},-1,\tfrac{1}{2}\right)\delta_{m_i,+3/2}\cdot\delta_{m_i m_i'}\quad] \qquad (6\text{-}76)$$

On evaluating the Clebsch-Gordan coefficients,

$$\begin{aligned} I_\perp &= |p(1/2)|^2/6 + |p(3/2)|^2/2 \\ &= \bar{\sigma}(1/2 \to 3/2\ 1/2)/6 + \bar{\sigma}(1/2 \to 3/2\ 3/2)/2. \end{aligned} \qquad (6\text{-}77)$$

Thus, we have only incoherent effects with

$$\begin{aligned} P &= [\,I_\parallel - I_\perp\,]/[\,I_\parallel + I_\perp\,] \\ &= [\,\bar{\sigma}(\tfrac{1}{2}\to\tfrac{3}{2}\,\tfrac{1}{2}) - \bar{\sigma}(\tfrac{1}{2}\to\tfrac{3}{2}\,\tfrac{3}{2})\,]\Big/[\,\tfrac{5}{3}\bar{\sigma}(\tfrac{1}{2}\to\tfrac{3}{2}\,\tfrac{1}{2}) + \bar{\sigma}(\tfrac{1}{2}\to\tfrac{3}{2}\,\tfrac{3}{2})\,] \end{aligned} \qquad (6\text{-}78)$$

E. DEPOLARIZATION EFFECTS DUE TO HYPERFINE STRUCTURE

Since the Na-atom has nuclear spin I=3/2, we have coupling with the initial excited total electronic angular momenta $j_i = 3/2[^2P_{3/2}$ -state] or $j_i = 1/2[^2P_{1/2}$ -state] so that the total coupled angular momenta $\vec{F}=\vec{I}+\vec{j}$ have the following hyperfine energy levels for $|FM_F>$-states. Now the frequency difference $\omega_{FF'}=\omega_F-\omega_{F'}$ within the initially excited $^2P_{3/2}$ (or within the $^2P_{1/2}$) state is bounded by 200 MHz which is considerably less than the bandwidth of the incident dye laser (3 GHz). Thus we have unresolved hyperfine structure within the $^2P_{3/2}$ band (or within the $^2P_{1/2}$ band). But the frequency gap between the 2 bands ($^2P_{3/2}$ and $^2P_{1/2}$) is equal to 5000 GHz so that the bands themselves are easily resolved from each other. Moreover, the hyperfine components of the excited state will fluoresce coherently. For illustrative

purposes, consider the effect of fluorescence from two experimentally indistinguishable levels (a) and (b) in the $^2P_{3/2}$ band. Since the frequency gap in the final hyperfine ground state $^2S_{1/2}$ is 1.7 GHz., we shall assume the detector can resolve the F=2 and F=1 levels. Hence we consider the fluorescence of these two excited levels into the same (c) level [we have illustrated F=3 and F=2 in $^2P_{3/2}$ fluorescing to F=2 in $^2S_{1/2}$]. Since the bandwidth of the incident non-resonant laser is greater than the frequency gap $\omega_{FF'} = \omega_{ab}$, the states (a) [F=3] and (b) [F=2] will be excited coherently. Thus the intensity of the emitted radiation $\left| \langle (c)|\hat{\epsilon}\cdot\vec{r}|(a)\rangle + \langle (c)|\hat{\epsilon}\cdot\vec{r}|(b)\rangle \right|^2$, and because of the coherent term it will exhibit quantum beats [i.e. interference effects due to the cross term time dependence $\cos(\omega_{ab})\, t$ arising from $|(a)(t)\rangle = |a_o\rangle \exp(-i E_a t/\hbar)$ and $|(b)(t)\rangle = |b_o\rangle \exp(-i E_b t/\hbar)$ with $h\omega_{ab} = E_a - E_b$]. Since these oscillations are too rapid to be observed within the time resolution of most experiments we must average this time dependence together with the life-time decay factor for the excited state $\exp(-t/\tau)$. Thus the time-dependence average yields

$$\int_0^\infty \exp(-t/\tau)\, \cos \omega_{F'F''} t \; dt \;=\; \tau / [1 + \omega^2_{F'F''}\tau^2] \qquad (6\text{-}80)$$

Fano and Macek [34] give a more detailed expositions of the treatment of nonstationary states.

We proceed from equation (6-62), but must express the initial and final states in the coupled representation $|jIFM_F>$. Thus the time-independent part of the initial wave function, averaged over the initial degeneracy

$$|\psi(j,Im_I)> = \sum_{m_j} p(m_j)\ |jm_j, Im_I> = \sum_{F,m_j} p(m_j).C(jIF|m_j\, m_I M_F)\ |F(I,j)M_F> \qquad (6\text{-}81)$$

where, as in equation (6-63), $p(m_j)$ is scattering amplitude obtained from the close-coupled theory and numerical code. Thus the resultant intensity of radiation of polarization q in the transition from either the D2 or the D1 line is given by

$$I = C_o \sum_{M_F}\Big[\sum_{F,F''}\sum_{\substack{m_j,m_j'\\ m_j''}} p^*(m_j').p(m_j'').C^2(jIF|m_j\, m_I M_F).C(j'IF'|m_j' m_I' M_F')$$

$$C(j'IF''|m_j''m_I''M_F'').\ <F'(Ij')M_F'|\hat{\epsilon}.\vec{r}\,|F(Ij)M_F>.$$

$$.<F(Ij)M_F|\epsilon^*.\vec{r}\,|F''(Ij')M_F''>\Big]\ \frac{1}{1+\omega^2_{F'F''}.\tau^2} \qquad (6\text{-}82)$$

For simplicity we have assumed the same detector geometry as before so that the rotation matrices are just the unit matrix. The primes denote the excited initial states. Again the angular integrations over the relevant angles in the scattering amplitude will lead to $m_j'=m_j''$.

We now apply the Wigner-Eckart theorem to $\sum_{k=-1}^{1} \epsilon_k^{(1)} \langle F'(Ij')M_F' \mid r_k^{(1)} \mid F(Ij)M_F \rangle$, noting that the first order irreducible transition dipole tensor operator acts only on one of the coupled systems making up the above coupled representation. In particular [c.f. Weissbluth equation (6.3-38),(6.3-39), Ref. 26]

$$\langle j'IF'M_F' \| r_k^{(1)} \| jIFM_F \rangle = (-1)^{k+I-j-F'} \cdot C(F1F' \mid M_F k M_F') \cdot \sqrt{(2F+1)(2j'+1)} \cdot W(jFj'F' \mid I1) \cdot \langle j' \| \vec{r}^{(1)} \| j \rangle \qquad (6\text{-}83)$$

$W(jFj'F' \mid I1)$ is the standard Racah coefficient which arises when one couples three angular momenta. Again, since we are interested in the degree of polarization of the transition line D2 (or of the transition line D1)

$$P = [\, I_{\parallel} - I_{\perp} \,]/[\, I_{\parallel} + I_{\perp} \,] = [\, I(\theta=\pi/2) - I(\theta=0) \,] \Big/ [\, I(\theta=\pi/2) + I(\theta=0) \,] \qquad (6\text{-}84)$$

which is a ratio of intensities, we will ignore constants like the reduced matrix element $\langle j' \| \vec{r}^{(1)} \| j \rangle$ which will cancel out in (6-84).

Equation (6-83) can be readily evaluated. The Clebsch-Gordon coefficient $C(F1F' \mid M_F k M_F')$ requires $F'-F=0$ or ± 1 and we also drop $I=3/2$, $j'=3/2$, $j=1/2$ from our notation so that $|jIFM_F\rangle = |FM_F\rangle$. We find for the D2 line

(i) $F'=3,\ F=3$

$$\langle F'=3, M_F'=2 | r_o^{(\omega)} | F=2, M_F=2\rangle = 1/\sqrt{3}$$

$$\langle 31 | r_o^{(\omega)} | 21\rangle = \sqrt{8/15}$$

$$\langle 30 | r_o^{(\omega)} | 20\rangle = \sqrt{3/5}$$

$$\langle 3,-2 | r_o^{(\omega)} | 2,-2\rangle = 1/\sqrt{3}$$

$$\langle 3,-1 | r_o^{(\omega)} | 2,1\rangle = \sqrt{8/15}$$

$$\langle 33 | r_1^{(\omega)} | 22\rangle = 1 = \langle 3,-3 | r_{-1}^{(\omega)} | 2,-2\rangle$$

$$\langle 32 | r_1^{(\omega)} | 21\rangle = \sqrt{2/3} = \langle 3,-2 | r_{-1}^{(\omega)} | 2,-1\rangle$$

$$\langle 31 | r_1^{(\omega)} | 20\rangle = \sqrt{2/5} = \langle 3,-1 | r_{-1}^{(\omega)} | 2,0\rangle$$

$$\langle 30 | r_1^{(\omega)} | 2,-1\rangle = \sqrt{1/5} = \langle 30 | r_{-1}^{(\omega)} | 2,1\rangle$$

$$\langle 3,-1 | r_1^{(\omega)} | 2,-2\rangle = \sqrt{1/15} = \langle 31 | r_{-1}^{(\omega)} | 22\rangle$$

etc....

Now the intensity

$$I = C_o \left[\langle j' \| \vec{r}^{(\omega)} \| j\rangle\right]^2 \sum_{\substack{M_F, M_F' \\ M_F''}} \sum_{\substack{F' \\ F''}} \sum_{\substack{m_j, m_j' \\ m_j''}} \sum_{k,k'} p(m_j').p(m_j'').$$

$$C^2(jIF | m_j m_I M_F).\ C(j'IF' | m_j' m_I' M_F').\ C(j'IF'' | m_j'' m_I' M_F'')$$

$$\hat{\epsilon}_k^{(\omega)} \hat{\epsilon}_{k'}^{*(\omega)} \langle F'M_F' | r_k^{(\omega)} | FM_F\rangle . \langle FM_F | r_{k'}^{(\omega)} | F''M_F''\rangle . \left[1+\omega_{F'F''}^2 \tau^2\right]^{-1}$$

F. POLARIZATION OF $^2P_{3/2} \longrightarrow {}^2S_{1/2}$

For $\theta = \pi/2$, from equation (6-65), we need $k=0$ with $\epsilon_o^{(\omega)} = 1$, while when $\theta = 0$ we need $k=\pm 1$ with $\epsilon_{\pm 1}^{(\omega)} = -i/\sqrt{2}$. Thus, dropping unimportant constants

$$I_{\parallel} = I\ (\theta=\pi/2)$$

$$= \sum_{\substack{M_F, M_F' \\ M_F''}} \sum_{\substack{m_j, m_j' \\ m_j''}} \sum_{F', F''} p^*(m_j').p(m_j'').C^2(\tfrac{1}{2}\tfrac{3}{2}F|m_j\, m_I M_F)$$

$$C(\tfrac{3}{2}\tfrac{3}{2}F'|m_j' m_I' M_F').C(\tfrac{3}{2}\tfrac{3}{2}F''|m_j''m_I''M_F'').\ \langle F'M_F'|r_o^{(1)}|FM_F\rangle$$

$$.\langle FM_F|r_o^{(1)}|F''M_F''\rangle.\ [1+\omega_{F'F''}^2.\tau^2\ ]^{-1}.\ \delta_{m_j' m_j''}$$

as there are over 1200 terms, this expression will not be algebraically simplified.

However, we note that since $I=3/2=j_i$ for $^2P_{3/2}$ state, the hyperfine structure will cause strong depolarization of the D2 line.

CHAPTER 7

RESULTS

It is convenient to first present the experimental results of Havey,et.al.[13] for the Na-Ar system. For fixed detuning Δ , the intensities of the atomic Na D1 and D2 lines were recorded as a function of the Ar pressure and we present their data for various detunings in Figure 2. The ratio of these line intensities measures the relative number of atoms produced in each of the fine structure states, while the dependence on the Ar pressure arises because of the effects of fine structure changing collisions of the excited Na atoms with the Ar atoms. To compare this experimental data to our theoretical calculations, we must extrapolate the data in Figure 2 to zero Ar pressure since it is this limit that we are interested in examining the redistribution process. In Figure 3, we present the experimental data, extrapolated to zero pressure, for the D1/D2 ratio as a function of the detuning Δ . It is seen, from Figure 3 for the Na-Ar system, that in the far blue-wing excitation the intensity ratio D1/D2 $\longrightarrow$ 1.6 while in the far red wing excitation D1/D2 ratio $\longrightarrow$ 0.5.

A. POTENTIAL FITS AND D1/D2 INTENSITIES

In discussing our theoretical results and comparing them to the experimental results we must first discuss the Born-Oppenheimer potentials, our least squares fit to these potentials, and the sensitivity of our results for the intensity ratio D1/D2 as a function of detuning on variations in these least square fits.

For the Na-rare gas systems we used the functional forms of Tellinghuisen [37] to fit the Born-Oppenheimer molecular ground $X^2\Sigma_{1/2}$ and excited $B^2\Sigma_{1/2}$ states

$$V_\Sigma(R) = D_e \left\{1 - \exp\left[-a_1 (R - R_e) \right]\right\}^2 \cdot \left\{1 - a_2 \exp\left[- (R - a_3)^2/a_4^2 \right]\right\} - D_e \qquad (7\text{-}1)$$

with the coefficients a_1, a_2, a_3, a_4 being determined by a standard least square fitting program to the potential data of Saxon, Olson, and Liu [27]. D_e is the dissociation energy for the particular molecule under consideration and R_e is the radial location of that particular potential. In Table 4, we give the numerical values used for these coefficients. Length is expressed in units of Bohr radii a_o, while energy D_e is given in cm^{-1} [a_1 has dimensions of $(\text{length})^{-1}$, a_2 is dimensionless and both a_3 and a_4 have dimensions of length]. The $A^2\pi$ B-O potential for NaAr is fitted by a Thakkar potential of the form

TABLE 4

Coefficients of a least squares fit to the $X\Sigma$ and $B\Sigma$ potential curves for NaAr, NaNe, NaHe

	NaAr		NaNe		NaHe	
	$X\Sigma$	$B\Sigma$	$X\Sigma$	$B\Sigma$	$X\Sigma$	$B\Sigma$
a_1	0.472	0.313	0.492	0.273	0.492	0.338
a_2	0.137	-0.595	-0.024	0	0.477	0
a_3	5.444	7.594	5.233	-	4.419	-
a_4	0.882	1.516	0.483	0.292	2.999	0.0292
D_e	41.00	32.00	9.37	4.408	2.38	0.51
R_e	9.437	12.86	10.00	14.50	12.00	19.00

$$\text{NaAr}: \quad V_{\pi}(R) = D_o \left[\left(1 - R_e/R \right)^{p} \right] \cdot \left[1 + \sum_{i=2}^{6} b_i \left(1 - R_e/R \right)^{i} \right] - D_e \qquad (7\text{-}2)$$

with the dissociation energy D_e given by

$$D_e = D_o \; 1 + \sum_{i=2}^{6} b_i \qquad (7\text{-}3)$$

The parameters used are the following: $D_o = 510.481$ cm , $R_e = 5.75\ a_o$, $p = 4.841$ and the least square fitting program gives $b_2 = -0.454$, $b_3 = 0.301$, $b_4 = 0.297$, $b_5 = -0.235$, and $b_6 = 0.059$. For the NaNe and NaHe B-O potentials we ued the functional form

NaNe and NaHe :

$$V_{\pi}(R) = D_o \exp\left[-c_o R\right] - C_6 / (10R)^6 - C_8 / (10R)^8 - C_{10} / (10R)^{10} \qquad (7\text{-}4)$$

with the coefficients listed in Table 5.

The difference between the $A^2\Pi_{1/2}$ and $A^2\Pi_{3/2}$ potential curves comes from the atomic Na spin-orbit interaction which we treat here as independent of the internuclear separation for the three molecules under consideration. This is a common approximation [2],[22].

We present these potentials for NaAr, NaNe , and NaHe in Figure 7 where it is immediately apparent that as one moves to the lighter mass molecules (NaAr → NaNe → NaHe) the

TABLE 5

The coefficients for a least square fit to $A\,\pi$ potential curves for NaHe and NaNe

	NaNe	NaHe
	Aπ	Aπ
c_0	4.04	4.03
c_6	13.64	16.55
c_8	-3.25	-3.11
c_{10}	0.09	0.12
D_0	4.04E7	4.04E7

FIGURE 7

Born-Oppenheimer potentials for (a) NaAr, (b) NaNe, (c) NaHe

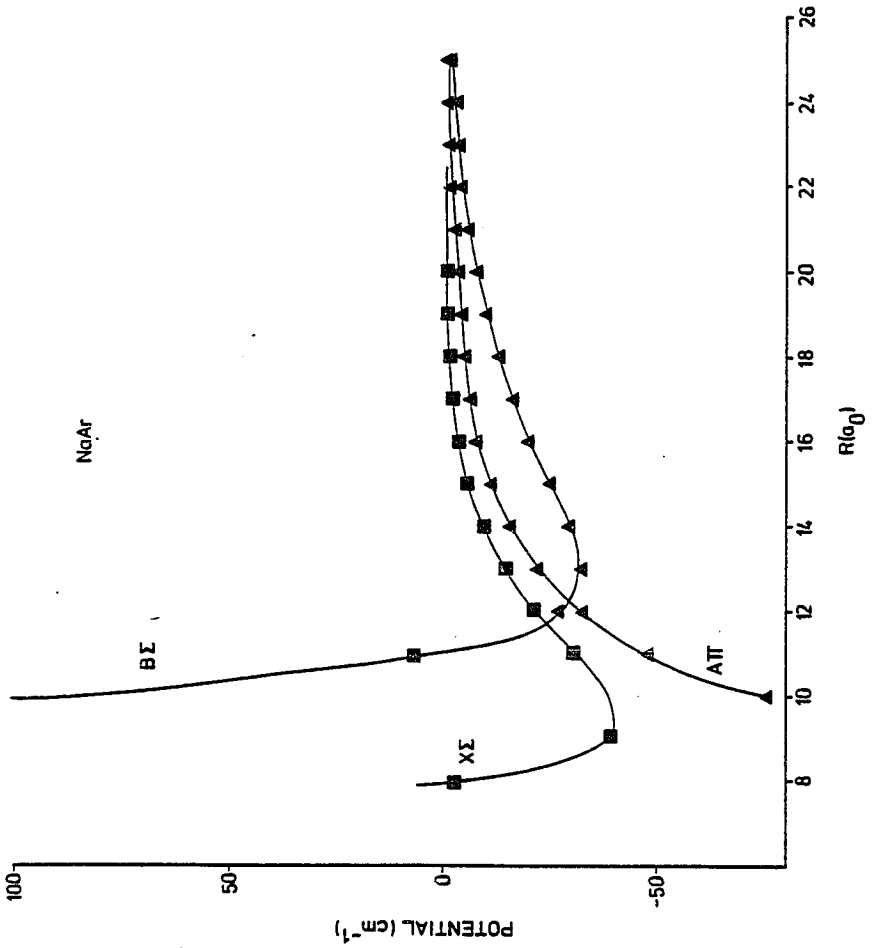

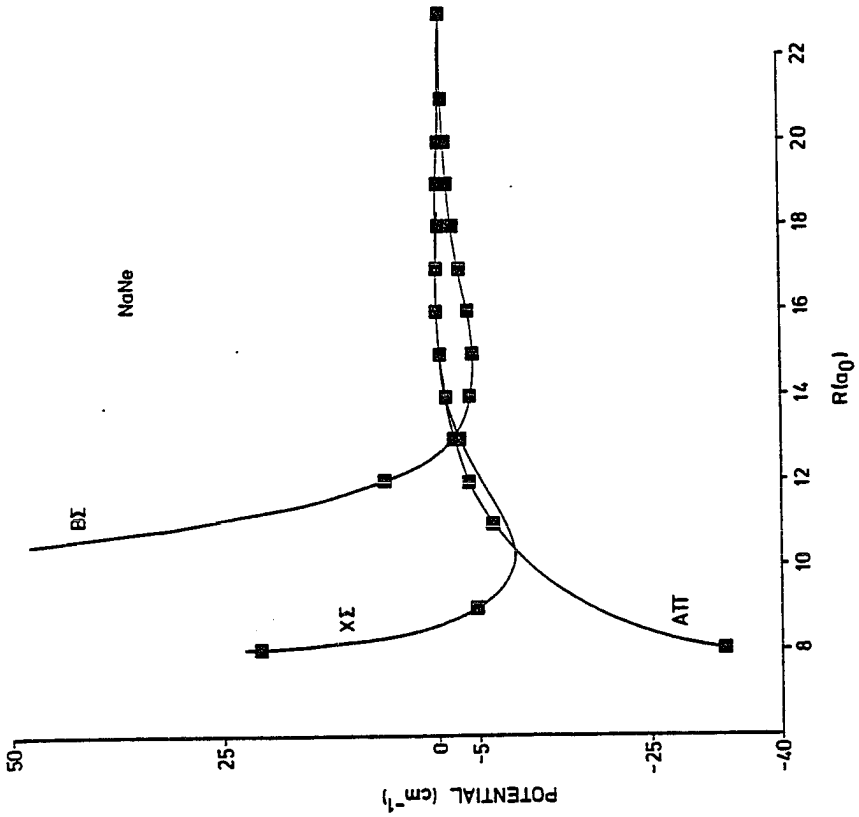

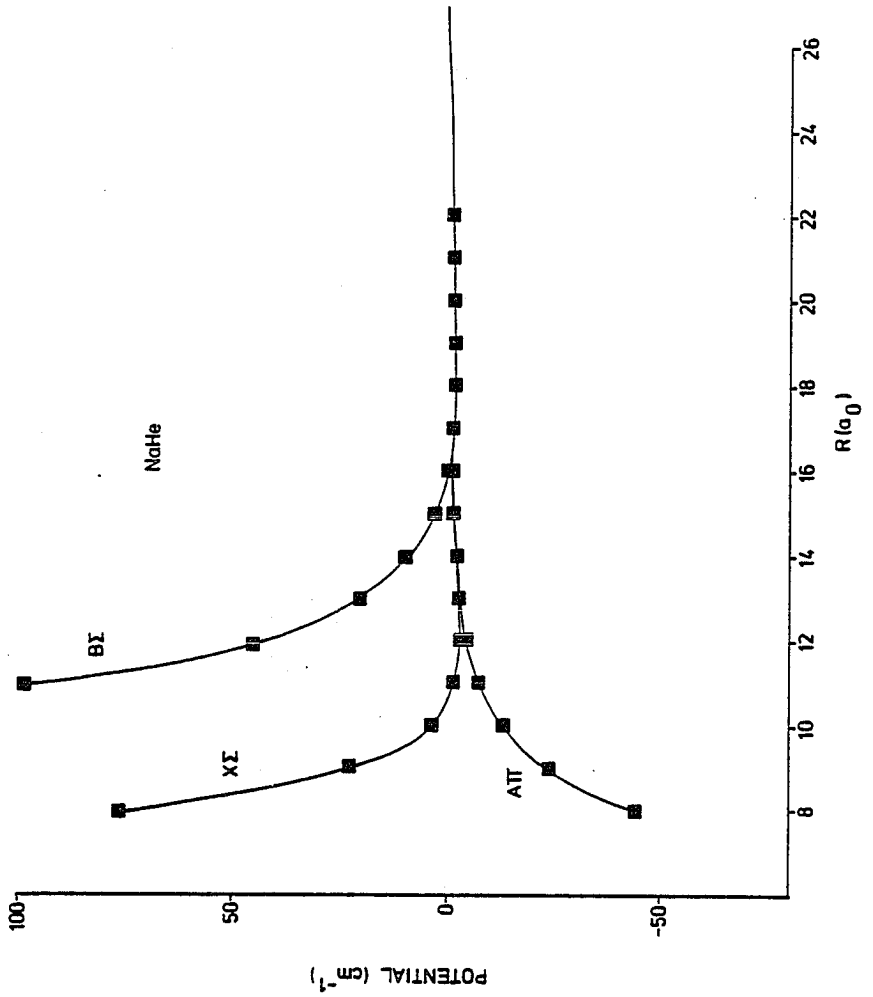

potential wells for the $B\Sigma^-$ and $X\Sigma^-$ states are considerably reduced till the NaHe case where they are nearly totally eliminated. All the potentials are normalized so that $V(R) \rightarrow 0$ as $R \rightarrow \infty$. In Figure 8, we plot the potential differences as a function of the internuclear separation R for the three molecules NaAr, NaNe, and NaHe.

The zero rare-gas pressure extrapolation of the atomic Na D1/D2 line intensity ratio is plotted in Figure 9 for NaAr for various detunings Δ at collsion energy E=200 cm^{-1}, while the corresponding plots for NaNe and NaHe are shown in Figures 10 and 11 respectively.

For the NaAr case we can compare our results to the experimental data of Havey et.al.[13] and the recently published close-coupling model results of Kulander-Rebentrost [22]. The Kulander-Rebentrost [22] results were obtained using the potentials of Duren et.al. [28] and the R-matrix propagation technique of Light and Walker [38]. It appears that they solved the full 10 X 10 close-coupled set of equations. In our case we work with the Gordon algorithm for solving the close-coupled equations which we block into 3 (4 X 4) sets for the P , Q , and R branches (following Julienne [16]). We find good agreement of both theories with the experimental results. For the asymptotic far blue-wing excitation detuning, the intensity ratio $D1/D2 \longrightarrow 1$ while for the asymptotic far red-wing-excitation detuning $D1/D2 \rightarrow 0.5$.

FIGURE 8

Potentl differences for (a) NaAr, (b) NaNe, (c) NaHe

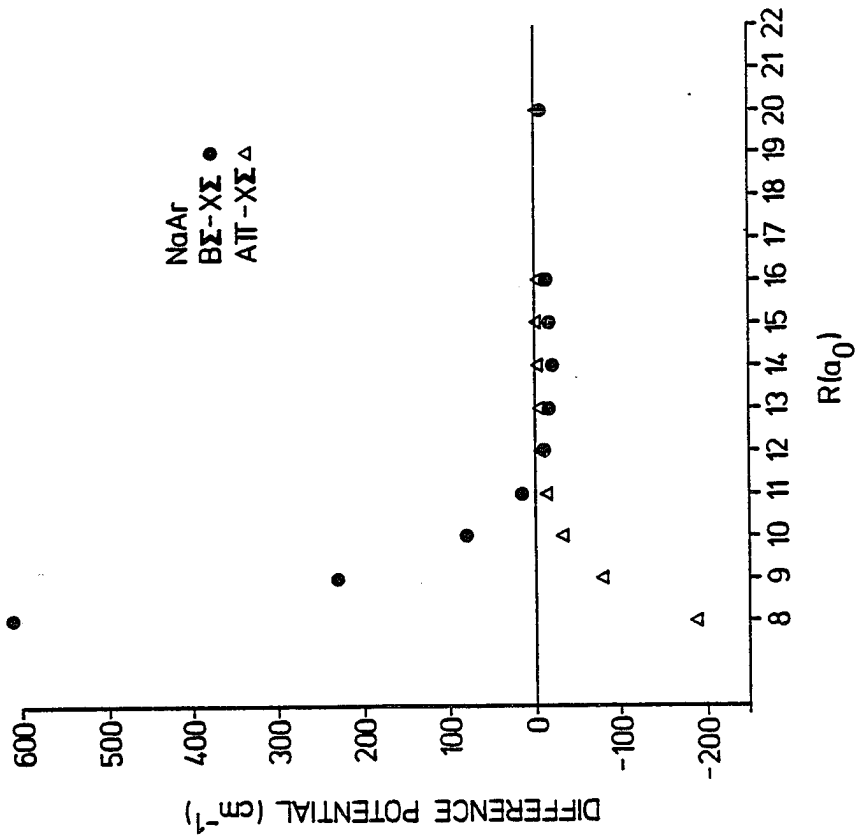

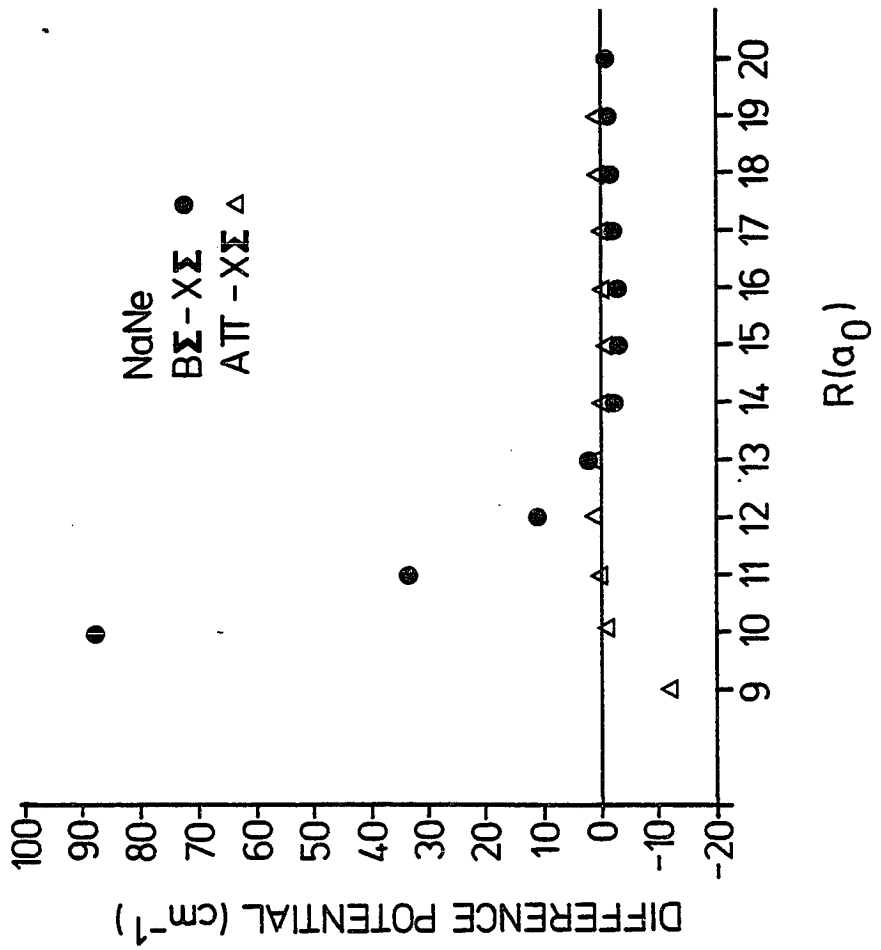

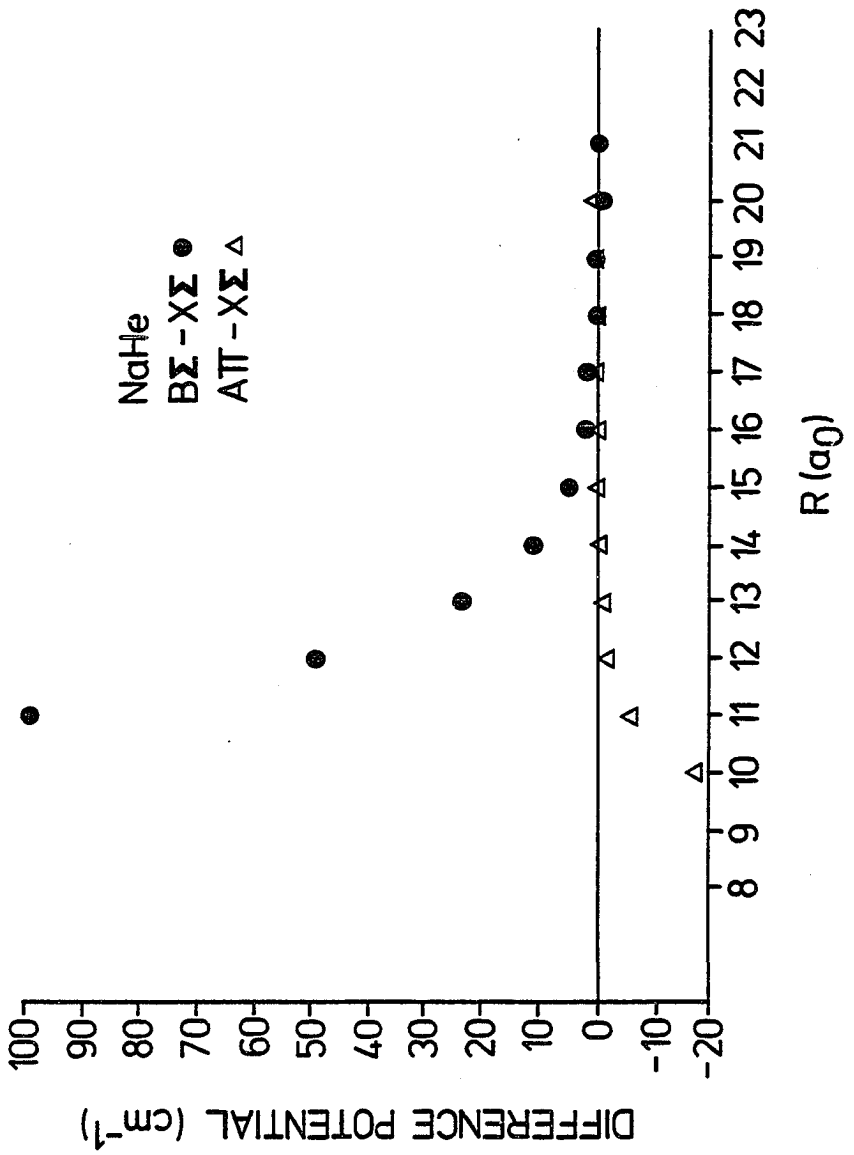

FIGURE 9

Numerically determined intensity ratio D1/D2 as a function of detuning for NaAr. The symbols + represent the experimental data of Havey [13], while the symbols • represent our calculated results

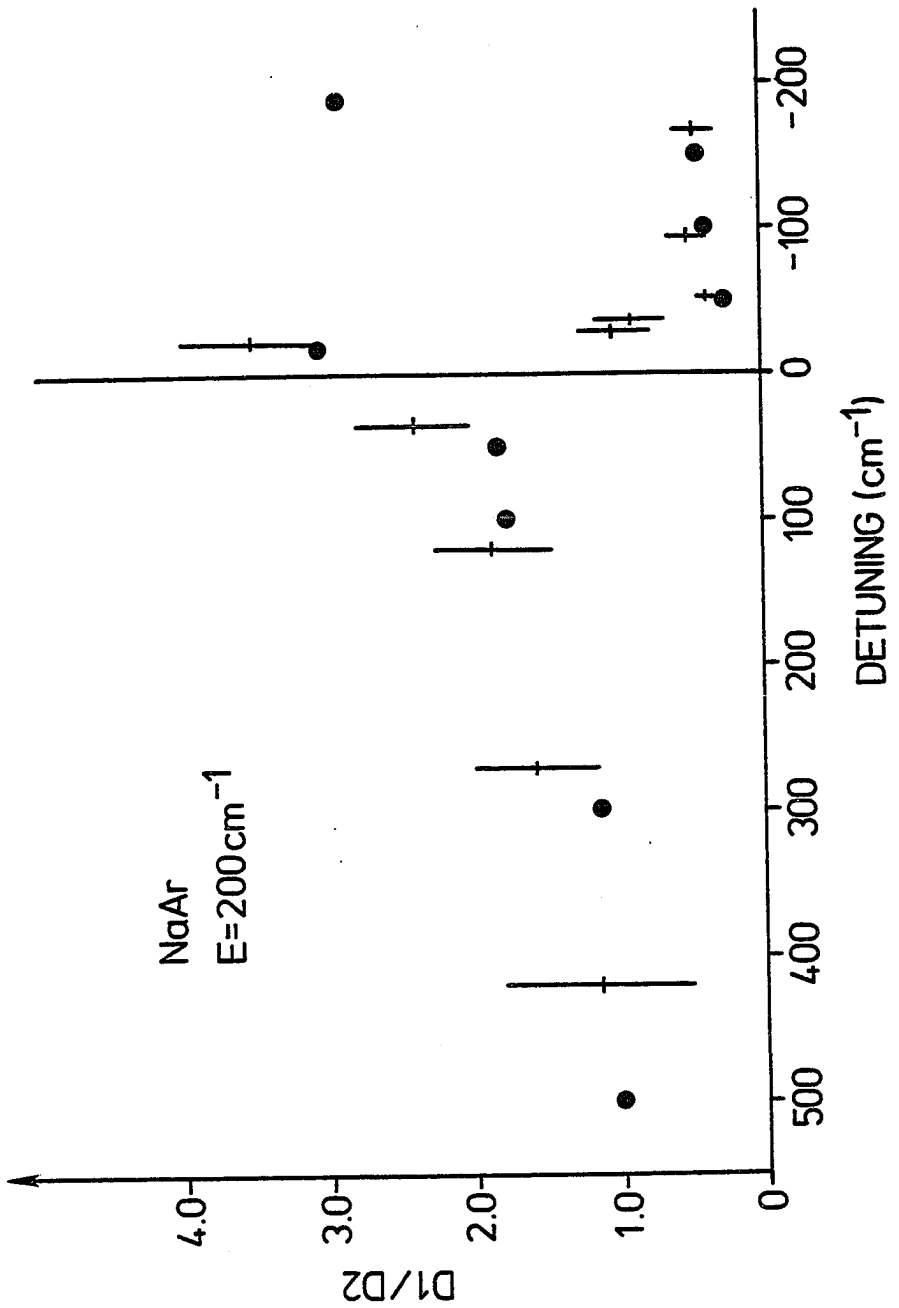

FIGURE 10

Numerically determined intensity ratio D1/D2
as a function of detuning for NaNe

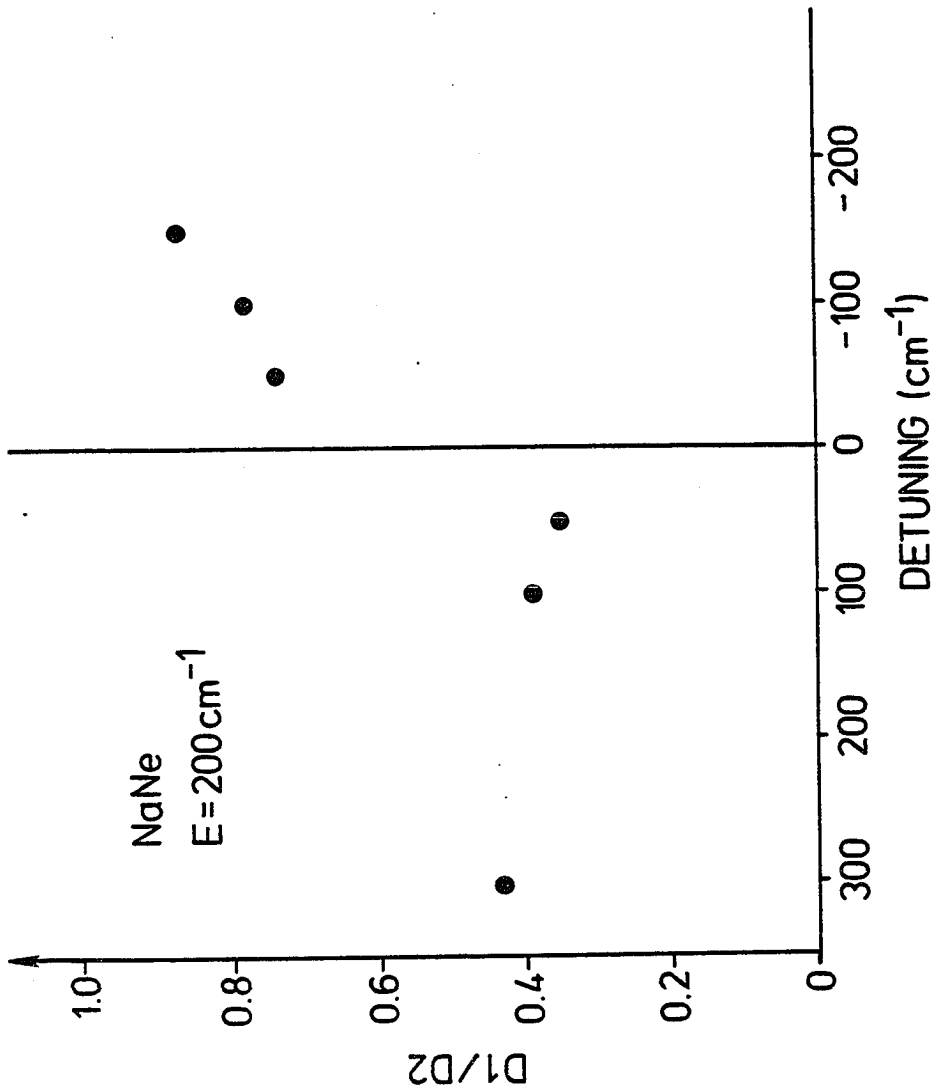

FIGURE 11

Numerically determined intensity ratio D1/D2
as a function of detuning for NaHe

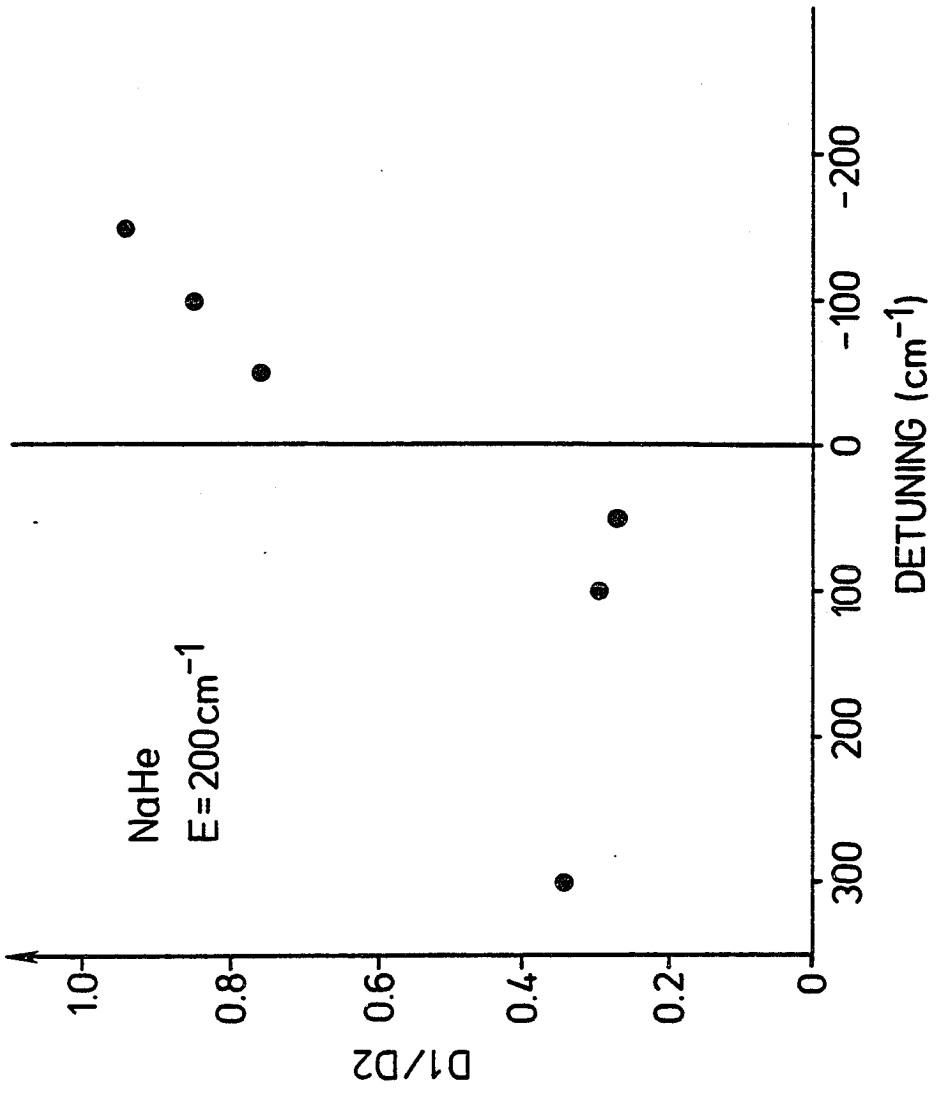

For NaNe, Figure 10, however we see that for blue-wing excitation the D1/D2 ratio increases with detuning, but is very significantly reduced over that for the NaAr case. Heuristically, this can be attributed to the potential difference between NaAr and NaNe. In particular, for blue-wing excitation the Na and rare gas atoms start to fly apart along the $B^2\Sigma_{1/2}$ potential. However, the $B^2\Sigma_{1/2}$ potential well for NaNe is considerably reduced from that of $B^2\Sigma_{1/2}$ for NaAr [see Figures 7a,7b], and the expected transition around the 'intersection' of $B^2\Sigma_{1/2}$ and $A^2\pi_{1/2}$ potentials is considerably reduced. Hence the probability of a transition from $B^2\Sigma_{1/2} \rightarrow A^2\pi_{1/2}$ state is decreased. Since the $A^2\pi_{1/2}$ state will dissociate into the excited Na $^2P_{1/2}$ state we thus expect the D1/D2 intensity ratio to decrease for NaNe over that for NaAr. This is clearly seen in Figures 10 and 11, and further reinforced for the NaHe case where there are extremely small potential wells for the $B^2\Sigma_{1/2}$ state making the transition coupling of $B^2\Sigma_{1/2} \rightarrow A\pi_{1/2}$ even further reduced over that of NaNe.

This same heuristic argument can qualitatively explain the far-red wing excitation results shown in figures 9-11. In the red-wing excitation the Na and rare gas atoms separate initially along the $A^2\pi$ states (i.e. both $A^2\pi_{1/2}$ and $A^2\pi_{3/2}$). However, due to the weak $B^2\Sigma_{1/2}$ potential wells of NaNe and the weaker well for NaHe, the probability of transitions of $A^2\pi_{1/2} \longrightarrow B^2\Sigma_{1/2}$ during the interaction region of these potentials is reduced in going from the

NaAr → NaNe → NaHe. Thus the extra population of the $^2P_{3/2}$ asymptotic excited Na atomic state from the molecular $^2A\Pi_{1/2}$ is reduced in going from NaAr → NaNe → NaHe since the $B^2\Sigma_{1/2}$ state dissociates asymptotically into the $^2P_{3/2}$ Na state. Since $A^2\Pi_{3/2}$ state also asymptotically dissociates into the Na $^2P_{3/2}$ state we see that the D1/D2 ratio is quite small for NaAr (with its significant coupling between $A\Pi_{1/2}$ and $B\Sigma_{1/2}$) and increases for NaNe and further increases for NaHe.

As expected, the intensity ratio of D1/D2 is sensitive to variations in the B-O potentials. For the NaAr system we have considered a Lennard-Jones $a_6 R^{-6} + a_8 R^{-8}$ fit for the $B^2\Sigma$ state for $R \approx R_e$, the potential well region, and $R > R_e$. For the small $R < R_e$ we assume a linear sharply repulsive potential. We found for far blue-wing excitation (detuning $\Delta \gg 0$) that asymptotically the intensity ratio D1/D2 $\approx$ .5 rather than 1.0 as seen experimentally. This intensity ratio D1/D2 $\approx$ 0.5 was insensitive to the rise of the repulsive linear potential core with slopes varying from 4.0 to 10.0.

We have also taken the potential minimum of the $B^2\Sigma_{1/2}$ of NaAr to be that given by the ab initio calculations of Saxon, Olson, Liu [27] to see the effects of the increased dissociation energy D_e over that used in generating Figures 9-11 [see Table 4]. The more recent work of Laskowski et. al.[29], as well as that of Duren et. al. [28], indicates that for NaAr, $D_e \approx 41.0$, rather than the Saxon, Olson, Liu

[27] result of $D \approx 55\ cm^{-1}$.

We find in this case, as also could have been expected from our earlier heuristic arguments, that the D1/D2 ratiio is increased significantly to $D1/D2 \approx 3.0$ over the experimental value of D1/D2 = 1.0.

We now expound a little on the heuristic argument for D1/D2 intensity ratio. For angular momentum coupling we see that

$$\begin{aligned} B^2\Sigma_{1/2} &\longrightarrow \sqrt{2/3}\ P_{3/2} + \sqrt{1/3}\ P_{1/2} \\ A^2\Pi_{1/2} &\longrightarrow \sqrt{1/3}\ P_{3/2} + \sqrt{2/3}\ P_{1/2} \\ A^2\Pi_{3/2} &\longrightarrow P_{3/2} \end{aligned} \qquad (7\text{-}5)$$

1. RED W1NG EXC1TAT1ON ($\Delta < 0$)

For red-wing excitation, the Na-rare gas system should initially separate on either the $\Pi_{1/2}$ or $\Pi_{3/2}$ potential curves. Assuming that it is equally probable to be on the $\Pi_{1/2}$ as on the $\Pi_{3/2}$ curve and that the 'mixing' of the potenial curves $A\Pi_{1/2}$ and $B\Sigma_{1/2}$ due to their 'overlap' is such that at this radial location there is a probability of a sudden transfer from the $\Pi_{1/2}$ state to the $B\Sigma_{1/2}$ state

$$\begin{aligned} \Pi_{1/2} &\approx \alpha B^2\Sigma_{1/2} + (1-\alpha)\Pi_{1/2} \\ &\longrightarrow 1/\sqrt{3}\,[\alpha/\sqrt{2} + (1-\alpha)\,].P_{3/2} \\ &\quad + 1/\sqrt{3}\,[\alpha + \sqrt{2}\,(1-\alpha)\,]\ P_{1/2} \end{aligned} \qquad (7\text{-}6)$$

on using equation (7-5). Thus asymptotically in R, the Na D1/D2 intensity ratio becomes

$$\frac{I(D1)}{I(D2)} = \frac{2 - \alpha}{1 + \alpha + 3} \qquad (7\text{-}7)$$

For very little 'overlap' between $A\Pi_{1/2}$ and $B\Sigma$, $\alpha \approx 0$ so that this simple argument predicts D1/D2 $\sim$ .5, while for strong 'overlap', $\alpha \sim 1$ so that D1/D2 is substantially reduced : D1/D2 = .2. Admittedly these ideas are very primitive, but they do give the correct qualitative trend between NaAr (strong overlap), NaNe (weak overlap) , NaHe (very weak overlap).

2. BLUE WING EXCITATION ($\Delta > 0$)

For blue wing excitation, the Na-rare gas is initally on the $B\Sigma_{1/2}$ curve so that with the subsequent overlap with the $\Pi_{1/2}$ curve having a probability of β of a sudden transition into the $\Pi_{1/2}$-state,

$$B^2\Sigma_{1/2} \approx \beta\Pi_{1/2} + (1 - \beta)\ B^2\Sigma_{1/2}$$

we have, following the primitive arguments given in the previous case, that

$$\frac{I(D1)}{I(D2)} = \frac{1 + \beta}{5 - \beta} \qquad (7\text{-}8)$$

Equation (7-8) predicts that

$$\left.\frac{I(D1)}{I(D2)}\right|_{NaAr} > \left.\frac{I(D1)}{I(D2)}\right|_{NaNe} > \left.\frac{I(D1)}{I(D2)}\right|_{NaHe}$$

which is qualitatively correct.

Of course, the true implications of the curve crossings, the magnitudes of the detuning can only be ascertained by a full quantum mechanical solution to the close-coupled equations and this is performed in this dissertation.

B. PARITY EFFECTS

Since the radiation-free Hamiltonian commutes with the parity operator, the wave functions describing the channel states are conveniently separated into parity $p_+ = (-1)^{J-1/2}$ and parity $p_- = (-1)^{J+1/2}$, where J is the initial total angular momentum of the molecular Hamiltonian operator. We now consider the difference between D1/D2 for parity p_+ over that for D1/D2 for parity

p_- as compared to the overall total D1/D2 intensity ratio as a function of the detuning Δ. These differences are shown in Figures 12, 13, and 14.

FIGURE 12

Parity difference as a function of detuning for NaAr

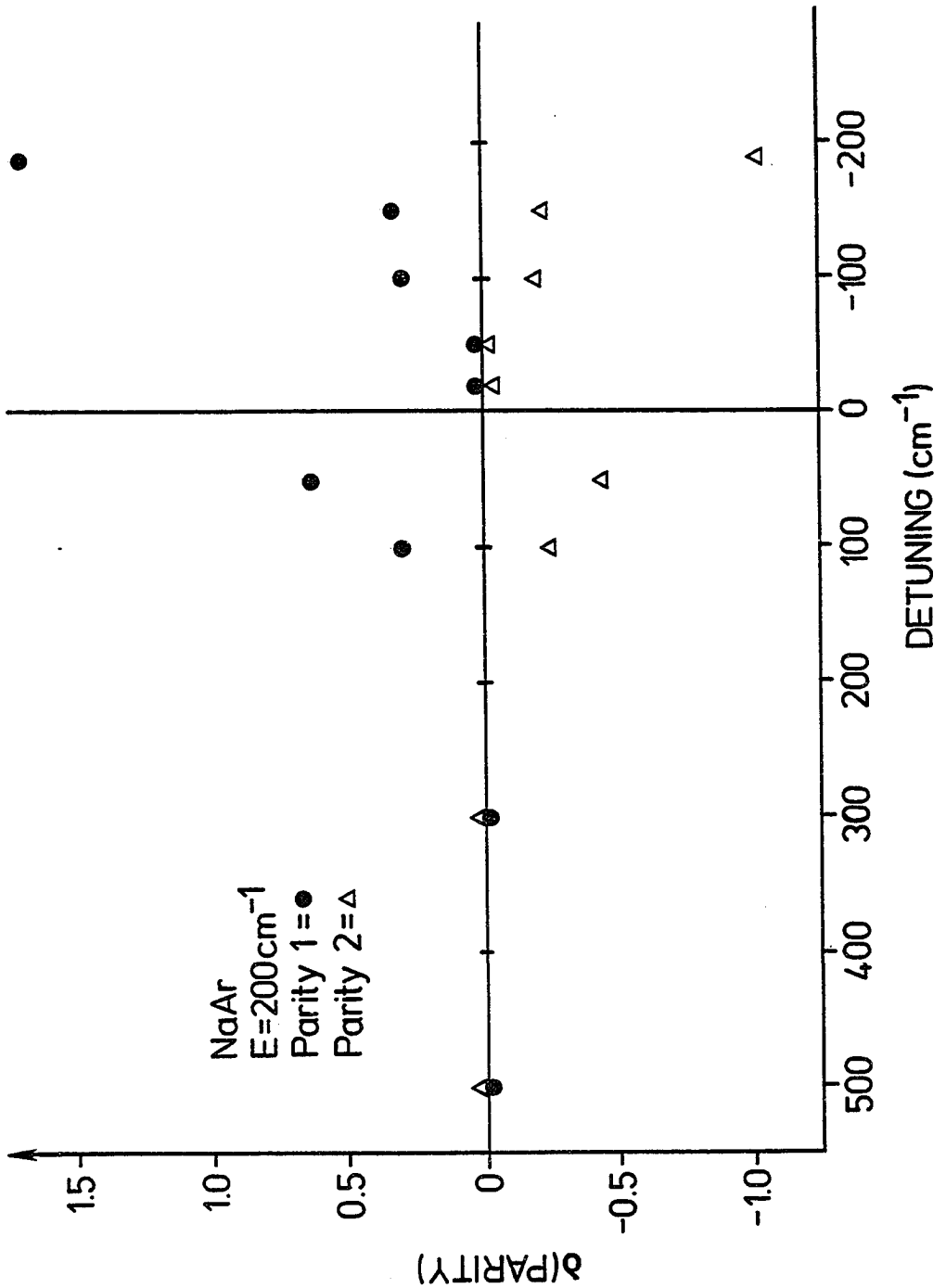

FIGURE 13

Parity difference as a function of detuning for NaNe

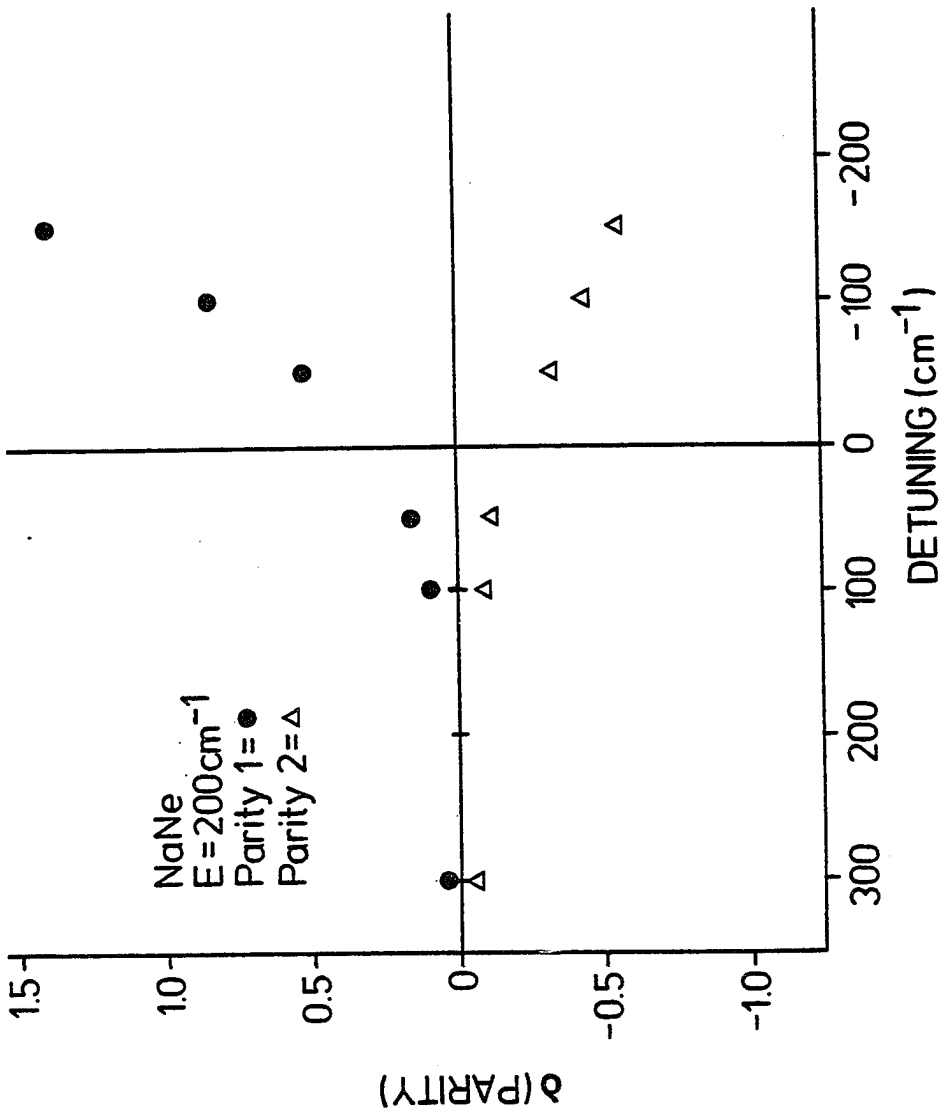

FIGURE 14

Parity difference as a function of detuning for NaHe

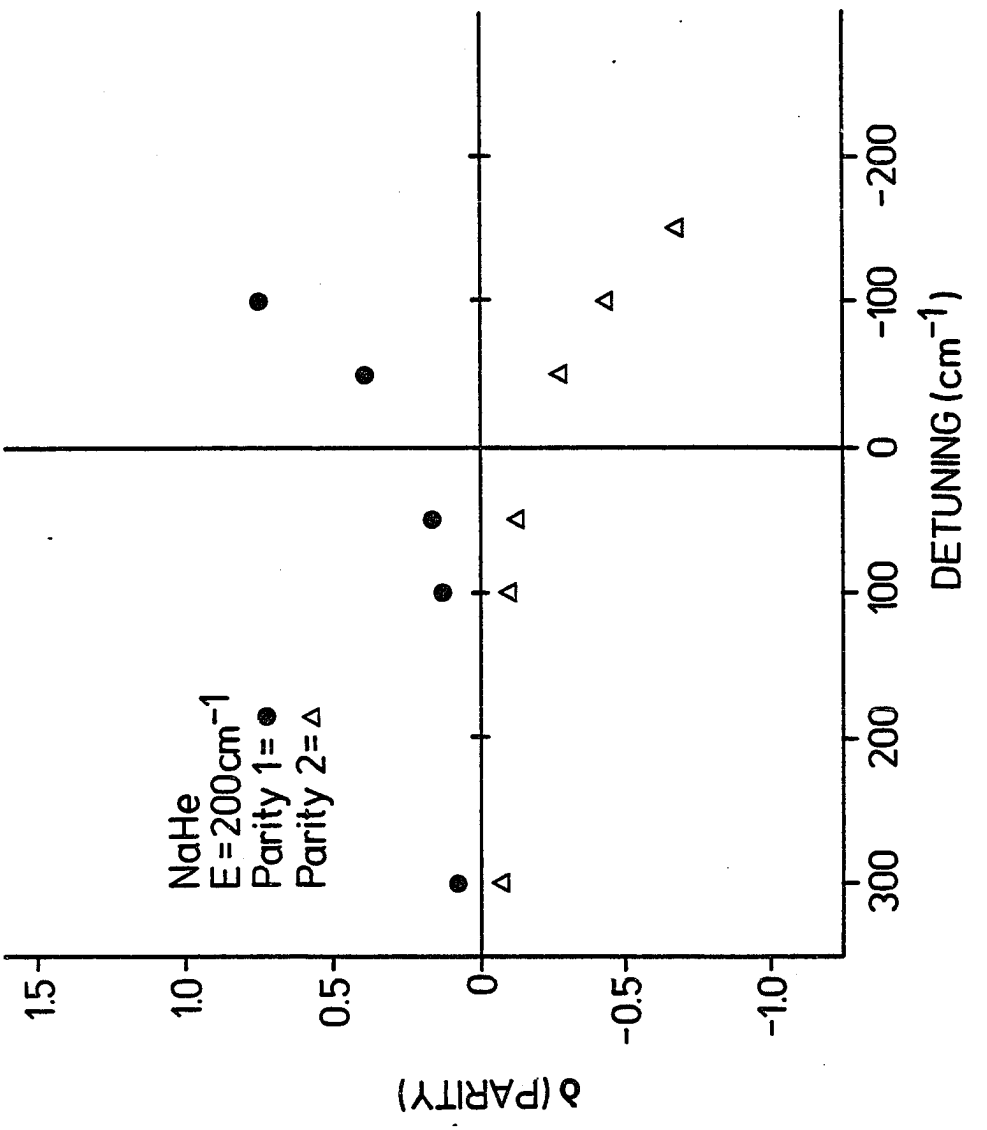

There is a dramatic difference between the NaAr case and the two cases of NaNe and NaHe. In particular both the NaNe and NaHe show a smooth monotonic change in the parity effect as the detuning is monotonically changed from the far blue-wing ($\Delta > 0$) to the far red wing ($\Delta < 0$). Moreover, there is a difference between parity $p_+=(-1)^{J-\frac{1}{2}}$ and parity $p_-=(-1)^{J+\frac{1}{2}}$. within each particular Na-rare gas molecule. Invariably, parity $p_+=(-1)^{J-\frac{1}{2}}$ shows a more pronounced effect as a function of detuning Δ. While this parity asymmetry suggests the effects discussed by Green and Zare [36], it is worth investigating further.

It is also very evident from the numerical results that for parity $p_+=(-1)^{J-\frac{1}{2}}$ the P-branch ($J_f=J-1$), and R-branch ($J_f=J+1$) have dominant contributions to the cross sections, while the contributions from the Q-branch ($J_f=J$) are negligible. However for parity $p_-=(-1)^{J+\frac{1}{2}}$, the situation is reversed: the major contribution to the cross sections comes from the Q-branch, while the P- and R-branches have negligible effect.

C. CROSS SECTIONAL DEPENDENCE ON ANGULAR MOMENTUM J

Foror the radiation-free Hamiltonian for the molecular system, the total angular momentum operator of the system commutes with this Hamiltonian. Thus J is a good quantum number. However, the introduction of a laser field with photon absorption implies that the total angular momentum of

the molecular (radiation-free) system is no longer conserved. The final angular momentum becomes

$$J_f = \begin{cases} J - 1 & , \quad \text{P-branch} \\ J & , \quad \text{Q-branch} \\ J + 1 & , \quad \text{R-branch} \end{cases}$$

for initial J. Thus, in essence, the cross sections could depend on all values of J, even $J \longrightarrow \infty$.

In figures 15-17, we present normalized cross-sections as a function of J for population of the Na $^2P_{1/2}$ and $^2P_{3/2}$ states. In figure 15, NaAr cross-sections for P-, Q-, and R- branches, and for both parities are given for a blue detuning of 100 cm^{-1}. Figure 16 and 17 show the J dependence of the normalized cross-sections for NaNe and NaHe, again for a blue detuning of 100 cm^{-1}. For these molecules, we present the results for only one parity, parity P_-. Note that in all of these figures J is incremented by two, as we do not wish to mix different parities.

We first see that the cross-sections, for a given J, are down by two orders of magnitude for the Q-branch as compared to the P-, and R- branches. For all cases, the cross-sections exhibit several oscillations up to some maximum J, after which the cross-section rapidly go to zero. The envelope of the oscillations is an increasing function of J. This behavior can be understood from elementary classical arguments; these are presented in the following paragraph. In all branches and parities, we also see that

FIGURE 15

Individual cross-sections as a function of J at detuning of $\Delta = 100\ cm^{-1}$ for the P-branch: (a) parity p_- for NaAr, (b) parity p_+ for NaAr, (c) parity p_- for NaNe, (d) parity p_- for NaHe

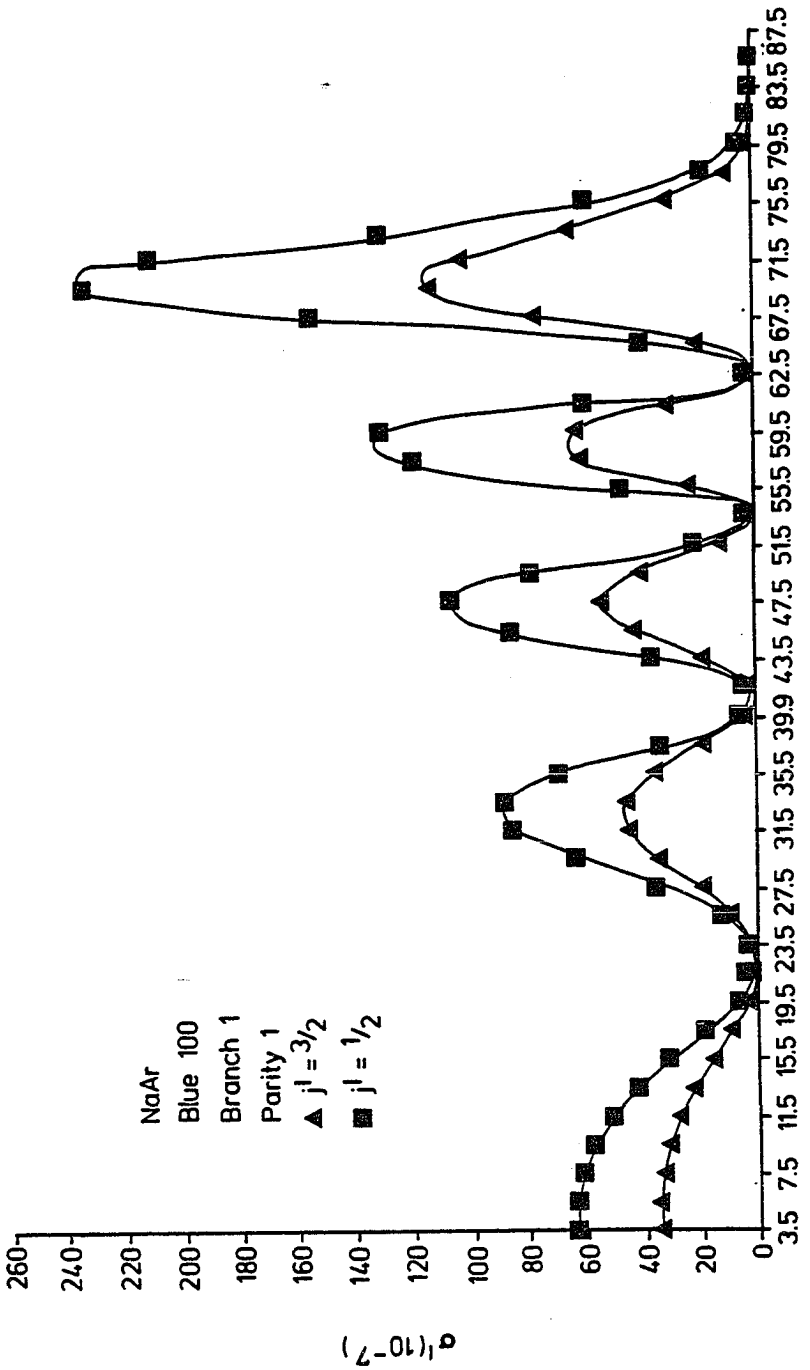

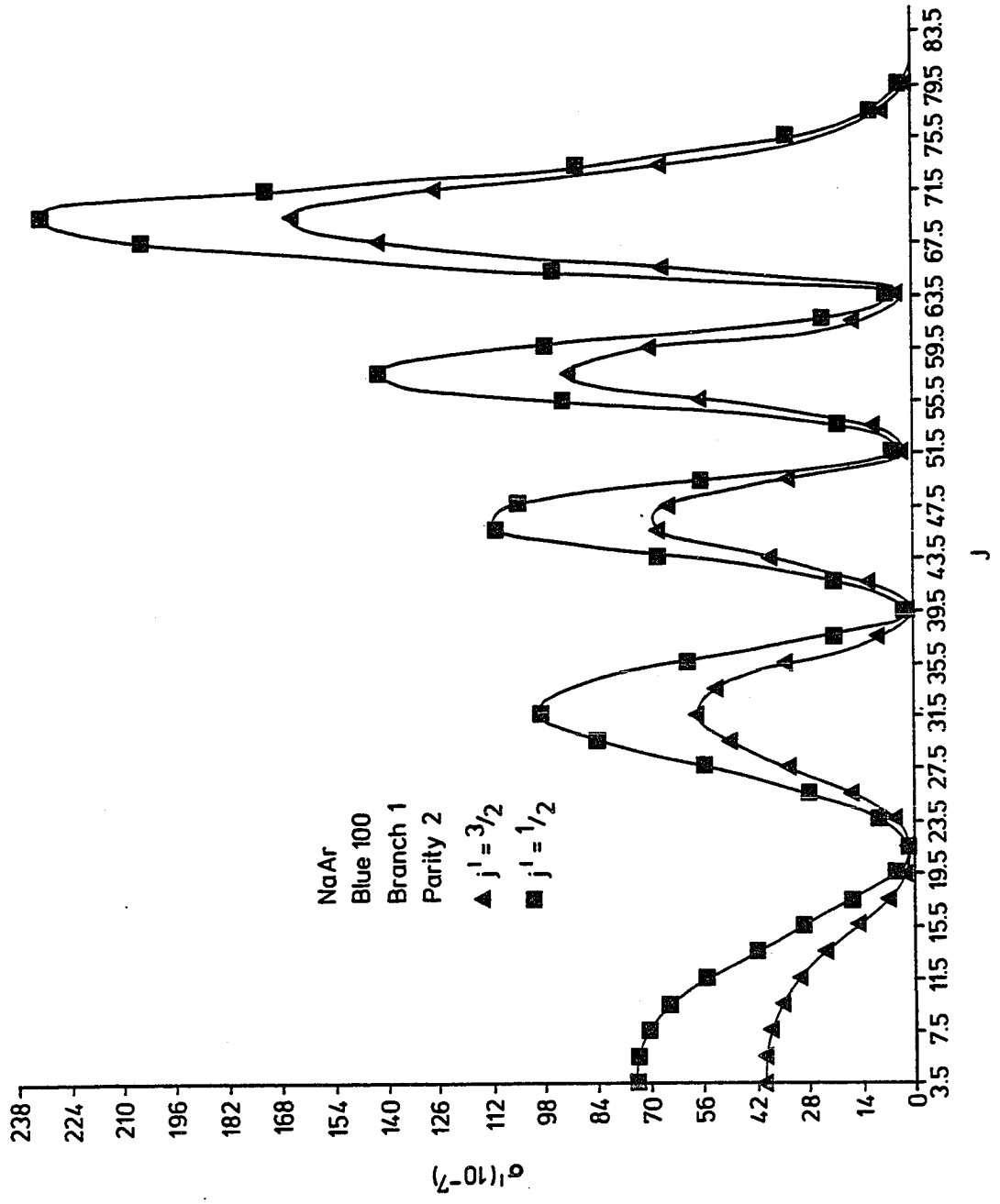

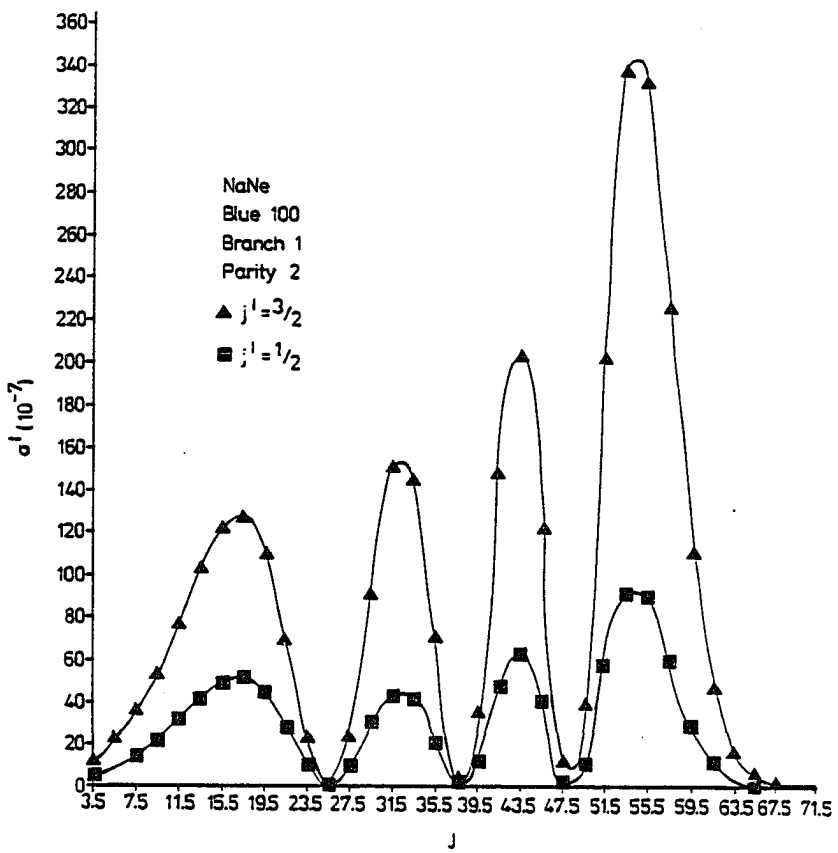

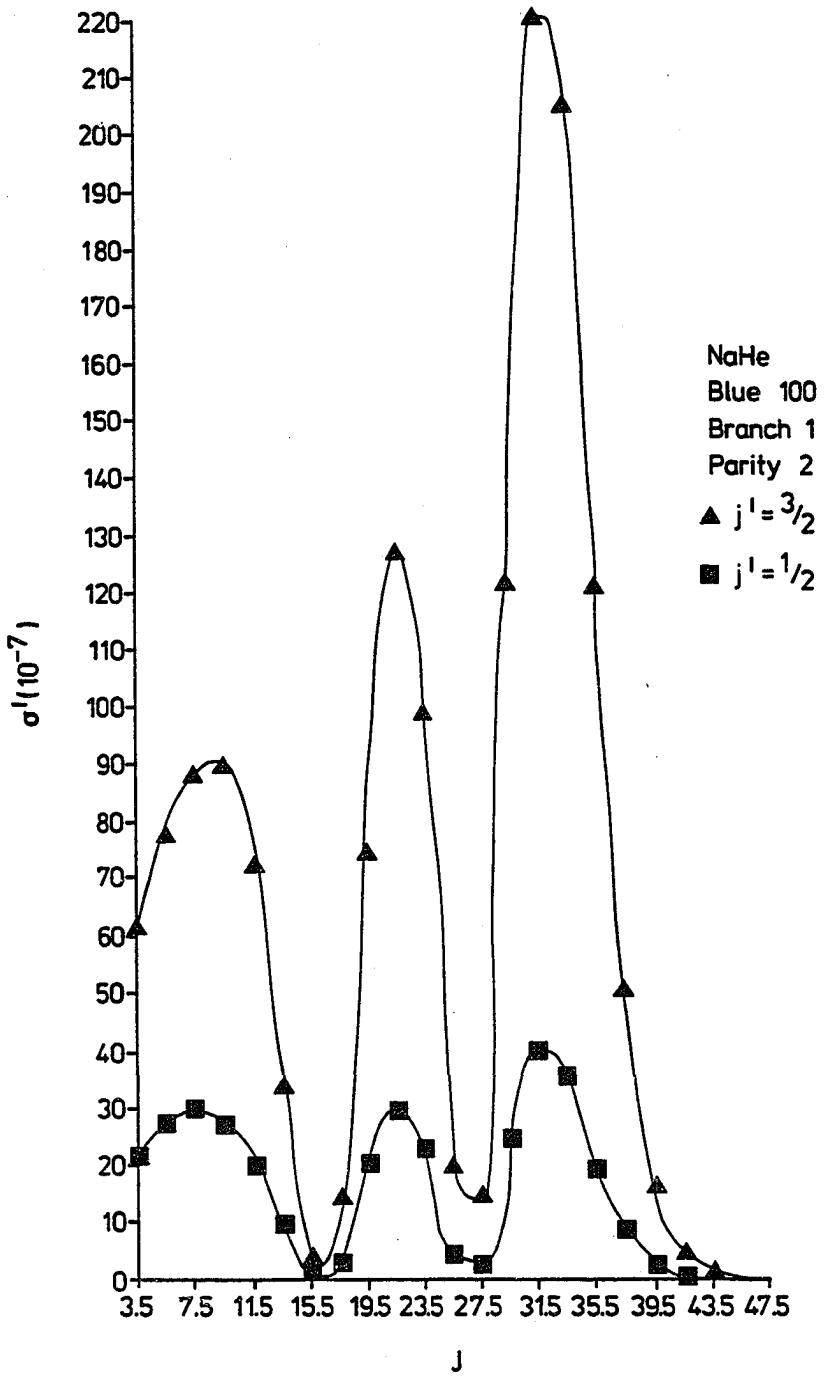

FIGURE 16

Individual cross-sections as a function of J at detuning of $\Delta = 100\ cm^{-1}$ for the Q-branch: (a) parity p_- for NaAr, (b) parity p_+ for NaAr, (c) parity p_- for NaNe, (d) parity p_- for NaHe

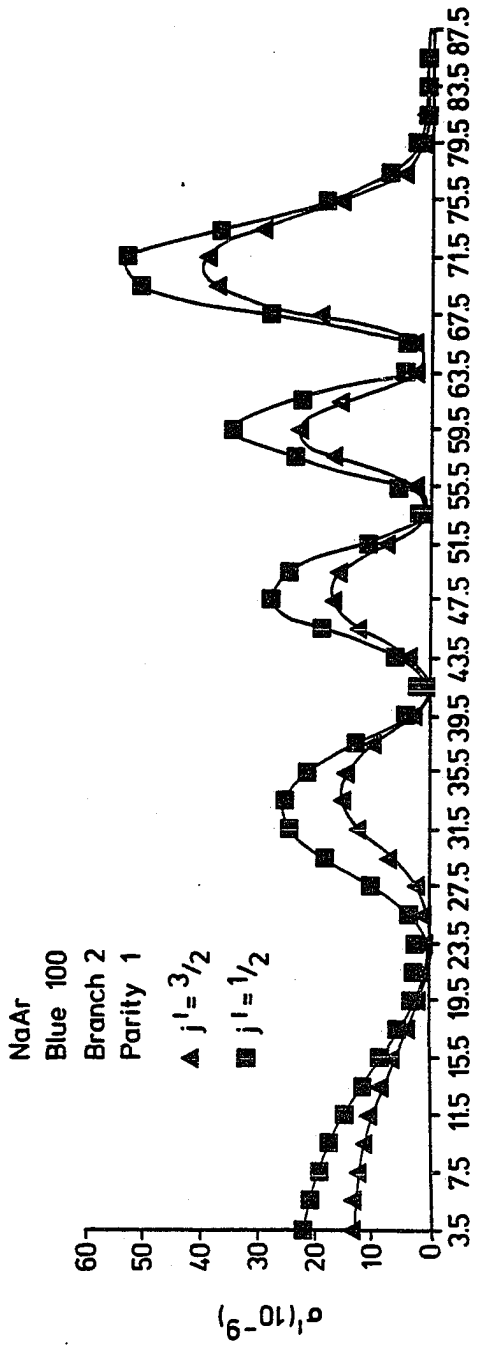

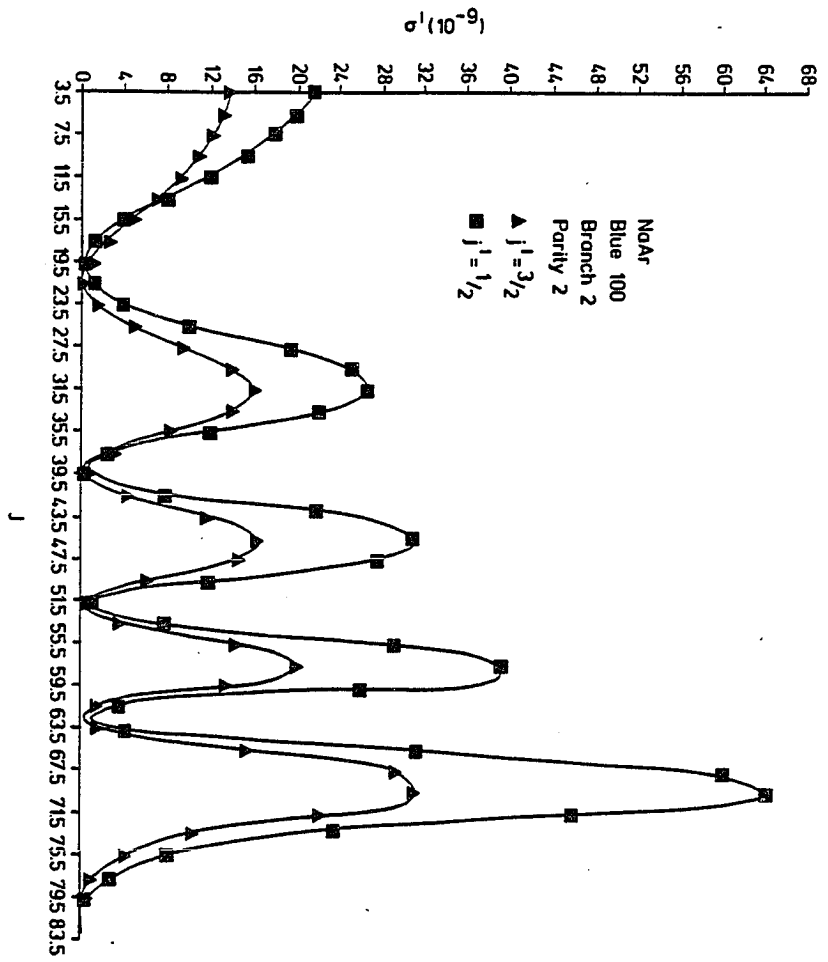

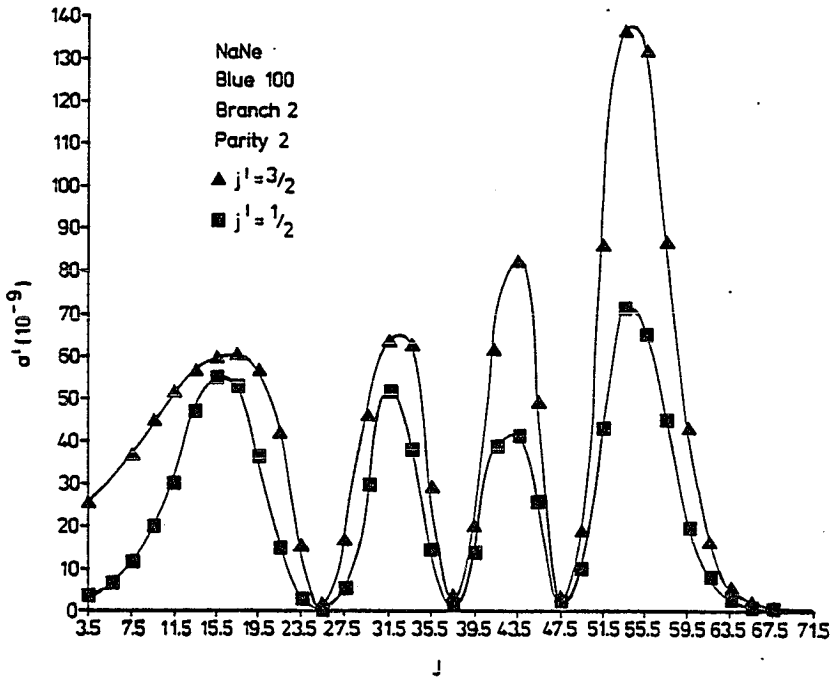

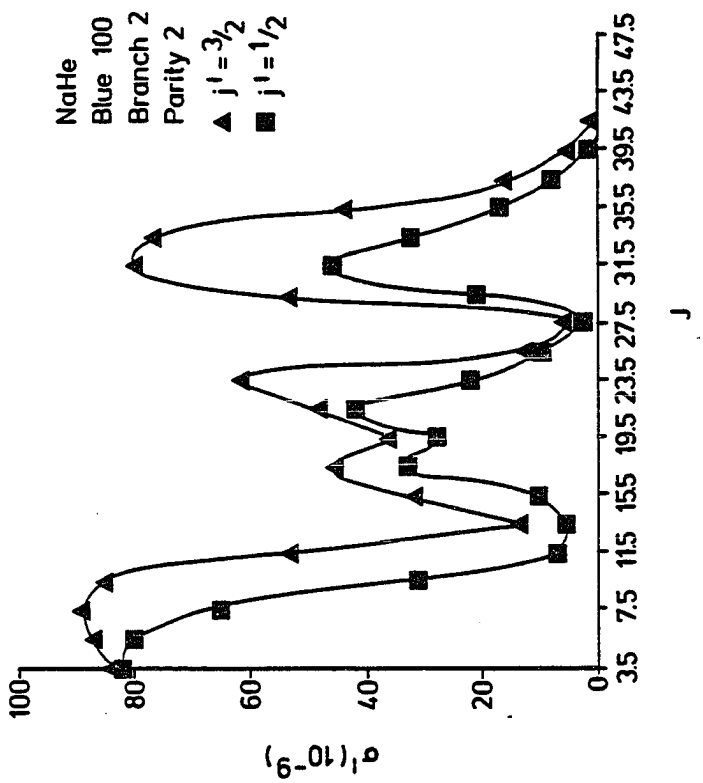

FIGURE 17

Individual cross-sections as a function of J at detuning of $\Delta = 100\ cm^{-1}$ for the R-branch: (a) parity p_- for NaAr, (b) parity p_+ for NaAr, (c) parity p_- for NaNe, (d) parity p_- for NaHe

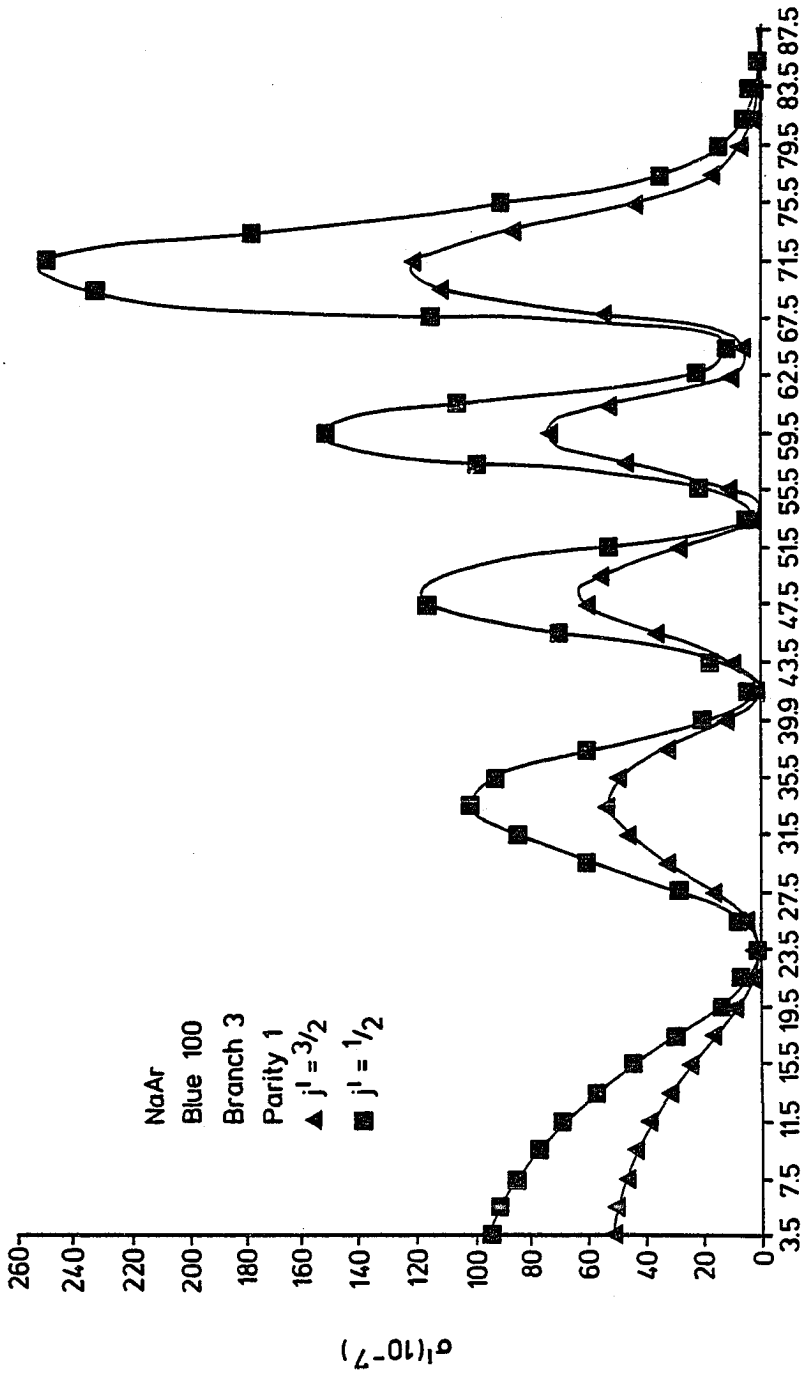

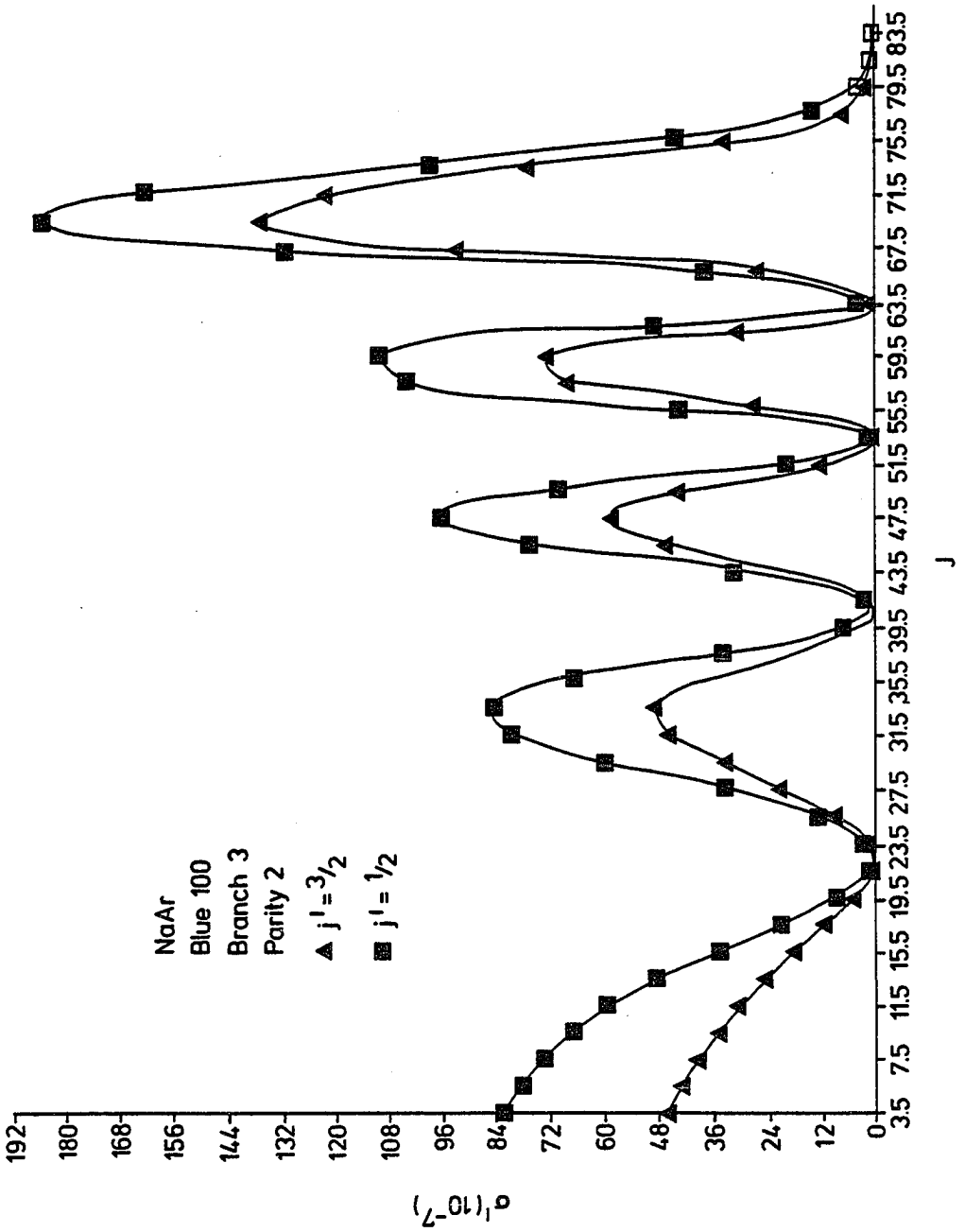

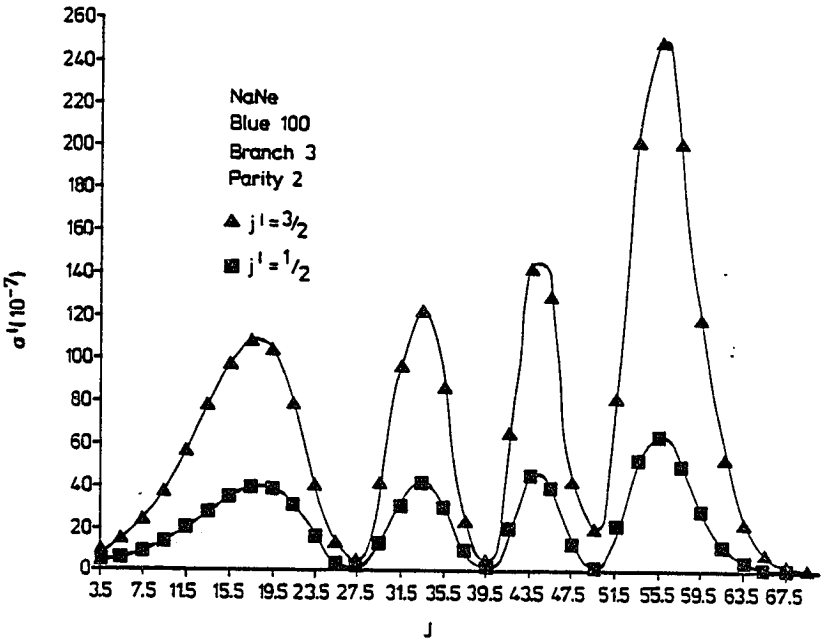

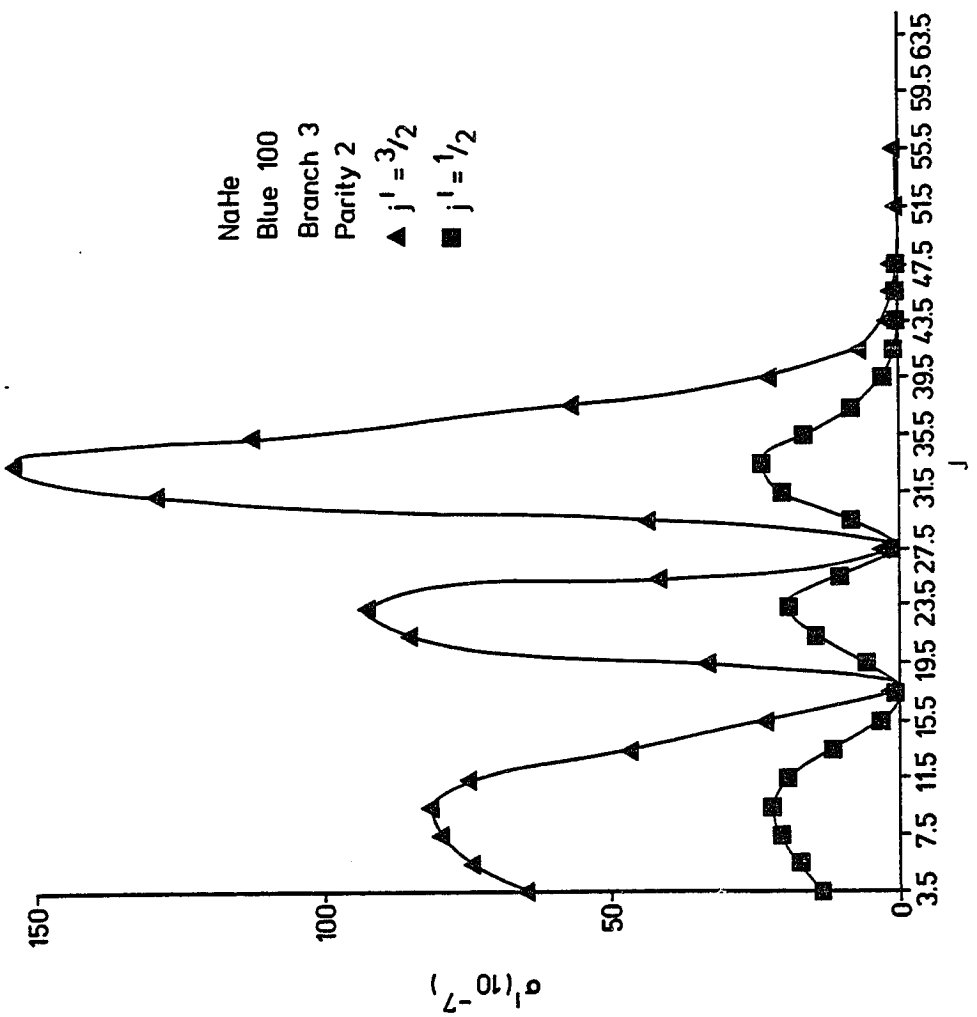

the oscillations, as function of J, are in phase. It also appears that,for a given molecule and parity, the relative maxima in the oscillations are shifted by J=2 for the P-branch relative to the R-branch.

The cutoff behavior of the cross sections with angular momentum J can be understood from a straight forward but oversimplified classical argument. Indeed if we assume the Franck-Condon principle applies so that transitions are most likely to occur at the classical turning points of a particle's trajectory we have in the center-of-mass coordinate system for the 'collision' of-Na and Ar atoms angular momentum

$$\ell \sim \mu v \quad b \quad \sim \sqrt{2 \mu E} \cdot b$$

where μ is the reduced mass, v the speed , E the impact energy and b the distance of closes approach. Let R_T be the maximum impact parameter radius so that

$$\frac{\ell_{(max)}}{\hbar} = \frac{2\pi \quad R_T}{\lambda_D}$$

where λ_D is the DeBroglie wavelength for NaAr: $\lambda_D = h/\sqrt{2\mu E}$ = 0.5 A. For blue wing excitation R_T = 10 a_o so that classically

$$\ell_{(max)}/\hbar \approx 63.5 \qquad (7\text{-}9)$$

Moreover, the classical geometrical cross section for hard sphere collisions, $\sigma_g = 4\pi R_T^2$ so that $\sigma_g \sim \ell^2$ until $\ell = \ell_{max}$ as sketched in Figure 18a. Now quantum mechanically, the analog of this (classical) orbital motion of Na and Ar atoms with respect to this center of mass is just the nuclear angular momentum operator $\vec{L}_R = -i\,\vec{R}\times\nabla_R \sim \hbar\ell$. Thus, from equation (7-9) we expect the cross section to have a maximum nuclear angular momentum before the cross section $\longrightarrow 0$. Moreover, R should be 'smeared' by quantum effects (typically, the fuzziness in the transition radius, $\delta R_T \sim 1\text{-}2\,\lambda_D$) leading to an increased ℓ_{max}. Also the location of the classical turning point R_T increases with ℓ, since for scattering energy E,

$$V(R_T) + \hbar^2\ell(\ell+1)/2\mu R_T^2 = E$$

so that for large ℓ, assuming $V(R_T) \ll E$

$$R_T \sim \sqrt{\hbar^2\ell(\ell+1)/2\mu E} \sim \lambda_D\ell/2\pi$$

(see Figure 18b) while for $\ell \sim 0$, R_T is the solution for $V(R_T) = E$. This increase of R_T with ℓ will also increase ℓ_{max} from that given in equation (7-9).

The oscillating behavior under the classical envelope seen in Figures 15-17 (remembering $\vec{J} = \vec{L}_R + \vec{j}$) is a quantum interference effect. Note also the quantum effects in the cross section for J near zero.

FIGURE 18

Schematic illustration of the classical behavior of the ground state scattering cross-section and the turning points as a function of orbital angular momentum

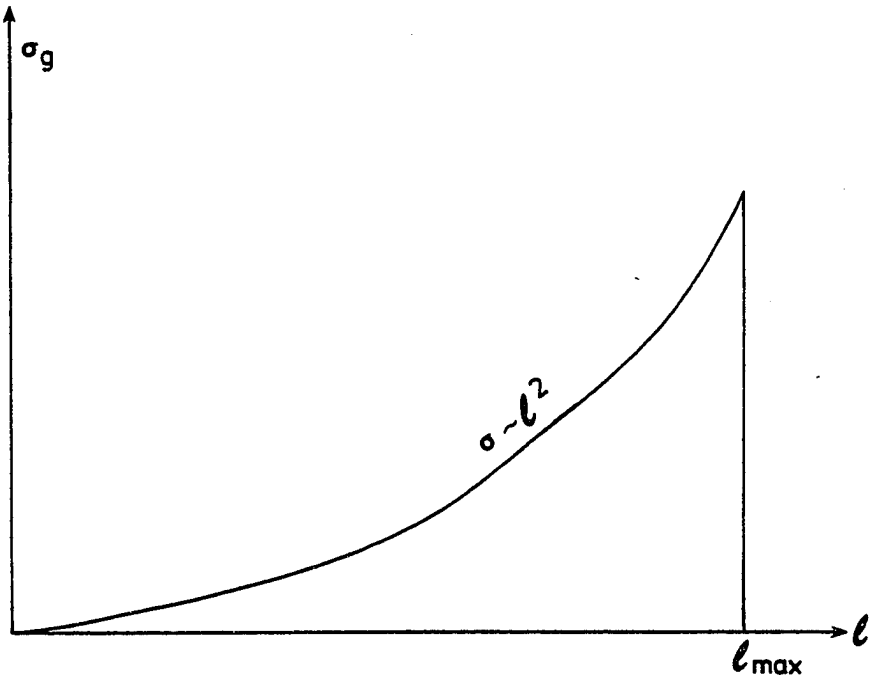

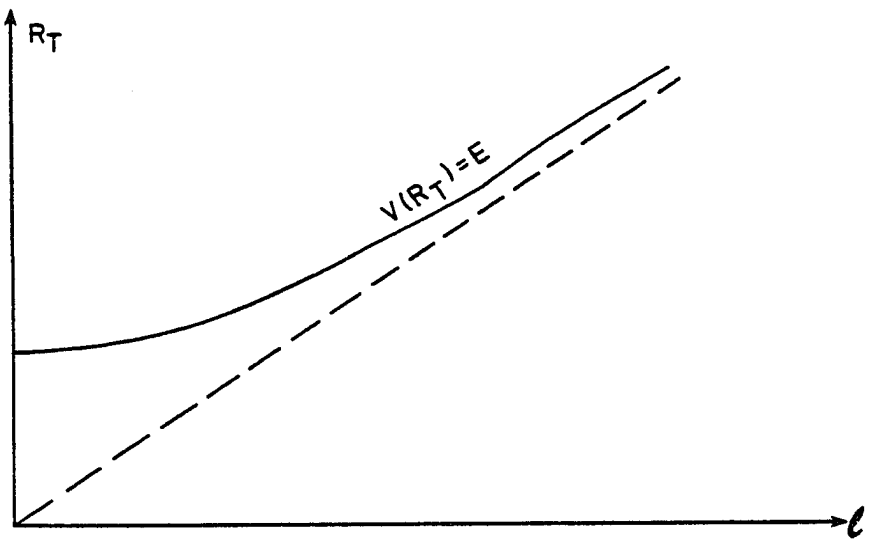

D. CROSS SECTIONAL DEPENDENCE ON INTIAL ENERGY E

Figure 19 is a plot of the $\sigma(1/2 \rightarrow 1/2)$ and $\sigma(1/2 \rightarrow 3/2)$ cross sections for both fixed red- and fixed blue-wing detuning as a function of the incident energy E. We see that $\sigma(1/2 \rightarrow 3/2)$ for red-detuning ($\Delta = -50$) has a maximum around $E = 200 cm^{-1}$ and then decreases monotonically, while all the other cross sections for both red-($\Delta = -50$) and blue-($\Delta = +100$) detuning monotonically decrease with energy.

We also plot the D1/D2 variation as a function of energy in Figure 20, and tabulate the results in Table 6.

E. POLARIZATION OF THE D2 LINE

As discussed in Chapter 6, there are strong hyperfine interactions in the Na $P_{3/2}$ state since j=3/2 and the nuclear spin I=3/2. This hyperfine interaction will destroy most of the alignment that might be produced by the far wing photon absorption leading to the excited $P_{3/2}$ - state. Experimentally, there are further depolarization effects due to collisional effects between the excited $P_{3/2}$ Na and the Ar atoms . Havey et. al.[13] report that an upper bound to the polarization of the D2 line is $\sim 10\%$ (on extrapolating to zero Ar pressure). Preliminary numerical work indicates the results listed in Table 7. Further work is planned.

FIGURE 19

Cross-section behavior as a function of energy for blue detuning of 100 cm^{-1}, and red detuning of 50 cm^{-1}

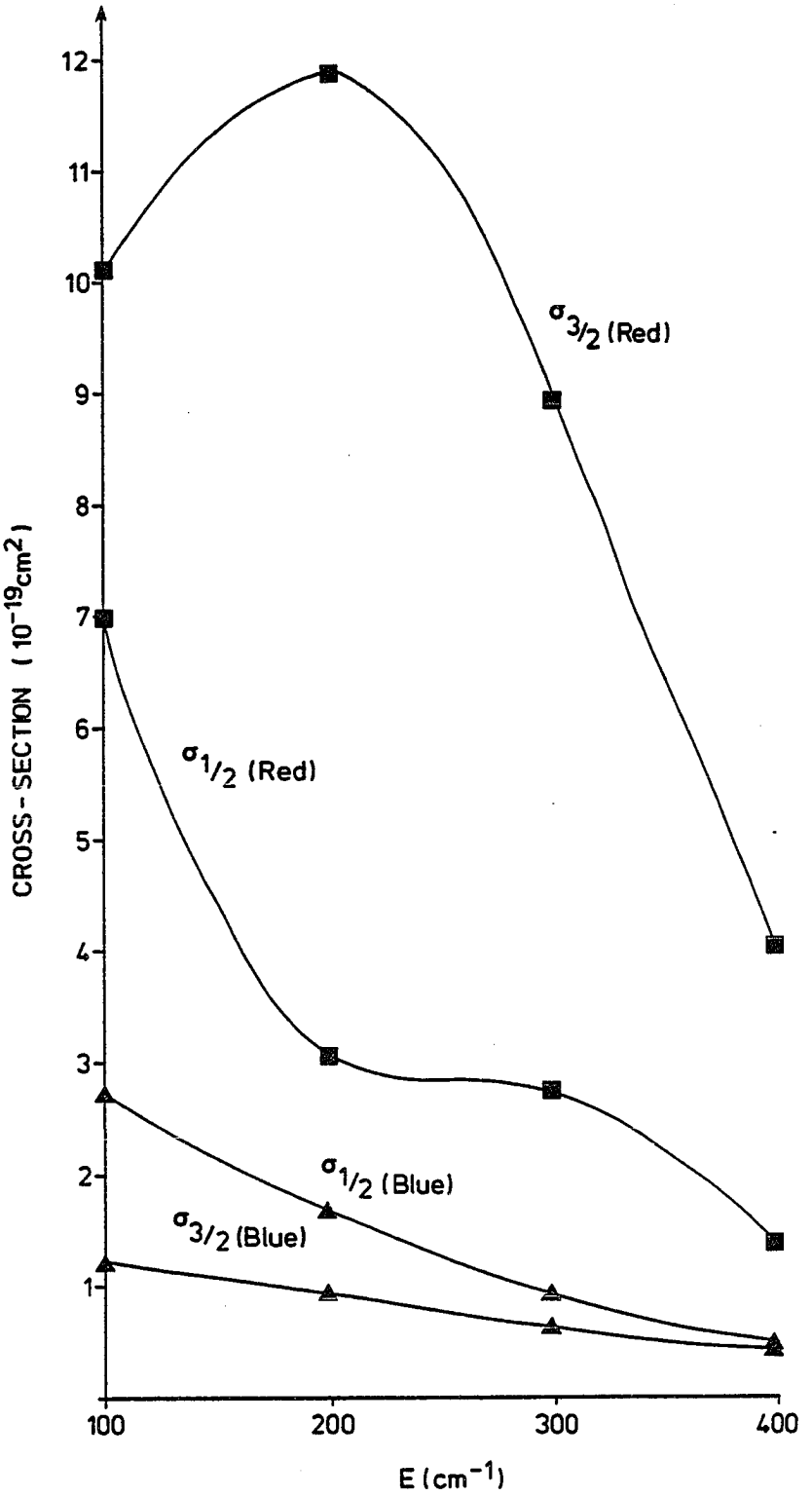

FIGURE 20

Intensity ratio D1/D2 as a function of energy for red(Δ =-50 cm^{-1}) and blue (Δ =+100 cm^{-1}) detuning. The indicated points ($\circ$) are for scattering energies of 100, 200, 300, and 400 cm^{-1}

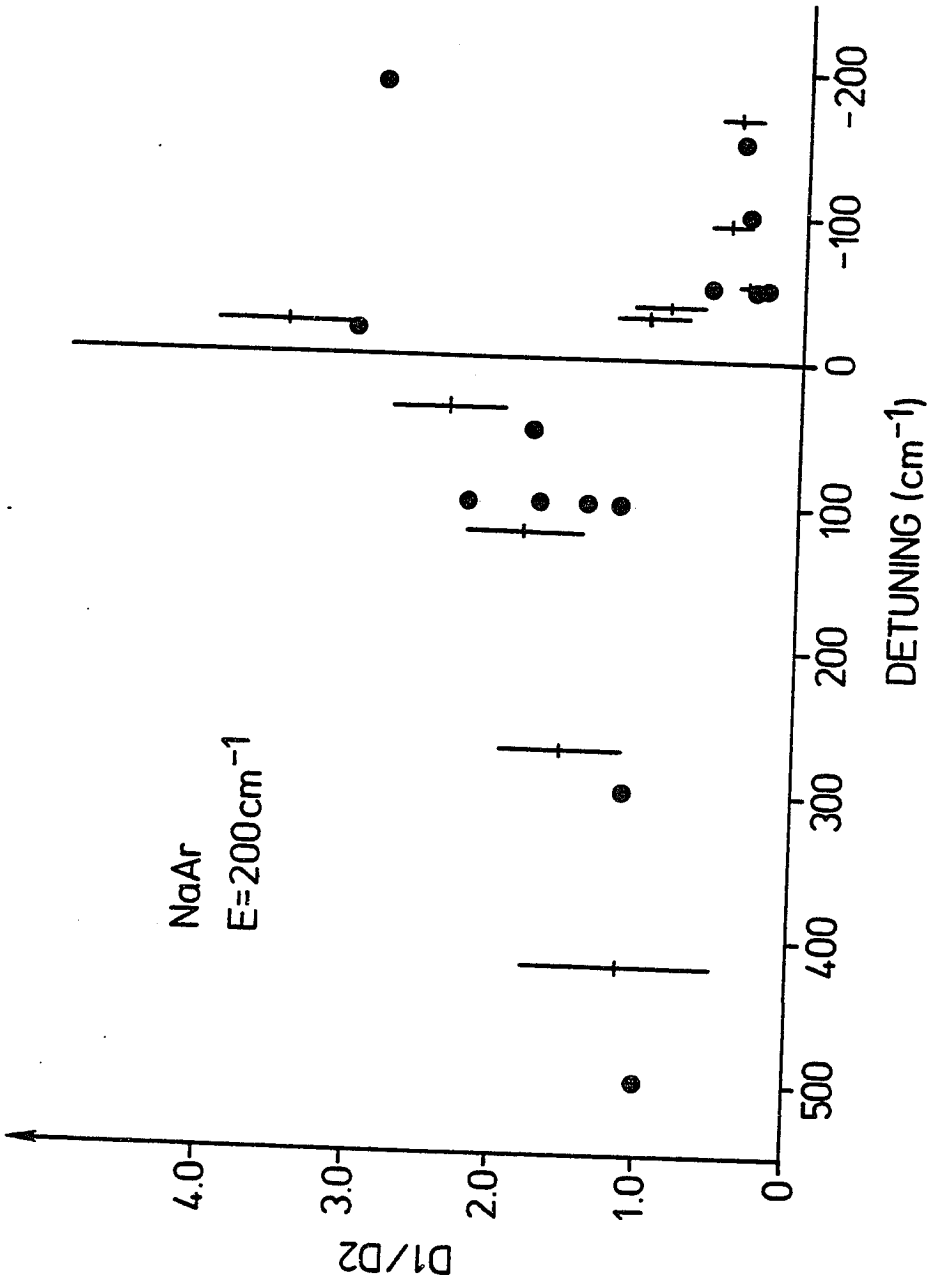

TABLE 6

The energy dependence of the intensity ratio I(D1)/I(D2) for red(Δ =-50 cm^{-1}) and blue (Δ =+100 cm^{-1}) detuning

D1/D2 RATIO

E(cm^{-1})	Red Detuning ($\Delta = -50 cm^{-1}$)	Blue Detuning ($\Delta = +100 cm^{-1}$)
100	0.64	2.25
200	0.25	1.73
300	0.31	1.44
400	0.35	1.20

TABLE 7

Cross-sections $\sigma(j\ m)$ for scattering into individual magnetic sublevels of the ^2P - state. ($\Delta = -100\ cm^{-1}$). Note that $\sigma(j\ m) = \sigma(j\ -m)$. The degree of linear polarization is given by P.

RED DETUNING ($100cm^{-1}$)

Parity	(1/2→3/2 1/2)	(1/2→3/2 3/2)
$(-1)^{J-1/2}$	0.025399	0.021827
$(-1)^{J+1/2}$	0.032692	0.037288

P =-0.7

F. EIGENFUNCTION BEHAVIOR VS. INTERNUCLEAR SEPARATION

In Figure 21 we show one of the eigenvectors for the P branch (detuning Δ =-100 cm^{-1}) for various internuclear separations R and various J. In particular, in solving the P branch, we are dealing with a 4 x 4 matrix in the Hund (a) representation c.f. Chapter 4

$$\begin{array}{c} {}^1\Sigma_u^+ \\ {}^1\Pi_{1/2} \\ {}^1\Pi_{3/2} \\ X\Sigma \end{array} \begin{bmatrix} * & * & * & * \\ * & * & * & * \\ * & * & * & * \\ * & * & * & * \end{bmatrix}$$

which in the process of solving the close coupled equations using the Gordon algorithm is diagonalized at the mid-point of each small grid interval in R. For each of the eigenvalues, we have a corresponding eigenvector which is projected onto the Hund (a) basis ($X\Sigma$, $B\Sigma$, $A\Pi_{1/2}$, $A\Pi_{3/2}$). For illustrative purposes, we look at the eigenvector which for all R has components predominantly in the $B\Sigma$ or $A\Pi_{1/2}$ states. Consider J= 3.5. For R < 12.1, $\psi \sim$(0,.999,.05,0), i.e. we have an $B\Sigma$- state. However , at a radial distance ~ 0.2 the eigenvector has suddenly changed predominantly into an $A\Pi_{1/2}$- state (0,.274,.962,0) at R=12.29, and which by R=12.45 is a 'pure' $A\Pi_{1/2}$ - state (0,.066,.998,0). However, for higher J we see that the transition from the $B\Sigma \rightarrow A\Pi_{1/2}$ state is far more gradual. We thus expect that the use of arguments based on sudden changes of molecular behavior along close Born-Oppenheimer

FIGURE 21

Projection of the scattering wavefunction onto Hund (a) basis as a function of internuclear separation

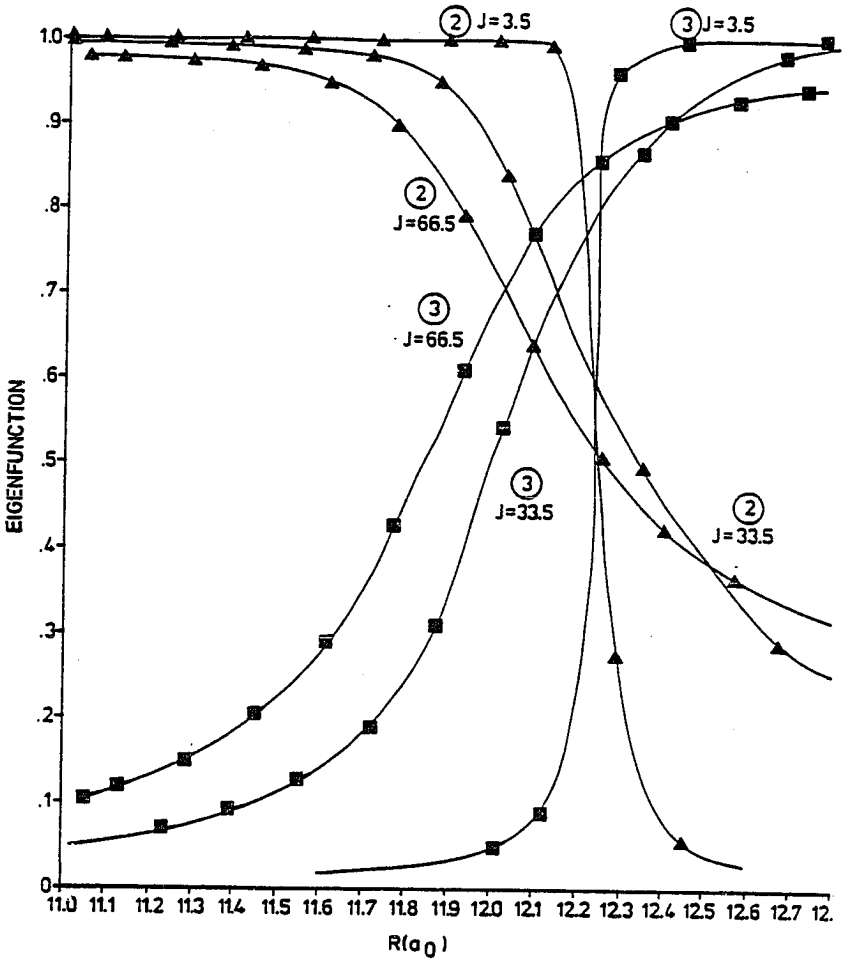

potential curves could lead to some errors since it is the larger J values that give the major contributions to the cross sections. In Figure 21, we see this effect more and more pronounced as J increases. We tabulate the coefficients in Table 8.

TABLE 8

Projection of eigenvectors at selected internuclear distances R onto the Hund (a) basis for blue detuning 100 cm^{-1}

Projection of Eigenvectors as a Function of R
onto Basis Vector ($X\Sigma$, $B\Sigma$, $A\pi_{1/2}$, $A\pi_{3/2}$)

R	J=3.5				J=33.5				J=65.5			
11.25	(0	1.000	0.006	0)	(0.070	0.995	0.070	0)	(0.142	0.978	0.152	0)
12.05	(0	0.999	0.050	0)	(0.017	0.838	0.545	0)	(0.031	0.636	0.771	0)
12.41	(0	0.066	0.998	0)	(0	0.495	0.869	0)	(0.024	0.426	0.904	0)
13.31	(0.001	0.019	1.000	0)	(0.025	0.182	0.983	0)	(0.056	0.264	0.963	0)
	$X\Sigma$	$B\Sigma$	$\pi_{1/2}$	$\pi_{3/2}$	$X\Sigma$	$B\Sigma$	$\pi_{1/2}$	$\pi_{3/2}$	$X\Sigma$	$B\Sigma$	$\pi_{1/2}$	$\pi_{3/2}$

CHAPTER 8

SUMMARY

The research presented here was motivated by the recent experiment of Havey, Copeland, and Wang [13] on fine-structure transitions occurring in collisional redistribution of far-off-resonant radiation. The experiments provided more detailed information than the usual cross-section measurements. The alkali-rare gas pair is very well suited for such experiments since the resonance lines (of the decaying alkali atom) are strong and in the visible frequency range. Moreover, we have relatively simple electronic structure since the alkalis can be taken as 1-electron atoms. However, complications are also present in both fine and hyperfine structure. For NaAr, NaNe, and NaHe, the Born-Oppenheimer potentials are sufficiently well known so as to make a full quantum mechanical calculation worth the effort.

We have employed the non-adiabatic theory of atomic collisions in the presence of a radiation field as developed by Mies [10] and Julienne [16], and by George and his collaborators [8,9]. The theory results in a coupled set of differential equations which incorporate, in a non-perturbative way, both the radiative and non-adiabatic

couplings in a time-independent molecular formulation. The good agreement in the D1/D2 intensities between the non-adiabatic theory and the experimental results of Havey et. al. [13] indicates the importance of the spin-orbit interaction in producing the fine-structure transitions occurring during the dissociation of the excited state molecule, and that it is properly treated by this time-independent formulation. We also note a related calculation by Kulander and Rebentrost [22] who used both a different set of Born-Oppenheimer potential curve fits and a different numerical procedure than we have presented here. They also find excellent agreement with the experimental results of Havey et. al. [13]. It should be noted that not all of the non-Born-Oppenheimer radial and angular couplings are included in the closed coupled set of equations which are solved numerically. Typically these terms arise from the dependence of the molecular basis on the internuclear separation R and so does not commute with the ∇_R^2 operator. However, it is believed [7-10,16] that for the low collision energies under consideration here that these effects are secondary to the main off-diagonal terms coming from the spin-orbit and rotational interactions. The good agreement between our results and those of Kulander and Rebentrost [22] to the experimental results of Havey et. al. [13] lends strong support for this commonly made approximation.

We have also investigated the effects of strong and weak mixing between the Born-Oppenheimer potentials by considering the molecular systems NaAr, NaNe, and NaHe. Parity effects were more pronounced than expected and warrant further investigation as do the hyperfine effects on the depolarization of the Na D2 line intensity.

REFERENCES

[1] D.R. Bates, Atomic and Molecular Processes (Academic Press, N.Y., 1962) pp. 597-621

[2] F.H. Mies, Physical Review 7A, 942, 958 (1973)

[3] E.E. Nikitin, Journal of Chemical Physics, 43, 744 (1965)

[4] E.E. Nikitin, Comments in Atomic Physics, 2, 122 (1970)

[5] R.W. Falcone, W.R. Green, J.C. White, J.F. Young, S.E. Harris, Physical Review A15, 1333 (1977)

[6] P.R. Brooks, R.F. Curl,Jr., R.S. Judson, R.S. Lowe, Physical Review Letters, 44,10, 587 (1980)

[7] M. Hutchinson, T.F. George, P.L. DeVries, Physical Review A28, 490 (1983)

[8] P.L. DeVries, T.F. George, Molecular Physics, 36, 151 (1978); 38, 561 (1979)

[9] P.L. DeVries, T.F. George, Physical Review, A18, 1751 (1978)

[10] F.H. Mies, in Theoretical Chemistry: Advances and Perspectives, edited by D. Henderson (Academic,.Y., 1981) vol. 6B, pp.127-198

[11] V. Kroop, W. Behmenburg, Z. Physik A294, 299 (1980)

[12] P.Thomann, K. Burnett, J. Cooper, Physical Review Letters, 45, 1325 (1980)

[13] M.D. Havey, G. Copeland, W. Wang, Physical Review Letters, 50, 1767 (1983)

[14] K. Burnett, J. Cooper, R.J. Ballagh, E.W. Smith, Physical Review A22, 2005 (1980)

[15] K. Burnett, J. Cooper, Review A22, 2027, 2(1980)

[16] P.S. Julienne, Physical Review A26, 3299 (1982)

[17] J. Ciurylo, L. Krause,JQSRT 28, 457 (1982)

[18] A.P. Hickman, Physical Review Letters, 47, 1585 (1981)

[19] M. Elbel, B. Niewitecka, L. Krause, Canadian Journal of Physics, 48, 29 (1970)

[20] J.C. White, G.A. Zdasiuk, J.F. Young, S.E. Harris, Physical Review Letters, 41,1709, (1978)

[21] C.B. Collins and J.A. Anderson, D. Popescu and Iovitzu Popescu, Journal of Chemical Physics, 74, 1043 (1981)

[22] K. Kulander, F. Rebentrost, Physical Review Letters, 51, 1262 (1983)

[23] R. Walkup, A.L. Migdall, D.E. Pritchard, Physical Review 25A, 3114 (1982)

[24] P.S. Julienne, F.H. Mies, Physical Review A25, 3399 (1982)

[25] I.M. Zimmerman, J-M. Yuan, T.F. George, Journal of Chemical Physics 66, 2638 (1977)

[26] M. Weissbluth, Atoms and Molecules (Academic, N.Y., 1978)

[27] R.P. Saxon, R.E. Olson, B. Liu, Journal of Chemical Physics, 67, 2692 (1977)

[28] R. Duren, E Hasselbrink, G. Moritz, Z. Physik, A307, 1 (1982)

[29] B.C. Laskowski, S.R. Langhoff, J.R. Stallcop, Journal of Chemical Physics, 75, 815 (1981)

[30] J.T. Hougen, NBS Monogram No. 115 (1970)

[31] L.C. Biedenharn, J.D. Louck, Angular Momentum in Quantum Physics (Addison-Wesley, Reading, 1981)

[32] M.E. Rose, Elementary Theory of Angular Momentum (Wiley, N.Y., 1957)

[33] R. Gordon, J. Chemical Physics 51, 14 (1969); Methods Computational Physics 10,81 (1971)

[34] U. Fano, J.H. Macek, Reviews of Modern Physics 45, 553 (1973)

[35] I.C. Percival, M.J. Seaton, Philosophical Transactions Royal Society of London, A251, 113 (1958)

[36] C.H. Greene, R.N. Zare, Journal Chemical Physics 73,6741 (1983); Annual Reviews of Physical Chemstry, 33, 119 (1982)

[37] J. Tellinghuisen, A. Ragore, S. Kim, D.J. Auerback, R.E. Smalley, L.Wharton, H.Levy, Journal of Chemical Physics, 71, 1283 (1979)

[38] J.C. Light, R.B. Walker, Journal of Chemical Physics, 65, 4272 (1976)

[39] M.D. Havey, unpublished

[40] J.B. Delos, Reviews of Modern Physics, 53, 287 (1981)

[41] P.S. Julienne, F.H. Mies, Journal of Physics, B14, 4335 (1981)

[42] F.H. Mies, Molecular Physics, 41, 973 (1980)

[43] F.H. Mies, W.J. Stevens, M. Krauss, Journal of Molecular Spectroscopy, 72, 303 (1978)

[44] C. Zener, Proceedings of the Royal Society 137A, 696 (1932)

APPENDIX 1

MOLECULAR HUND COUPLING CASES (a),(c),(e)

In the molecular electronic Hamiltonian H_{AB} there are three basic molecular interactions: the Coulomb, spin-orbit, and rotational interactions.

We introduce the following quantum numbers (internuclear axis $\vec{R}=R\hat{R}$) in Table 9.

Note that $\hat{R}.\vec{L}_R = 0$, i.e., the projection of the nuclear rotation angular momentum onto the nuclear axis is always zero.

The Hund coupling cases are limiting cases and we shall consider only those of interest to the Na-rare gas systems.

HUND (a)

In Hund (a), the Coulomb >> spin-orbit >> rotation interactions. Because of the strong internuclear electric field, the spatial part of the electronic wave function will rotate with the rotating internuclear axis. Thus the projection of the electronic orbital angular momentum onto the internuclear axis will be a good quantum number $|\Lambda| =$

TABLE 9

Notation used for the various angular momentum operators, their projections, and the associated eigenvalues

Operator	Quantum Numbers: Total	Projection onto Internuclear	Projection onto Space Fixed	Comments
Electronic Orbital Angular Mometum $\vec{L}$	L	Λ	M_L	
Electronic Spin Angular Momentum $\vec{S}$	S	Σ	M_S	
Total Electronic Angular Momentum $\vec{j}$	j	$\Omega = \Lambda + \Sigma$	m_j	$\vec{j}=\vec{L}+\vec{S}$
Nuclear Rotation Angular Momentum About Center of Mass $\vec{L}_R$	ℓ	0	M_ℓ	$\vec{L}_R = -i\vec{R} \times \nabla_R$
Total Angular Momentum $\vec{J}$	J	Ω	M_J	$\vec{J}=\vec{j}+\vec{L}_R$

0,1,2,..... giving rise to the $\Sigma^-, \pi^-, \Delta^-$ molecular states. On the other hand, the spherical symmetry of the system without Coulomb interaction is replaced by cylindrical symmetry about the internuclear axis. Hence the electronic orbital angular momentum operator $\vec{L}^2$ no longer commutes with the Hamiltonian for the interacting system so that L(L+1) is not a good quantum number.

The effect of the nuclear angular momentum operator $\vec{L}_R^2$ in the (noninertial) rotating frame is to introduce the equivalence of Coriolis and centrifugal forces which tend to decouple the electronic wave function from being fixed relative to the moving internuclear axis to being fixed in the inertial space-fixed frame. The spin-orbit interaction, being stronger than the decoupling Coriolis interaction in Hund case (a), tends to couple the spins with the internuclear axis in the rotating molecular frame. Thus the electronic spin angular momentum $\vec{S}^2$, and its projection onto the internuclear axis yield good quantum numbers.

The total wave function can be represented by the direct product of the vibrational/electronic part with the nuclear angular eigenfunctions. Thus Hund case (a) is specified by the quantum numbers $|\Lambda\ S\ \Sigma\ (p)\ ;\ J\ M_J\ (\Omega)\rangle$ where p is the parity operator discussed in Appendix 3 with $0 \leqslant \Lambda \leqslant L$, $-S < \Sigma < S$, and $0 \leqslant \Omega \leqslant \Lambda + S$. The nuclear rotational wavefunctions are chosen to be

eigenfunctions of the total angular momentum $\vec{J}^2$, and its space-fixed projection, since there is a weak but non-zero coupling between the nuclear and electronic angular momenta so that (j,m_j), (L,M_L), $(\vec{L}_R + \vec{L})^2$ and its projection are not qood quantum numbers.

Now for Hund (a), the electronic state follows the internuclear axis, giving rise to a non-zero angular momentum Λ along the internuclear axis. Hence one usually chooses the nuclear wave function $\Psi^{(\Omega)}_{JM_J}$ to be the symmetric top eigenfunctions of the total angular momentum operator $\vec{J}^2$ and its space-fixed projection [40].

$$\left[-(1/\sin\theta)\frac{\partial}{\partial\theta}\left(\sin\theta\frac{\partial}{\partial\theta}\right) + 1/\sin^2\theta\ \left(\frac{\partial}{\partial\varphi} - i\ \cos\theta\right)^2 - \Omega^2\right]\Psi^{(\Omega)}_{JM_J}$$

$$= J(J+1)\,\Psi^{(\Omega)}_{JM_J}$$

$$-i\frac{\partial}{\partial\varphi}\Psi^{(\Omega)}_{JM_J} = M_J\Psi^{(\Omega)}_{JM_J}$$

where (θ, φ) are the spherical angular coordinates of the internuclear axis relative to a space fixed frame. Ω is a parameter in these equations.

HUND (c)

In Hund (c) representation, the spin-orbit >> Coulomb >> rotational interaction. Since the spin-orbit interaction is dominant we go to the coupled electronic angular momentum representation so that the Hund (c) basis wave function is given by

$$\left| S\ j\ \Omega(p)\ ;\ J\ M_J\ (\Omega) \right>$$

with $|L - S| \leq j \leq L + S$ and $0 \leq \Omega \leq j$.

HUND (e)

For the Na-rare gas diatomic molecule the Coulomb potential of interaction is of the Van der Waal R^{-6} form, while the (Na-atomic) spin orbit interaction is sufficiently strong that spin-orbit >> rotational >> Coulomb interaction.

In this case the interatomic interactions are negligible and so we will eventually transform to this Hund (e) basis so as to apply the appropriate boundary conditions at infinity. One can use the coupled representation

$$|S\ j\ \ell\ ;\ J\ M_J\ (p)\rangle$$

with $|L - S| < j < L + S$, and $|J - j| < \ell < J + j$.

EXAMPLE FROM JULIENNE AND MIES [41]

Mies [42] has recently introduced the idea of adiabatic electronic-rotational (AER) states which span the whole space of electronic and nuclear rotational coordinates and which continuously (as function of internuclear separation R) diagonalizes the full molecular electronic rotational Hamiltonian. (The nuclear radial kinetic energy operator introduces coupling of the AER states which are treated perturbatively.) For the two lowest ungerade states of Hg_2, the Born-Oppenheimer potential curves [43] are given in Figure 22.

In Figure 22 we see the J=60 AER lowest adiabatic eigenstate projections onto the lowest eigenstate for pure Hund case (a) as a function of the internuclear separation R.

If the projection equals one, then we have a pure Hund coupling [for example for R > 8 a.u. we have pure Hund (c)]. Projections less than 1 imply that that there are no unique standard Hund coupling bases at that internuclear separation in which to represent the particular coupling operator under study.

FIGURE 22

Born-Oppenheimer potentials and eigenfunctions for Hg_2

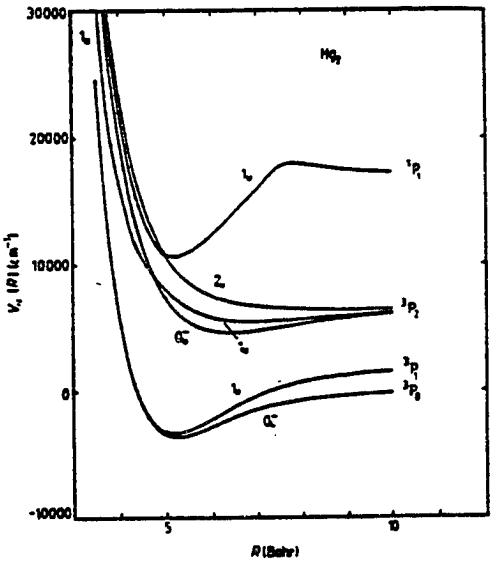

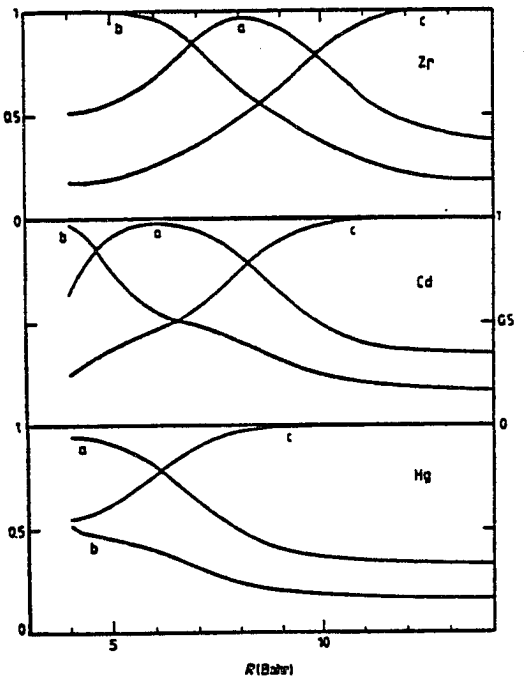

APPENDIX 2

ROTATION MATRICES: CLEBSCH-GORDON COEFFICIENTS

Here we review [30-32] some of the relevant aspects that we shall need concerning rotation matrices and Clebsch-Gordon coefficients. Rotation matrices are encountered when one transforms from space-fixed reference frame to the rotating molecular-fixed reference frame and vice-versa. Clebsch-Gordon coefficients are encountered when one switches from uncoupled to coupled representations, e.g., when one switches from Hund case (c) to (e).

A. ROTATION MATRICES

Let $\mathcal{R}(\alpha, \hat{n})$ correspond to a rotation about the axis $\hat{n}$ through and angle α in the right-hand sense. Thus, in rotating vectors we have for the position vector $\vec{r}$ where the origin is left fixed

$$\vec{R}' = \mathcal{R}(\alpha,\hat{n})\vec{r} = \vec{R}\cos\alpha + \hat{n}(\hat{n}\cdot\vec{r})(1-\cos\alpha) + (\hat{n}\times\vec{r})\sin\alpha \quad . \quad \text{(A2-1)}$$

The set of all rotations keeping the origin fixed but possibly having different rotation axes forms a group. If we consider the set of all rotations having a common axis of

rotation then this set will form an Abelian subgroup

$$\mathcal{R}(\alpha_1,\hat{n})\ \mathcal{R}(\alpha_2,\hat{n}) = \mathcal{R}(\alpha_2,\hat{n})\ \mathcal{R}(\alpha_1,\hat{n}) = \mathcal{R}(\alpha_1+\alpha_2,\hat{n}) \quad . \quad \text{(A2-2)}$$

The elements of the elements rotation group can be structured into equivalence classes characterized by the angle of rotation irrespective of the particular rotation axis; i.e. we can find a similarity transformation which which takes $\mathcal{R}(\alpha,\hat{n}')$ into $\mathcal{R}(\alpha,\hat{n})$. Indeed, choosing the rotation $\mathcal{J}:\hat{n}\rightarrow\hat{n}'$, then

$$\mathcal{R}(\alpha,\hat{n}') = \mathcal{R}(\alpha,\mathcal{J}\hat{n}) = \mathcal{J}\,\mathcal{R}(\alpha,\hat{n})\,\mathcal{J}^{-1} \quad . \qquad \text{(A2-3)}$$

Introduce a fixed coordinate frame with orthornormal vectors $(\hat{e}_1,\hat{e}_2,\hat{e}_3)$. A passive rotation is one in which the coordinate frame is rotated, but the physical object under consideration is kept fixed, while an active rotation transforms the physical object but leaves the coordinate frame fixed. Thus a passive rotation through an angle is equivalent to an active rotation of the object through an angle $-\alpha$.

Now for an arbitrary vector $\vec{y} = \sum y_i\ \hat{e}_i$,

$$\mathcal{R}\vec{y} = \sum_i \left(\sum_j R_{ij}\, y_j\right) \hat{e}_i = \vec{y}' \qquad \text{(A2-4)}$$

where we define $R_{ij} = \hat{e}_i\,\mathcal{R}\,\hat{e}_j$. Thus to each rotation $\mathcal{R}$

there is a corresponding matrix R which forms a representation of the rotation group since to any rotation projection $\mathcal{R}_1, \mathcal{R}_2$ there corresponds a matrix product $R_1 R_2$. This set of all 3 x 3 real orthogonal matrices with determinant = 1 forms the group SO (3). It should be noted that this representation is defined relative to a fixed reference frame.

We parametrize this group SO (3) by the Euler angles $(\alpha\ \beta\ \gamma)$, which relative to the fixed frame $(\hat{e}_1, \hat{e}_2, \hat{e}_3)$, are defined by the sequence of rotations (see Figure 23)

$\mathcal{R}_1$: rotation about $\hat{n}_1 = (0,0,1)$ through angle α

$\mathcal{R}_2$: rotation about $\hat{n}_2 = (-\sin\alpha, \cos\alpha, 0)$ through angle β

$\mathcal{R}_3$: rotation about $\hat{n}_3 = (\cos\alpha \sin\beta, \sin\alpha \sin\beta, \cos\beta)$ through angle γ . (A2-5)

Thus

$$\mathcal{R}(\alpha\beta\gamma) = \mathcal{R}_3(\gamma, \hat{n}_3)\ \mathcal{R}_2(\beta, \hat{n}_2)\ \mathcal{R}_1(\alpha, \hat{n}_1) \quad . \quad \text{(A2-6)}$$

Alternatively this rotation $\mathcal{R}(\alpha\beta\gamma)$ can be described relative to the fixed frame $(\hat{e}_1, \hat{e}_2, \hat{e}_3)$ by the successive rotations

$\mathcal{R}_3'$: rotation about $\hat{e}_3 = (0,0,1)$ through angle γ

$\mathcal{R}_2'$: rotation about $\hat{e}_2 = (0,1,0)$ through angle β (A2-7)

$\mathcal{R}_1'$: rotation about $\hat{e}_3 = (0,0,1)$ through angle α

FIGURE 23

Definition of the Euler angles (α , β , γ)

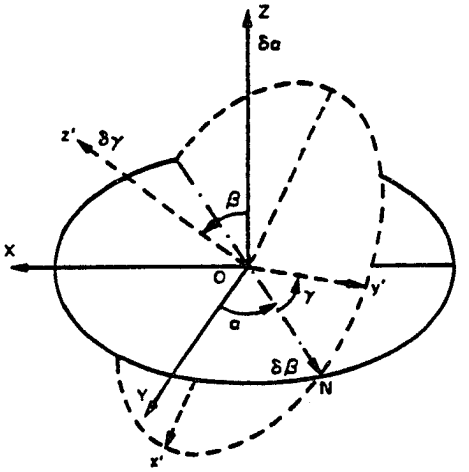

with

$$\mathcal{R}(\alpha\beta\gamma) = \mathcal{R}_1'(\alpha,\hat{e}_3)\ \mathcal{R}_2'(\beta,\hat{e}_2)\ \mathcal{R}_3'(\gamma,\hat{e}_3) \quad . \qquad \text{(A2-8)}$$

The Euler angles are such that $\alpha\in(0,2\pi)$, $\beta\in(0,\pi)$ and $\gamma\in(0,2\pi)$.

For passive rotations, the final coordinate system $(\hat{f}_1,\hat{f}_2,\hat{f}_3)$ is related to the fixed reference frame $(\hat{e}_1,\hat{e}_2,\hat{e}_3)$ by equation (6) with the matrix $\mathcal{R}(\alpha\beta\gamma)$ given by the direction cosines

$$\mathcal{R}(\alpha\beta\gamma) = \hat{e}_i \quad \hat{f}_j \quad .$$

For active rotations, $\mathcal{R}(\alpha\beta\gamma)$ maps an arbitrary vector $\vec{y}$ into the new vector $\vec{y}'$ with

$$\vec{y}' = \mathcal{R}(\alpha\beta\gamma)\,\vec{y},$$

and

$$\mathcal{R}(\alpha\beta\gamma) = \begin{bmatrix}\cos\alpha & -\sin\alpha & 0\\ \sin\alpha & \cos\alpha & 0\\ 0 & 0 & 1\end{bmatrix}\begin{bmatrix}\cos\beta & 0 & \sin\beta\\ 0 & 1 & 0\\ -\sin\beta & 0 & \cos\beta\end{bmatrix}\begin{bmatrix}\cos\gamma & -\sin\gamma & 0\\ \sin\gamma & \cos\gamma & 0\\ 0 & 0 & 1\end{bmatrix}$$

Note that

$$R^{-1}(\alpha\beta\gamma) = R(2\pi-\gamma,\ \pi-\beta,\ 2\pi-\alpha) \qquad \text{(A2-10)}$$

An alternative parametrization of the group SO(3) in terms of the set $(\alpha, \hat{n})$ by a rotation operator

$$U(\alpha,\hat{n}) = \exp(-i\alpha\,\hat{n}\cdot\vec{J}), \quad \alpha\in(0,2\pi) \qquad \text{(A2-11)}$$

where $\vec{J}$ is a vector operator with Hermitian components J_1, J_2, J_3. Thus $\vec{J}\times\vec{J} = i\vec{J}$, making $\vec{J}$ an angular momentum operator. For fixed eigenvalue J, consider the basis $\{|J\ M\rangle$ with $M = -J....J\}$, and the action of the unitary rotation operator U on it. $\vec{J}^2$ commutes with $U(\alpha,\hat{n})$, equation (A2-11), so that

$$\vec{J}^2\ U(\alpha,\hat{n})\ J\ M\rangle = U(\alpha\langle\hat{n})\ \vec{J}^2\ |J\ M\rangle$$
$$= J(J+1)\ U(\alpha,\hat{n})|J\ M\rangle .$$

Thus $U(\alpha,\hat{n})|J\ M\rangle$ is an eigenfunction of $\vec{J}^2$ with eigenvalue $J(J+1)$ so that it must be expressible as some linear combination of the $(2J+1)$ independent basis vectors $\{|J\ M\rangle, M = -J,....J\}$ of $\vec{J}^2$ with fixed J, i.e., there exists coefficients $D^{J}_{M'M}(\alpha,\hat{n})$ such that

$$U(\alpha,\hat{n})\ |J\ M\rangle = \sum_{M'=-J}^{J} D^{J}_{M'M}(\alpha,\hat{n})\ .\ |J\ M'\rangle . \qquad \text{(A2-12)}$$

Hence, from equation (A2-11), the elements of the rotation

matrix $D^{J}(\alpha,\hat{n})$ are given by

$$D^{J}_{M'M}(\alpha,\hat{n}) = \langle J\,M' \mid \exp(-i\alpha\,\hat{n}\cdot\vec{J}) \mid J\,M\rangle \qquad \text{(A2-13)}$$

In the Euler angle parametrization, the unitary rotation operator from equation (A2-11), is defined by

$$U(\alpha\,\beta\,\gamma) = \exp(-i\alpha J_z)\exp(-i\beta J_y)\exp(-i\gamma J_z) \qquad \text{(A2-14)}$$

In the fixed coordinate system $(\hat{e}_1,\hat{e}_2,\hat{e}_3) = (\hat{x},\hat{y},\hat{z})$. The corresponding rotation matrix elements are

$$D^{J}_{M'M}(\alpha\,\beta\,\gamma) = \langle J\,M' \mid U(\alpha\,\beta\,\gamma) \mid J\,M\rangle$$
$$= \exp(-i\alpha M')\langle J\,M' \mid \exp(-i\beta J_y) \mid J\,M\rangle \exp(-i\gamma M)$$

making use of equation (A2-14) and the expression

$$\langle J\,M' \mid \exp(-i\alpha J_z) =$$

$\langle \exp(i\alpha J_z)\,J\,M' \mid = \exp(-i\alpha M')\langle J\,M' \mid$ which holds since J_z is Hermitian and the angle α is real. Introducing the matrix elements

$$d^{J}_{M'M}(\beta) = \langle J\,M' \mid \exp(-i\beta J_y) \mid J\,M\rangle\,, \qquad \text{(A2-16)}$$

equation (A2-15) can be written in the form

$$D^{J}_{M'M}(\alpha\beta\gamma) = \exp(-i\alpha M')\,d^{J}_{M'M}(\beta)\exp(-i\gamma M). \qquad \text{(A2-17)}$$

Although explicit forms [30-32] can be given for $d^{J}_{M'M}(\beta)$ these are somewhat unenlightening. By unitarity

$$d^{J}_{M'M}(\beta) = d^{J}_{MM'}(-\beta)$$

while from the explicit forms $d^{J}_{M'M}(\beta)$ we can show that

$$d^{J}_{M'M}(+\beta) = (-1)^{M'-M} \cdot d^{J}_{MM'}(\beta) \qquad \text{(A2-18)}$$
$$= d^{J}_{-M,-M'}(\beta) \quad ,$$

i.e. ,

$$d^{J}_{M'M}(\beta) = (-1)^{M'-M} \cdot d^{J}_{-M,-M'}(\beta) \; . \qquad \text{(A2-19)}$$

Also,

$$d^{J}_{M'M}(\pi - \beta) = (-1)^{J-M'} \cdot d^{J}_{M,-M'}(\;) \qquad \text{(A2-20)}$$

Now, from equation (A2-14)

$$U^{-1}(\alpha\beta\gamma) = \exp(i\,\gamma\,J_z)\exp(i\,\beta\,J_y)\exp(i\,\alpha\,J_z), \qquad \text{(A2-21)}$$

so that, physically, the inverse rotation operator is related to the rotation operator by reversing the order of axes rotation and rotating through the negative angles. Since U is unitary

$$\langle J\,M' \mid U^{-1}(\alpha\beta\gamma) \mid J\,M \rangle = \langle J\,M \mid U(\alpha\beta\gamma) \mid J\,M' \rangle^{*}$$

Using equation (A2-21) and equation (A2-15), we obtain

$$\langle J\ M' \mid \exp(i\gamma J_z)\exp(i\beta J_y)\exp(i\alpha J_z) \mid J\ M\rangle = D^J_{M'M}(-\gamma,-\beta,-\alpha) = D^{J*}_{MM'}(\alpha\beta\gamma) \quad . \tag{A2-22}$$

Another useful relation is derived as follows: from equation (A2-17) and the reality of the $d^J_{M'M}$,

$$D^{J*}_{M'M}(\alpha\beta\gamma) = \exp(i\alpha M').d^J_{M'M}(\beta).\exp(i\gamma M)$$
$$= (-1)^{M'-M}\exp(M'i\alpha).d^J_{-M',-M}(\beta)\exp(i\gamma M)$$

by the equation (A2-20). Thus, from equation (A2-17)

$$D^{J*}_{M'M}(\alpha\beta\gamma) = (-1)^{M'-M}.D^J_{-M',-M}(\alpha\beta\gamma) \tag{A2-23}$$

B. SYMMETRIC TOP WAVE FUNCTIONS

Consider the Euler angles parametrization of the rotation matrices about the same coordinate frame

$$D^J(\alpha\beta\gamma) = \exp(-i\alpha J_z)\exp(-i\beta J_y)\exp(-i\gamma J_z)$$

Thus

$$\frac{\partial}{\partial\alpha}D^J(\alpha\beta\gamma) = -i J_z D^J(\alpha\beta\gamma) \tag{A2-24}$$

$$\frac{\partial}{\partial\beta}D^J(\alpha\beta\gamma) =$$

$$
\begin{aligned}
&-i \exp(-i\alpha J_z)\, J_y \exp(-i\beta J_y)\, \exp(-i\gamma J_z) \\
&= -i \exp(-i\alpha J_z) J_y \left[\exp(i\alpha J_z)\exp(-i\alpha J_z)\right] \\
&\qquad \cdot \exp(-i\beta J_y)\exp(-i\gamma J_z) \\
&= -i \left[\exp(-i\alpha J_z)\, J_y \exp(i\alpha J_z) D^J (\alpha\beta\gamma) \right. \\
&= -i \left[-J_x \sin\alpha + J_y \cos\alpha \right] . D^J (\alpha\beta\gamma) , \qquad \text{(A2-25)}
\end{aligned}
$$

since the rotation operator $U(\theta, \hat{n})$:

$$
\begin{aligned}
&\vec{J} \longrightarrow \vec{J}' = \exp(-i\theta\, \hat{n}\cdot\vec{J})\, \vec{J}\, \exp(i\theta\, \hat{n}\cdot\vec{J}) \\
&= \vec{J}\cos\theta + \hat{n}(\hat{n}\cdot\vec{J})(1-\cos\theta) - (\hat{n}\times\vec{J})\sin\theta \qquad \text{(A2-26)}
\end{aligned}
$$

Similarly,

$$
\begin{aligned}
&\frac{\partial}{\partial\gamma} D^J (\alpha\beta\gamma) = -i \left[D^J (\alpha\beta\gamma)\, J_z\, (D^J (\alpha\beta\gamma))^{-1}\right] D^J (\alpha\beta\gamma) \\
&= -i \left[J_x \cos\alpha \sin\beta + J_y \sin\alpha \sin\beta + J_z \cos\beta\right] D^J (\alpha\beta\gamma) \\
&\qquad\qquad\qquad\qquad\qquad\qquad\qquad\qquad\qquad\qquad \text{(A2-27)}
\end{aligned}
$$

Equations (A2-4), (A2-23), (A2-27) can be written in the operator form

$$
-\vec{g}\, D^J (\alpha\beta\gamma) = \vec{J}\, D^J (\alpha\beta\gamma) \qquad \text{(A2-28)}
$$

with

$$
\begin{aligned}
g_x &= i\cos\alpha\cot\beta\, \frac{\partial}{\partial\alpha} + i\sin\alpha\, \frac{\partial}{\partial\beta} - i\left[\cos\alpha/\sin\beta\right] \frac{\partial}{\partial\gamma} \\
g_y &= i\sin\alpha\cot\beta\, \frac{\partial}{\partial\alpha} - i\cos\alpha \frac{\partial}{\partial\beta} - i\left[\sin\alpha/\sin\beta\right] \frac{\partial}{\partial\gamma} \qquad \text{(A2-29)} \\
g_z &= -i\frac{\partial}{\partial\alpha} \quad .
\end{aligned}
$$

$\vec{g}$ is an angular momentum operator, since with the introduction of the negative sign in equation (A2-28), $\vec{g} \times \vec{g} = i\,\vec{g}$.

Defining $g_{\pm} = g_x \pm i\, g_y$

$$
\begin{aligned}
g_{\pm}\, D^{J*}_{M'M}(\alpha\beta\gamma) &= \sqrt{J(J+1) - M(M\pm1)}\; D^{J*}_{M'\pm1,M}(\alpha\beta\gamma) \\
g_{z}\, D^{J*}_{M'M}(\alpha\beta\gamma) &= M'\, D^{J*}_{M'M}(\alpha\beta\gamma) \\
\vec{g}^{\,2}\, D^{J*}_{M'M}(\alpha\beta\gamma) &= J(J+1)\, D^{J*}_{M'M}(\alpha\beta\gamma)
\end{aligned}
\qquad \text{(A2-30)}
$$

where $\vec{g}^{\,2} = \vec{g}\cdot\vec{g}$,

$$
\begin{aligned}
\vec{g}^{\,2} = -\Big[&(1/\sin\beta)\,\frac{\partial}{\partial\beta}\left(\sin\frac{\partial}{\partial\beta}\right) \\
&+ (1/\sin^2\beta)\left(\frac{\partial^2}{\partial\alpha^2} + \frac{\partial^2}{\partial\gamma^2} - 2\cos\beta\,\frac{\partial^2}{\partial\alpha\,\partial\gamma}\right)\Big] .
\end{aligned}
\qquad \text{(A2-31)}
$$

Thus the rotation matrices $D^{J*}(\alpha\beta\gamma)$ are eigenfunctions of the angular momentum operator $\vec{g}$ referred to a space-fixed frame.

Consider the orbital angular momentum of a particle $\vec{\mathcal{L}} = \vec{r} \times \vec{p} = -i\vec{r} \times \nabla$ (avoiding factors of $\hbar$). Using spherical polar angles (θ, φ)

$$
\begin{aligned}
\mathcal{L}_x &= i\cos\varphi\cot\theta\,\frac{\partial}{\partial\varphi} + i\sin\varphi\,\frac{\partial}{\partial\theta} \\
\mathcal{L}_y &= i\sin\varphi\cot\theta\,\frac{\partial}{\partial\varphi} - i\cos\varphi\,\frac{\partial}{\partial\theta} \\
\mathcal{L}_z &= -i\,\frac{\partial}{\partial\varphi}
\end{aligned}
\qquad \text{(A2-32)}
$$

Thus $\vec{\mathcal{L}} = \vec{g}$, from equations (A2-29) and (A2-32), on

identifying $\beta = \theta$ and $\alpha = \varphi$ provided $\frac{\partial}{\partial \gamma} = 0$ in g. That is, defining

$$P_z = -i \frac{\partial}{\partial \gamma} \tag{A2-33}$$

we immediately find that

$$P_z \; D^{J*}_{M'M}(\alpha \beta \gamma) = M \; D^{J*}_{M'M}(\alpha \beta \gamma) \; . \tag{A2-34}$$

Hence $\vec{\mathcal{L}} = \vec{g}$ provided M= 0 so that the rotation matrices, which are eigenfunctions of $\vec{g}^2 = \vec{\mathcal{L}}^2$ if M = 0, reduce to the standard spherical harmonics in this special case

$$Y_{LM'}(\theta, \varphi) = \sqrt{(2L + 1)/4\pi} \; D^{L*}_{M'0}(\varphi \theta \gamma) \tag{A2-35}$$

When M=0 in $D^{L*}_{M'M}(\varphi \theta \gamma)$, $D^{L*}_{M'0}$ becomes independent of the Euler angle γ .

It is interesting to note that the operator P_z is related to the angular momentum operator $\vec{g}$, from equation (A2-29) and (A2-33), by

$$\begin{aligned} P_z &= \sin\beta \cos\alpha \, g_x + \sin\beta \sin\alpha \, g_y + \cos\beta \, g_z \\ &= \sum_i R_{iz}(\alpha \beta \gamma) g_i \end{aligned} \tag{A2-36}$$

Here $R(\alpha\beta\gamma)$ is the real orthogonal matrix equation (A2-9). Let us define the three operators

$$P_j \quad (j=1,2,3) \qquad = \sum_i R_{ij}(\alpha\beta\gamma)\, g_i \qquad \text{(A2-37)}$$

thus denoting the inertial space-fixed frame by the unit vectors $(\hat{e}_1, \hat{e}_2, \hat{e}_3)$ and the noninertial (molecular) frame with unit vectors $(\hat{f}_1, \hat{f}_2, \hat{f}_3)$ where the instantaneous orientation, relative to the inertial frame, is given by the Euler angles

$$f_j = \sum_i R_{ij}(\alpha\beta\gamma)\, \hat{e}_i \qquad \text{(A2-38)}$$

we come to the conclusion that while $\vec{g} = \hat{e}_1 g_1 + \hat{e}_2 g_2 + \hat{e}_3 g_3$ (and also denoted above by $\hat{e}_1 g_x + \hat{e}_2 g_y + \hat{e}_3 g_z$) is the total angular momentum of the physical system, P_j

$$P_j = \hat{f}_j \cdot \vec{g} = \sum_i R_{ij}(\alpha\beta\gamma)\, g_i \qquad \text{(A2-39)}$$

is the component of the total angular momentum referred to the moving (noninertial molecular) frame axis $\hat{f}_j$. Moreover, the commutation relation

$$\vec{P} \times \vec{P} = -i\vec{P} \qquad \text{(A2-40)}$$

says that $\vec{P}$ does not obey the usual angular momentum commutation relations. Rather, $-\vec{P}$ satisfies the canonical

angular momentum commutation relations.

From equation (A2-37) we find using subscripts 1,2,3 to refer to the axes in the noninertial molecular frame

$$P_{\pm} = P_1 \pm i P_2 = \exp(\mp i\gamma)\left[-i \cot\beta \frac{\partial}{\partial\gamma} \pm \frac{\partial}{\partial\beta} + (i/\sin\beta)\frac{\partial}{\partial\alpha}\right] \quad \text{(A2-41)}$$

$$P_3 = -i \frac{\partial}{\partial\gamma} \quad ,$$

so that

$$\begin{aligned} P_+ \; D^{J*}_{M'M}(\alpha\beta\gamma) &= \sqrt{J(J+1) - M(M-1)}\; D^{J*}_{M',M-1}(\alpha\beta\gamma) \\ P_- \; D^{J*}_{M'M}(\alpha\beta\gamma) &= \sqrt{J(J+1) - M(M+1)}\; D^{J*}_{M',M+1}(\alpha\beta\gamma) \qquad \text{(A2-42)} \\ P_3 \; D^{J*}_{M'M}(\alpha\beta\gamma) &= M\, D^{J*}_{M'M}(\alpha\beta\gamma) \quad . \end{aligned}$$

We thus see, that because of the negative sign in the commutation relations (A2-40), P_+ is a lowering operator while P_- is a raising operator in contrast to the standard angular momentum operators g_+ being a raising operator and g_- a lowering operator as in equation (A2-30).

SUMMARY

We have thus shown that the wave functions $D^{J*}_{M'M}(\alpha\beta\gamma)$ are the wave functions of a rotating symmetric top (i.e. a rigid object with center of mass fixed in space). g_3 is the z-component of the angular momentum referred to the inertial space-fixed frame, while P_3 is the angular

momentum referred to the noninertial molecular axis of symmetry. g_+ and P_- are raising operators on M' and M respectively, while g_- and P_+ are lowering operators on M' and M.

An alternative way of seeing that the rotation matrices $D^J(\alpha\beta\gamma)$ are the wave functions of the symmetric top is to note that the Schrodinger equation (moments of inertia $\underline{\underline{I}} = I_1(\hat{f}_1\hat{f}_1 + \hat{f}_2\hat{f}_2) + I_3\hat{f}_3\hat{f}_3$ in the noninertial molecular frame) is

$$T\,\psi_{LKM}(\alpha\beta\gamma) = E\,\psi_{LKM}(\alpha\beta\gamma) \qquad \text{(A2-43)}$$

where the kinetic energy operator T for a rigid body with symmetry axis $\hat{f}_3$ and which rotates about its center of mass is given by

$$T = (\hbar^2/2I_1)(\mathcal{L}_1^2 + \mathcal{L}_2^2) + (\hbar^2/2I_3)\mathcal{L}_3^2 \qquad \text{(A2-44)}$$

where the angular momentum operator

$$\vec{\mathcal{L}} = \mathcal{L}_1\hat{f}_1 + \mathcal{L}_2\hat{f}_2 + \mathcal{L}_3\hat{f}_3 ,$$

the projections being in the non-inertial molecular frame axes. But $d^{L*}_{KM}(\alpha\beta\gamma)$, with integers K, M running through -L to L, form a basis for $\vec{\mathcal{L}}$. Hence the rotation matrices are the symmetric top wave functions.

C. CLEBSCH-GORDON COEFFICIENTS

The Clebsch-Gordon coefficients occur in the unitary transformation from an uncoupled angular momentum representation in which the commuting operators $(\vec{J}_1^2, J_{1z}, \vec{J}_2, J_{2z})$ are diagonal to a diagonal coupled angular momentum representation $(\vec{J}^2, J_z, \vec{J}_1^2, \vec{J}_2^2)$ where

$$\vec{J} = \vec{J}_1 + \vec{J}_2$$
$$J_z = J_{1z} + J_{2z} \qquad \text{(A2-45)}$$

i.e.

$$|J\ M\ (J_1\ J_2)\rangle = \sum_{M_1, M_2} C\ (\ J_1\ J_2\ J\ ;\ M_1\ M_2\ M\ )\ .\ |J_1\ M_1\ ,\ J_2\ M_2\rangle \qquad \text{(A2-46)}$$

The Clebsch-Gordon coefficients have the property that

$$C(J_1\ J_2\ J\ ;\ M_1 M_2 M\ ) = 0 \qquad \text{(A2-47)}$$

unless $J = J_1 + J_2,\ J_1 + J_2 - 1,\ \ldots,\ |J_1 - J_2|$; algebraically $M_1 + M_2 = M$ and the typical restrictions $|M_1| < J_1, |M_2| < J_2$, $|M| = |M_1 + M_2| < J$. Because of the restriction $M = M_1 + M_2$ for the existence of nontrivial Clebsch-Gordon coefficients equation (A2-46) is sometimes abbreviated to

$$|J\ M\rangle = \sum_{M_1} C\ (\ J_1\ J_2\ J\ |\ M_1\ ,\ M-M_1\ )\ .\ |J_1 M_1\ ,\ J_2\ M-M_1\rangle \qquad \text{(A2-48)}$$

since $M_2 = M - M_1$.

The standard phase convention for the Clebsch-Gordon coefficients is that they be real. Thus the unitary real matrix of C-G coefficients is necessarily orthogonal

$$\sum_{M_1} C\,(J_1 J_2 J \mid M_1, M - M_1).C\,(J_1 J_2 J' \mid M_1, M - M_1) = \delta_{JJ'} \tag{A2-49}$$

so that the inverse transformation from coupled to uncoupled representations is given by

$$|J\ M\ ; J\ M - M_1\rangle = \sum_{J} C(J_1 J_2 J \mid M_1, M - M_1).|J\ M\ (J_1 J_2)\rangle \tag{A2-50}$$

Hence, it can be shown, from equation (A2-50) that

$$\sum_{J} C(J_1 J_2 J \mid M_1, M - M_1).C\,(J_1 J_2 J \mid M_1', M' - M_1') = \delta_{M_1 M_1'}.\ \delta_{MM'} \tag{A2-51}$$

The following symmetry relations (with $\vec{J}_3 = \vec{J}_1 + \vec{J}_2$, and algebraically $M_3 = M_1 + M_2$) can readily be shown [30-32].

$$C(J_1\ J_2\ J_3 \mid M_1\ M_2\ M_3) =$$

$$(-1)^{J_1+J_2+J_3}.C(J_1\ J_2\ J_3 \mid -M_1\ -M_2\ -M_3)$$

$$= (-1)^{J_1+J_2-J_3}.C(J_2\ J_1\ J_3 \mid M_2\ M_1\ M_3) \tag{A2-52}$$

$$= (-1)^{J_1-M_1}\sqrt{[(2J_3+1)/(2J_2+1)]}.C(J_1\ J_3\ J_2 \mid; M_1\ -M_3\ -M_2)$$

and similar results by intercombining these equations.

D. ROTATION MATRICES AND CLEBSCH-GORDON COEFFICIENTS

Equation (A2-50) gives the connection between the uncoupled and coupled representations, $|J_1\ M_1\rangle . |J_2\ M_2\rangle = \sum_J C(J_1\ J_2\ J \mid M_1, M_2, M_1 + M_2) . |J\ M_1 + M_2\rangle$ while if a coordinate system is rotated through the Euler angles $(\alpha\beta\gamma)$ the angular momentum eigenfunctions transform as those in equation (A2-12) or equation (A2-15) do .

$$U(\alpha\beta\gamma)\ |J_1\ M_1\rangle = \sum_{M_1'} D^{J_1}_{M_1' M_1}(\alpha\beta\gamma)\ |J_1\ M_1'\rangle$$

Thus for the Euler angle rotations $(\alpha\beta\gamma)$:

$$U\ |J_1\ M_1\rangle .\ |J_2\ M_2\rangle = \sum_{M_1', M_2'} D^{J_1}_{M_1' M_1} . D^{J_2}_{M_2' M_2}\ |J_1\ M_1'\rangle . |J_2\ M_2'\rangle$$

$$= \sum_J C(J_1\ J_2\ J \mid M_1, M_2, M_1 + M_2) . U\ |J, M_1 + M_2\rangle$$

$$= \sum_{J,M} C(J_1\ J_2\ J \mid M_1, M_2, M_1 + M_2)\ D^{J}_{M, M_1 + M_2}\ |J\ M\rangle$$

$$= \sum_{J,M} \sum_{M_1'} C(J_1\ J_2\ J \mid M_1, M_2, M_1 + M_2)$$

$$C(J_1\ J_2\ J \mid M_1', M_2', M_1' + M_2')\ D^{J}_{M, M_1' + M_2'} |J_1, M_1'\rangle |J_2, M - M_1'\rangle$$

making use of equation (A2-48). By relabelling the eigenvectors in the uncoupled representation, we thus get the Clebsch-Gordon series

$$D^{J_1}_{M_1' M_1}(\alpha\beta\gamma)\ D^{J_2}_{M_2' M_2}(\alpha\beta\gamma) = \sum_J C(J_1\ J_2\ J \mid M_1'\ M_2', M_1' + M_2')$$

$$\cdot C\,(J_1\ J_2\ J \mid M_1\ M_2, M_1+M_2)\ D^{J}_{M_1+M_2,\,M_1'+M_2'}(\alpha\beta\gamma) \qquad \text{(A2-53)}$$

Finally, the rotation matrices, besides being unitary so that

$$\sum_{M} D^{J*}_{M'M}(\alpha\beta\gamma)\cdot D^{J}_{M''M}(\alpha\beta\gamma) = \delta_{M'M''}$$

$$\sum_{M'} D^{J*}_{M'M}(\alpha\beta\gamma)\cdot D^{J}_{M'M''}(\alpha\beta\gamma) = \delta_{MM''}$$

can be shown to be orthogonal on the surface of the unit sphere (with

$$\int d\Omega = \int_0^{2\pi} d\alpha \cdot \int_0^{\pi} d\beta\ \sin\beta \int_0^{2\pi} d\gamma = 8\pi^2 \quad)$$

$$\int d\Omega\, D^{J_1*}_{M_1'M_1}(\alpha\beta\gamma)\cdot D^{J_2}_{M_2'M_2}(\alpha\beta\gamma) =$$

$$(8\pi^2/(2J+1))\cdot \delta_{M_1'M_2'}\cdot \delta_{M_1M_2}\cdot \delta_{J_1J_2} \qquad \text{(A2-54)}$$

where the 2J+1 factor is due to the number of basic elements $|J, M_1>$ for given J . For symmetric top problems,

$$\int_0^{2\pi} d\alpha \int_0^{\pi} d\beta\ \sin\beta\ \ D^{L*}_{M0}(\alpha\beta 0)\cdot D^{L'}_{M'0}(\alpha\beta 0) = (4\pi/(2L+1))\cdot \delta_{MM'}\cdot\delta_{LL'} \qquad \text{(A2-55)}$$

Using Clebsch-Gordon coefficients we can also show that

$$\int d\Omega\ D^{J_3*}_{M_3'M_3} D^{J_2}_{M_2'M_2} D^{J_1}_{M_1'M_1} = (8\pi^2/(2J_3+1))\ \ C\,(J_1\ J_2\ J_3 \mid M_1'\ M_2', M_1'+M_2')$$

$$C\,(J_1\ J_2\ J_3\ |\ M_1\ M_2, M_1 + M_2)\,. \qquad \text{(A2-56)}$$

$$\cdot\ \delta_{M_1'+M_2',\,M_3'}\ \cdot\ \delta_{M_1+M_2,\,M_3}$$

APPENDIX 3

PARITY OF HUNDS CASE (a) WAVE FUNCTION [1]

Since the total molecular Hamiltonian without the radiation terms is invariant under parity in the lab frame, the matrix elements of the Hamiltonian are split into two non-interacting sub matrix blocks: one with even parity, the other with odd parity. The eigenfunctions of the Hamiltonian can be expressed with definite , either odd or even.

Let $\vec{i}_{sp}$ be the parity operator which in a space-fixed frame performs an inversion through the origin of all the spatial coordinates needed to describe the system, i.e.

$$\vec{i}_{sp} : (\vec{r}_i', \vec{R}') \longrightarrow (-\vec{r}_i', \vec{R}') \qquad \text{(A3-1)}$$

where $\vec{r}_i'$ is the spatial coordinate of the ith electron in the space-fixed frame, and $\vec{R}'$ is the internuclear separation vector. In the space-fixed frame parity does not act on the spin "coordinates"

$$\vec{i}_{sp} : \quad \vec{\sigma}' \longrightarrow \vec{\sigma}' \qquad \text{(A3-2)}$$

The full Hund (a) wave equation is given by

$$| n v \Lambda \; S \; \Sigma ; \; J \; M_J \Omega > \; .$$

For the electron vibration state $| n v >$, Λ is the projection of the total electron orbital angular momentum onto the moving internuclear axis. Σ is the projection of the total electron spin angular momentum S also onto the moving internuclear axis. J is the quantum number associated with the total angular momentum of the system, with projections M_J onto a space-fixed axis, and Ω onto the moving internuclear axis. This wavefunction can be written as a product of the nuclear rotation function $| J \; M_J \; \Omega >$ and the electronic-vibrational wave function in the moving molecular frame $| n v \Lambda \; S \Sigma >$:

$$| \; n v \; \Lambda S \Sigma \; ; \; J \; M_J \Omega > \; = \; | \; n v \Lambda \; S \Sigma > \; . \; | J \; M_J \Omega > \qquad \text{(A3-3)}$$

Thus, the nuclear rotation wave function is just the normalized symmetric top wave function discussed in (A2-17)

$$| \; J \; M_J \; \Omega \; > = \sqrt{[\; (2J+1)/8\pi^2 \;]} \; . D^{J*}_{M_J \Omega} (\; \alpha \beta \gamma \;) \; , \qquad \text{(A3-4)}$$

where $(\alpha\beta\gamma)$ the Euler angles that give the orientation of moving molecular frame relative to the space-fixed frame . The origin of both frames coincides with the center-of-mass of the molecule. The electronic-vibrational wave function

can be factored into a vibrational part $F_{nv}(R)$. An electron spatial coordinate $\vec{r}_i$ and a spin coordinate are measured in the moving molecular frame.

$$|nv\Lambda S\Sigma\rangle = F_{nv}(R) \cdot {}^{2s+1}\Phi_{\Lambda}(\vec{r}_i\,\sigma_i\,;R) \qquad \text{(A3-5)}$$

In discussing the parity of the full wave function $|\, nv\,\Lambda S\Sigma\,;\ J\ M_J\,\Omega\,\rangle$ it is sufficient to consider the effect of parity on the projection wave functions, equation (A3-4) and equation (A3-5), separately.

Consider first the nuclear rotation wave function. From Appendix 2, equations (A2-6) and (A2-9), in the moving molecular frame

$$\vec{i}_{sp} : (x,y,z) \longrightarrow (-x,y,z) \qquad \text{(A3-6)}$$

and the Euler angles

$$\vec{i}_{sp} : (\alpha\,\beta\,\gamma) \longrightarrow (\pi+\alpha\,,\pi-\beta\,,\gamma) \qquad \text{(A3-7)}$$

Now for linear molecules like NaAr, with fixed center of mass, there are only two rotational degrees of freedom $(\alpha\,,\beta)$ with the angle γ being redundant and we choose phases such that $\gamma=0$. Thus with $\alpha\in(0,2\pi)$ and $\beta\in(0,\pi)$, the normalization of the symmetric top wave function, equation (A3-4) , changes to

$$\left| J\ M_J\ \Omega \right> = \sqrt{(2J+1)/4\pi}\quad D^{J*}_{M_J\Omega}(\alpha, \beta, o) \qquad \text{(A3-8)}$$

From the properties of the Jacobi polynomial $d^{J}_{M'M}(\beta)$ [equations (A2-19) and (A2-20)] ,

$$d^{J}_{M_J\Omega}(\pi-\beta) = (-1)^{J-M_J}\cdot d^{J}_{\Omega,-M_J}(\beta)$$

$$d^{J}_{M_J\Omega}(\beta) = d^{J}_{-\Omega,-M_J}(\beta) \qquad \text{(A3-9)}$$

so that from equation (A2-17) and equation (A3-7) :

$$\vec{i}_{sp}\, D^{J*}_{M_J\Omega}(\alpha\ \beta\ 0) = D^{J*}_{M_J\Omega}(\pi+\alpha, \pi-\beta, 0)$$

$$= \exp[i(\pi+\alpha)M_J]\cdot d^{J}_{M_J\Omega}(\pi-\beta)$$

$$= (-1)^{J}\ \exp(i\alpha M_J)\cdot d^{J}_{\Omega,M_J}(\beta) = (-1)^{J}\cdot\ \exp(i\alpha M_J)\cdot d^{J}_{M_J,-\Omega}(\beta)$$

$$= (-1)^{J}\cdot D^{J*}_{M_J,-\Omega}(\alpha\ \beta\ 0) \quad , \qquad \text{(A3-10)}$$

on using equation (A3-9) and $\exp(i\pi M_J) = (-1)^{M_J}$. Thus, under parity, the nuclear rotation wave function transforms like

$$\vec{i}_{sp}\left| J\ M_J\ \Omega \right> = (-1)^{J}\left| J\ M_J,-\Omega \right> \qquad \text{(A3-11)}$$

Since the virbational part of the wave function $F_{nv}(R)$ can be considered to come from an anti-symmetrized linear combination of spin-orbitals $\Phi_{\Lambda}(\vec{r}_i ; \vec{R}) . \chi_{S\Sigma}(\sigma_i)$. Now for Hund case (a), the spin coordinates are in the (moving) molecular frame and can be related to the wave function with spin projection M_s on the space-fixed axis by the appropriate rotation matrix

$$\chi_{S\Sigma} = \sum_{M_S} D^{S}_{M_S\Sigma}(\alpha\beta 0) . \chi_{SM_S} \qquad \text{(A3-12)}$$

But since χ_{SM_S} is the spin wave function in the space-fixed frame it is invariant under parity

$$\vec{i}_{sp} \chi_{SM_S} = \chi_{SM_S} \qquad \text{(A3-13)}$$

while the parity operator on the rotation matrix D^S yields, from equation (A3-10)

$$\vec{i}_{sp} D^{S}_{M_S\Sigma}(\alpha\beta 0) = (-1)^S . D^{S}_{M_S,-\Sigma}(\alpha\beta 0) \qquad \text{(A3-14)}$$

Hence, from equation (A3-12)

$$\vec{i}_{sp} \chi_{S\Sigma} = (-1)^S . \chi_{S,-\Sigma}$$

(A3-15)

The orbital wave function $\Phi_\Lambda(\vec{r}_i;\vec{R})$ has explicit dependence on Λ :

$$\Phi_\Lambda(\vec{r}_i;\vec{R})\exp(i\Lambda\xi_e)$$

where ξ_e is some arbitarily chosen electronic reference angle. Thus, since the molecular state has cylindrical symmetry the electron coordinates $\vec{r}_i$ are most easily expressed in cylindrical coordinates

$$\begin{aligned} x_i &= r_i \cos\xi_i \\ y_i &= r_i \sin\xi_i \\ z_i &= z_i \end{aligned} \qquad \text{(A3-16)}$$

with $r_i^2 = x_i^2 + y_i^2$ and the polar angle ξ_i measured relative to the reference angle ξ_e . Hence, from equations (A3-6) and (A3-16)

$$\vec{i}_{sp}\ (r_i, \xi_i, z_i) = (r_i, \pi - \xi_i, z) \qquad \text{(A3-17)}$$

Σ - STATES

When $\Lambda = 0$, there can be two independent Σ-states: Σ^+- state which is invariant under a reflection through the plane embedding the internuclear axis (e.g. in the

molecular frame, the plane y-z where $\hat{z}$ is the internuclear direction), and a Σ^--state which changes parity under this reflection.

$$\vec{i}_{sp}\,\Phi_{\Lambda=0} = (-1)^s\,\Phi_{\Lambda=0} \quad , \tag{A3-18}$$

with s= 1 , Σ^--state

= 0 , Σ^+-state

NON-Σ -STATES

We choose phases such that

$$\Phi_\Lambda(\vec{r}_i\,,\vec{R}) = \exp(i\pi\Lambda/2).\Phi_{|\Lambda|}\exp(i\Lambda\xi_e)$$

so that

$$\vec{i}_{sp}\,\Phi_\Lambda = \Phi_{-\Lambda} \quad . \tag{A3-19}$$

For the Na-rare gas diatomic molecule, we only have Σ^+-states.

Combining equations (A3-18) and (A3-19) , we have

$$\vec{i}_{sp}\,\Phi_\Lambda = (-1)^s\,\Phi_{-\Lambda} \quad , \tag{A3-20}$$

with s=1 , Σ^-state

$=0$, all non-Σ^- states

Therefore, from equations (A3-3),(A3-11), (A3-5), (A3-12), (A3-16) and (A3-21)

$$\vec{i}_{sp} \left| nv\,\Lambda S\Sigma\,;\Omega J\ M_J \right> = (-1)^{J+S+s} \left| vn\text{-}\Lambda S\text{-}\Sigma;\ -\Omega\ J\ M_J \right> \qquad \text{(A3-21)}$$

where s=1 for Σ^--state, s=0 for all non-Σ^- states. Defining the parity

$$p_+ = -(-1)^{J+S+s}$$

$$p_- = +(-1)^{J+S+s} \qquad \text{(A3-22)}$$

we have the parity full wave functions for Hund (a)

$$\left| nv\ \Lambda\ S\Sigma\ p_+;\Omega J\ M_J \right> = (1/2)^{1/2}\ [\ \left| nv\,\Lambda S\Sigma\ ;\ \Omega\ J\ M_J \right> + \left| nv,\ -\Lambda\ S\ -\Sigma\ ;\ -\Omega\ J\ M_J \right> \ ] \qquad \text{(A3-23)}$$

$$\left| nv\ \Lambda\ S\Sigma\ p_-\ ;\Omega J\ M_J \right> = (1/2)^{1/2}\ [\ \left| nv\,\Lambda S\Sigma\ ;\ \Omega\ J\ M_J \right> - \left| nv,\ -\Lambda\ S\ -\Sigma\ ;\ -\Omega\ J\ M_J \right> \ ] \ .$$

APPENDIX 4

TRANSFORMATION FROM HUND (a) TO HUND (c) REPRESENTATION

To solve the close-coupled equations one chooses an appropriate angular momentum coupling scheme as a basis representation. In particular, for the potential energy curves under study in this dissertation, we find three possible Hund coupling schemes of interest:

(i) Hund (a) basis $|J\ M\ p\ ;\ S\ \Lambda\ \Omega\rangle$ which leads to small off-diagonal elements in the molecular Hamiltonian for small internuclear separations. The large internuclear electric field leaves the orbital and spin angular momentum projections, Λ and Ω, onto the moving molecular axis good quantum numbers. $\Omega = \Lambda + \Sigma$.

(ii) Hund (c) basis $|J\ M\ p\ ;\ S\ j\ \Omega\rangle$ which leads to small off-diagonal elements in the molecular Hamiltonian for intermediate internuclear separations. Now the spin-orbit interaction uncouples the orbital angular momentum projection onto the molecular axis, Λ , from being a good quantum number. $\vec{j}$ is the total electronic angular momentum. $\vec{j} = \vec{L} + \vec{S}$.

(iii) Hund (e) basis $|J\ M\ p\ ;\ S\ j\ \ell\ >$ with small off-diagonal elements for very large internuclear separations, $R \longrightarrow \infty$. This space-fixed representation is needed to extract the S-matrix and the polarization information for subsequent comparison to experiment.

In deriving the transformation that leads from Hund (a) to Hund (e) representation, it is easier to first consider the transformation from Hund (a) to Hund (c) and then the transformation from Hund (c) to Hund (e). In particular, the transformation from Hund (a) to Hund (c) can be viewed as transforming from the uncoupled to coupled representation for the addition of 2 angular momenta $\vec{S} + \vec{L}$: i.e. ,

$$|J\ M\ p;\ S(L)\ j\ \Omega\ > = \sum_{\Lambda} C\ (S\ L\ j\ |\ \Omega - \Lambda\ ,\ \Lambda\ ,\ \Omega\ ).\ |J\ M\ p\ ;\ (L)\ S\ \Omega\ \Lambda\ > \ , \tag{A4-1}$$

C is the usual Clebsch-Gordon coefficient. The transformation from Hund (c) to Hund (e) is more complicated since we will also have to transform from molecule-fixed to a space-fixed representation. We can show that

$$|J\ M\ p;\ S\ j\ell\ > = \sqrt{(2-\delta_{o\Omega})}\ .\ (-1)^{j+\Omega}\ .C(J\ j\ \ell\ |\ -\Omega\ \ \Omega\ \ 0)\ \ |J\ M\ p;\ S\ j\ \Omega\ > \tag{A4-2}$$

so the final transformation from Hund (a) to Hund (e) is given by

$$|J\ M\ p;\ S\ j\ \ell> =$$

$$\sqrt{(2-\delta_{o\Omega})}\ .\ (-1)^{j+\Omega}\ C(J\ j\ \ell|\ -\Omega\ ,\Omega,\ 0)$$

$$.\ \sum_{\Lambda\geq 0} C\ (S\ L\ j\ |\ \Omega-\Lambda\ ,\ \Lambda\ ,\Omega)\ .\ |J\ M\ p;\ S\ \Omega\Lambda\ >\ .$$

(A4-3)

In Table 10 we present the results for the two parities.

TABLE 10

Elements of the unitary Hund (a) to Hund (e) transformation matrix

HUND (a) / HUND (e)	$^{B}\Sigma_{1/2}$	$\Pi_{1/2}$	$\Pi_{3/2}$
$-\ ^{J}_{3/2}\ -\ ^{1}_{J_f+3/2}\ -$	$\sqrt{\frac{2J_f+3}{4(J_f+1)}}$	$\sqrt{\frac{2J_f+3}{8(J_f+1)}}$	$-\sqrt{\frac{2J_f-1}{8(J_f+1)}}$
$3/2 \quad J_f-1/2$	$-\sqrt{\frac{2J_f-1}{12(J_f+1)}}$	$-\sqrt{\frac{2J_f-1}{24(J_f+1)}}$	$-\sqrt{\frac{3(2J_f+3)}{8(J_f+1)}}$
$1/2 \quad J_f-1/2$	$\sqrt{\frac{1}{3}}$	$-\sqrt{\frac{2}{3}}$	0

HUND (a) / HUND (e)	$^{B}\Sigma_{1/2}$	$\Pi_{1/2}$	$\Pi_{3/2}$
$-\ ^{J}_{3/2}\ -\ ^{1}_{J_f-1/2}\ -$	$-\sqrt{\frac{2J_f+3}{12J_f}}$	$-\sqrt{\frac{2J_f+3}{24J_f}}$	$\sqrt{\frac{3(2J_f-1)}{8J_f}}$
$3/2 \quad J_f-3/2$	$\sqrt{\frac{2J_f-1}{4J_f}}$	$\sqrt{\frac{2J_f-1}{8J_f}}$	$\sqrt{\frac{(2J_f+3)}{8J_f}}$
$1/2 \quad J_f+1/2$	$-\sqrt{\frac{1}{3}}$	$\sqrt{\frac{2}{3}}$	0

BIOGRAPHY

Linda Lindroth Vahala was born in Chicago, Illinois on October 18, 1947. She entered the University of Illinois at Champaign-Urbana in 1965, and received her B.S in Physics in of Iowa. She married Mr. George Vahala in December 1970. In the summer of 1971 she was awarded an NSF Fellowship for best teacher, and received her M.S in Physics in January 1972 with a thesis on a variational solution of the Lippmann-Schwinger equation (High Energy Physics). The next nine months were spent at the University of Tennessee - Knoxville with her graduate studies being interrupted by a two year stay in New York, followed by a move to Williamsburg, Virginia. During this time, she collaborated with her husband in research in plasma physics, a collaboration which extended to summer stays at Oak Ridge National Laboratory. In the meantime, she became principal of a private school from 1976- January 1982. In September 1981 she entered O.D.U as a parttime student, and switched to full-time status after one semester of graduate studies. Besides her 4 publications (with 4 papers in the process of being submitted for publication), she has presented over 12 contributed talks at various scientific and International meetings on subjects ranging from plasma physics, high speed switching devices to atomic physics.

She is a member of the Society of Women Engineers, the American Association of Physics Teachers, and the American Physical Society.

PUBLICATIONS:

Vahala, G., Vahala, L., Montgomery, D., and Joyce, D., "Comments on 'Fluctuations in Guiding Center Plasmas in Two Dimensions' ". Phys. Fluids 17, 2298 (1974)

Vahala, G., and Vahala, L., "Wall Stabilization in a Collisionless Bumpy 0 Pinch". J. Plasma Phys. 18, 317 (1977)

Vahala, G., and Vahala, L., "Stable Equilibrium Statistical States for Spheromaks". Phys. Fluids 22, 871 (1979)

Vahala, G., Vahala, L., Harris, J. H., Waddell, B. V., Bateman, G., Dunlap, J. L., Pare, V. K., and Burris, R. D., "Perturbed Magnetic Field Phase Slip for Tokamaks". Nucl. Fusion 20, 17 (1980)